Werking en functie van ASB eiwitten in de regulatie van compartimentgrootte

Proefschrift

ter verkrijging van de graad van doctor aan de

Erasmus Universiteit Rotterdam

op gezag van de

rector magnificus

Prof. dr. H. G. Schmidt

en volgens besluit van het College voor Promoties.

De openbare verdediging zal plaatsvinden op

25 mei 2011 om 11.30 uur

door

Maria Augusta Sartori da Silva

geboren te Piracicaba-SP, Brazil

The research described in this thesis was financially supported by ALW Grant #817.02.002.

Printed by Wöhrmann Print Service.

Action and function of ASB proteins in compartment size regulation

Thesis

to obtain the degree of Doctor from the

Erasmus University Rotterdam

by command of the

Rector Magnificus

Prof. dr. H. G. Schmidt

and in accordance with the decision of the Doctorate Board

The public defence shall be held on

25 May 2011 at 11.30 hrs

by

Maria Augusta Sartori da Silva

born at Piracicaba-SP, Brazil

ERASMUS UNIVERSITEIT ROTTERDAM

Promotor:

Prof. dr. M. P. Peppelenbosch

Copromotor:

Dr. D. Guardavaccaro

Other members:

Prof. dr. F. G. Grosveld

Prof. dr. E. J. Kuipers

Prof. dr. C. P. Verrijzer

“Veni, vidi, vici!”

- Julius Caesar -

Contents

Outline of this thesis

In the research described in this thesis I investigated the function of the ankyrin repeat and SOCS box-containing protein 11 (ASB11) as a key protein involved in the regulation of cell proliferation and differentiation during zebrafish embryogenesis. Zebrafish (*Danio rerio*) is a valuable model organism for studies of vertebrate development and gene function allowing biologists to identify many genes involved in embryogenesis and human diseases. A brief introduction on zebrafish biology is given in the **Chapter 1**.

In **Chapter 2**, I reviewed the current knowledge of biological functions of the ASB family with particular emphasis on the regulation of protein levels by the ubiquitin-proteasome pathway and the occurrence of human malignancies as a consequence of the disruption of this regulating system. The evidences suggested that ASB proteins are crucial regulators of cell fate decisions in different compartments, however many details of its molecular mode of function need to be resolved. This thesis will contribute to uncover some of these details.

In **Chapter 3**, I reported on the role of d-Asb11 as a positive regulator of Notch signaling, acting at the level of DeltaA ubiquitylation, important in fine-tuning the lateral inhibition gradients between DeltaA and Notch and thereby regulating Notch signaling activity in a non cell-autonomous manner. The function of the different subdomains in d-Asb11 and especially the cullin box domain remained to be determined. To this end, in **Chapter 4**, I generated a zebrafish germline having a deletion of the cullin box subdomain of the d-Asb11 SOCS box and showed that this deletion resulted in loss of d-Asb11 activity. As a consequence, the animals were defective for Notch signaling and proper cell fate specification within the neurogenic regions of zebrafish embryos. My results established the first *in vivo* evidence that the cullin box is required for SOCS box functionality. Subsequently, experiments were initiated to identify further *in vivo* functions of d-Asb11, also using the hypomorphic mutant fish as a tool.

In **Chapter 5**, I provided evidence that d-Asb11 is important in maintaining myogenic proliferation in the stem cell compartment of zebrafish embryos

and muscle regenerative responses in adult animals. This finding is supported by the highly specific d-Asb11 expression found in proliferating satellite cells and revealed the new function of d-Asb11 as a regulator of zebrafish myogenesis. The apparent importance of d-Asb11 in multiple germ lines enforces the urgency to define its mode of action in molecular terms and especially to identify new binding partners. Thus, in **Chapter 6**, I have applied immunoaffinity chromatograpy followed by tandem mass spectrometry to identify human ASB11 interacting proteins. My data confirmed the role of human ASB11 as a substrate-recognition that targets proteins for ubiquitylation and proteasomal degradation via the canonical ECS ubiquitin ligase complex. Furthermore, I speculated on a specific function of ASB11 in governing cellular fate of membrane proteins not only by mediating proteasome degradation but also by influencing protein stability, activity and intracellular localization.

Finally, a summarizing discussion is given in **Chapter 7**. Altogether my results provide important new insight on the action and function of ASB proteins, and especially ASB11, in regulating progenitor compartment expansion, possibly by controlling protein levels in the cells.

CHAPTER 1

Biology of zebrafish

Carmen V. Ferreira[1], Maria A. Sartori da Silva[2], Giselle Z. Justo[3]

[1]Laboratory of Bioassays and Signal Transduction, Institute of Biology, University of Campinas, Campinas-SP, Brazil.

[2]Department of Gastroenterology and Hepatology, Erasmus MC-University Medical Center Rotterdam, Rotterdam, The Netherlands.

[3]Departament of Biochemistry and Departament of Biological Sciences, Federal University of São Paulo, São Paulo-SP, Brazil.

Adapted from

Chapter 12: Zebrafish as a suitable model for evaluating nanocosmetics and nanomedicines. In: NANOCOSMETICS AND NANOMEDICINES: New approaches for skin care

Springer Publishing Company

2001

Zebrafish (Fig.1), a popular aquarium fish, is a freshwater cyprinoid teleost placed in the order of ray-finned fishes, Cypriniformes [1]. It was first described in *An Account of the Fishes Found in the River Ganges and its Branches*, published by Francis Hamilton in 1822 [2]. The name Danio means ‘‘of the rice field’ and derives from the Bengali name ‘‘dhani’’. Zebrafish are native to the streams of South-eastern Himalayan region, being distributed throughout South and Southeast Asia. They are most commonly encountered in slow-moving or standing water bodies, often connected to rice cultivation [2].

Figure 1: Zebrafish.

Zebrafish are small, rarely exceeding 4 cm (from the tip of the snout to the origin of the caudal fin). It has a fusiform and laterally compressed body shape, with a terminal mouth directed upwards. Males are slender and torpedo shaped while gravid females have more rounded body shape. The fish’s popular name is due to its color pattern composed of five to seven uniform dark blue longitudinal stripes on the side of the body, extending from behind the operculum into the caudal fin. Males have gold stripes between the blue stripes and tend to have larger anal fins with more yellow coloration. Females have silver stripes instead of gold and adult females exhibit a small genital papilla in front of the anal fin origin. However the sex of juveniles cannot be properly distinguished without dissection [3,4].

Domestic strains used in laboratories may exhibit distinguished features. The ‘‘leopard’’ Danio displays a spotted color pattern instead of stripes caused by a spontaneous mutation of the wild-type, whereas the ‘‘longfin’’ Danio has a dominant mutation resulting in elongated fins. The TL or Tubingen long-fin, commonly used wild-type strain, displays both the ‘‘leopard’’ and ‘‘longfin’’ mutations [2].

The approximate generation time for zebrafish is 3-4 months. Fertilization and subsequently embryonic development are external and occur synchronously in large clutches. Females, in the presence of males, can spawn every 2-3 days laying several hundred of eggs per mating. Spawning

activity, in domesticated zebrafish, is influenced by photoperiod and usually commences within the first minute of exposure to light following darkness, continuing for about an hour [5]. Zebrafish eggs are relatively large and embryos are completely transparent during the first 24 hours post fertilization, allowing the visualization of developing organs through the chorion. Embryos develop rapidly; a beating heart and erythrocytes can be seen by 24 hours. Precursors of all major vertebrate organs arise within 36 hours, including brain, eyes, ear and internal organs. The organs are like a minimalist version with far fewer cells compared to higher vertebrates having an equivalent function in the organism. Within five days, the larva hatches from the egg and is able to swim, displaying food seeking and active avoidance behaviors [6]. The first three months following hatching, zebrafish growth rate is most rapid and it starts to decrease, approaching zero, by about 18 months. Life-span in captivity is around 2-3 years, although in ideal conditions, may extend to 5 years [7].

Zebrafish biological characteristics, in general, make it particularly tractable to experimental manipulation and concede valuable advantages for its use as an animal model system. In the late 1970s, George Streisinger, at the University of Oregon, recognized the virtues of the zebrafish and pioneered its use as a model organism for studies of vertebrate development and gene function [8]. Later, methods for high-efficiency mutagenesis were developed and large scale genetic screens characterized several mutants and identified numerous genes. By now, zebrafish genome is almost completely sequenced. It has approximately 2.0 gigabases in size, divided up into 25 chromosomes (1n) (http://www.sanger.ac.uk/Projects/D_rerio/). Although the absolute number of genes is still unknown, a large set of genes has been cloned and found to have conserved coding and regulatory sequences between zebrafish and humans. Furthermore, by 120 hours after fertilization, zebrafish develop discrete organs and tissues, including brain, heart, liver, pancreas, kidney, intestines, bone, muscles, nerve systems and sensory organs. These organs and tissues have been demonstrated to be similar to their mammalian counterparts at the anatomical, physiological and molecular levels. Thus, the zebrafish has become a powerful model

system for providing novel insights into the processes of embryonic development, physiology and a wide range of human disorders, such as cancer, diabetes, neurodegenerative and cardiovascular diseases [9-13].

In this thesis, zebrafish is utilized as a model organism for vertebrate neural and muscle development. We have focused on the role of the ankyrin repeat and SOCS box-containing protein 11 (Asb11) in governing molecular events during early neurogenesis and myogenesis in zebrafish embryos as well as in adult muscle regeneration. Moreover, the characterization of an *asb11* mutant line provided additional clues to understanding the function of the protein.

References

1. Mayden RL, Tang KL, Conway KW, Freyhof J, Chamberlain S, Haskins M, Schneider L, Sudkamp M, Wood RM, Agnew M, Bufalino A, Sulaiman Z, Miya M, Saitoh K, He S (2007). J Exp Zool B Mol Dev Evol 308:642-654.
2. Spencer R, Gerlach G, Lawrence C, Smith C (2008). Biol Rev Camb Philos Soc 83:13-34.
3. Laale HW (1977). J Fish Biol 10:121-173.
4. Barman RP (1991). Record Zool Surv India Occas Pap 137:1-91.
5. Darrow KO, Harris WA (2004). Zebrafish 1:40-45.
6. Kimmel CB, Ballard WW, Kimmel SR, Ullmann B, Schilling TF (1995). Dev Dyn 203:253-310.
7. Spence R, Smith C (2007). Ethology 113:62-67.
8. Streisinger G, Walker C, Dower N, Knauber D and Singer F (1981). Nature 291:293-296.
9. Müller F, Blader P, Strähle U (2002). Bioessays 24:564-572.
10. Amatruda JF, Patton EE (2008). Int Rev Cell Mol Biol 271:1-34.
11. Kinkel MD, Prince VE (2009). Bioessays 31:139-152.
12. Chico TJ, Milo M, Crossman DC (2010). J Pathol 220:186-197.
13. Sager JJ. Bai Q, Burton EA (2010). Brain Struct Funct 214:285-302.

CHAPTER 2

Size matters: the emerging role of ASB proteins in controlling cell fate decisions and cancer development

Maria A. Sartori da Silva[1,2] and Maikel P. Peppelenbosch[2]

[1]Hubrecht Institute-KNAW & University Medical Center Utrecht, Utrecht, The Netherlands.

[2]Department of Gastroenterology and Hepatology, Erasmus MC-University Medical Center Rotterdam, Rotterdam, The Netherlands.

(Submitted)

Abstract

One of the most important and defining processes during development is the establishment of the relative sizes of the various compartments in the vertebrate body. The molecular regulators guiding compartment size are only now emerging, but involve the ankyrin and SOCS box containing protein family (ASBs). ASBs are among the most conserved genes in the chordate phylum. Studies revealed roles of ASBs in regulating both normal and pathological (i.e. cancer) compartment size in various systems in different vertebrates. Although mechanistically important roles for ASB-mediated ubiquitylation effects on physiology have been established, many questions remain. Nevertheless it is evident that further knowledge on these systems will prove useful combating compartment size-related diseases.

Introduction

One of the most important and defining processes during development is the pattern formation of the various compartments in embryos. Compartments are composed of distinct cell populations divided into functional units limited in specific areas. As a concept they were first defined in the *Drosophila melanogaster* wing imaginal discs and, later, this concept was expanded to vertebrates (for an impression of compartments see Fig.1). The fate of these compartments is highly organized and regulated, controlling patterning, polarity, proliferation and differentiation into diverse tissues [1-5].

Developing organisms require the generation of cells in appropriate numbers prior to acquisition of specialized functions, therefore the expansion of a progenitor compartment is essential before further differentiation ensues [6, 7]. However, the mechanisms behind the regulation of overall compartment dimensions remain unclear at best.

In adult tissues, the size of the stem cell compartment is under tight genetic control [8]. The stem cells, a restricted subpopulation of cells, continue

proliferating and undergo either to self-renewal or differentiate into committed cell types with less proliferative potential. Deregulation of these processes result in uncontrolled cell growth and is implicated in many serious pathologies, as cancer [9]. Hence to comprehend the biology of cancer, it is necessary to characterize the mechanisms that multi-cellular organisms evolved to control their proliferative capacity into appropriate compartments, and understand how these mechanisms are regulated in normal cells and how they become deregulated in cancer. Nevertheless, knowledge as to the factors driving expansion of the stem cell compartment remains obscure and elucidation of the underlying molecular mechanisms that define compartment size represents an important scientific question, being hardly a pursuit only of academic interest.

Efforts to discover the participants involved in regulating compartment size have revealed gene products whose presence are essential for maintaining proliferation of progenitors during embryogenesis and adult life. One of these genes, emerged from a genetic screen, was *asb11* (Ankyrin repeat and SOCS box-containing protein 11). Asb11 was down-regulated at the start of terminal cell commitment in zebrafish embryos and subsequent experiments revealed that Asb11 is a major determinant regulating the size of the central nervous system [10]. As the *asb11* gene, together with the highly homologous *asb5*, *asb9*, and *asb13* are among the most conserved genes in the chordate *phylum* (Fig.2) [10], we and others hypothesise that ASBs have a vertebrate *subphylum*-wide significance for maintaining expansion of progenitor compartments [10].

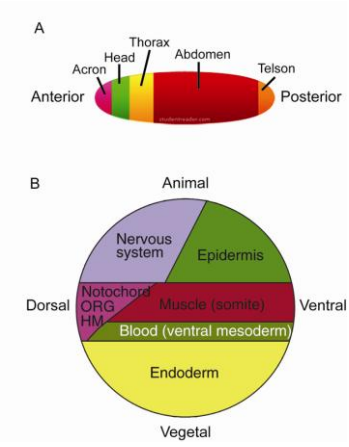

Figure 1. Schematic embryonic fate maps of (**A**) *Drosophila* and (**B**) a vertebrate organism (Xenopus). Lateral views. ORG: organizer, HM: head mesoderm. Adapt from Lemaire et al 2008 (59) and studentreader.com.

Clues as to the possible molecular action of Asb11 come from the presence of the conserved ankyrin repeats and SOCS box domains [11] (Fig. 3A). SOCS box proteins regulate the turnover of protein substrates by interacting with and targeting them to degradation via the ubiquitin-proteasome pathway [12]. Accordingly, ASB proteins, as well as Asb11, have been reported to bring target proteins to the ubiquitylation machinery, leading these proteins to degradation [13-15]. Targeted degradation of proteins controls numerous cellular processes and alterations in the ubiquitin pathway are associated with various human disorders including neurodegenerative diseases and cancer [16, 17]. These findings propose a role of ASBs in important biological functions and prompt a dedicated review on the ASB family.

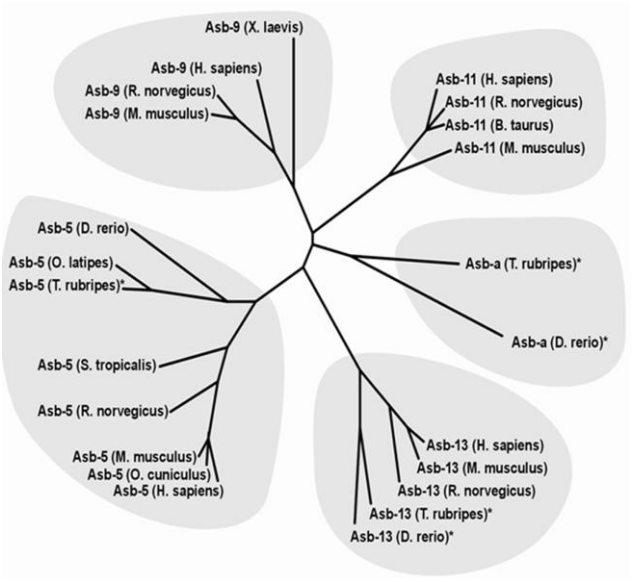

Figure 2. Phylogenetic tree of the homologous vertebrate genes *ASB5, ASB9, ASB11,* and *ASB13.*

In the present piece we summarise the current knowledge of ASB proteins with particular emphasis on the regulation of cell fate, possibly by degradation of key proteins, and the human malignancies caused by the disruption of this regulating cell system.

ASB family structure and function

The ASB family constitutes a chordate-unique gene family whose members are characterized by variable numbers of N-terminal ankyrin repeats and a C-terminal SOCS box [11] (Fig.3A). SOCS box proteins have been subdivided into different protein families based on the structural differences of their substrate-binding domains. The families include the SOCS family (SH2 domain), von Hippel–Lindau disease protein (pVHL) (β-domain), the ankyrin repeat and SOCS box (ASB) family (ankyrin repeat), WSB1 and WSB2 (WD40 repeat), the SSB family (SPRY domain) and the RAR-like proteins (GTPase domain) [11]. The eighteen mammalian ASB proteins constitute the largest family of SOCS box-containing proteins and they were first identified by Hilton et al (1998). Other species present a lesser number of ASB proteins, however they show very high conservation.

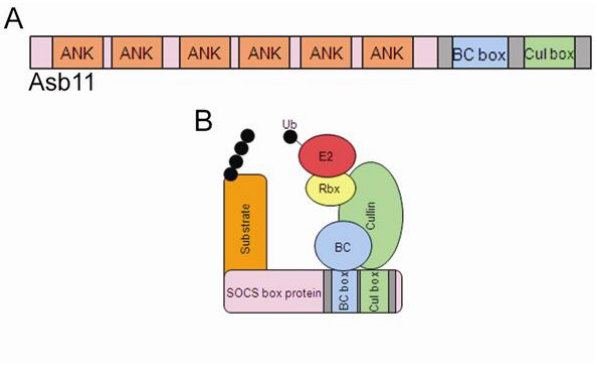

Figure 3. Schematic representation of the Asb11 protein and the ECS ubiquitin ligase complex.
(**A**) Illustration of the *d-asb11* gene product containing the ankyrin repeat domain (ANK) in its N-terminal region and the SOCS box domain divided into BC box and Cullin box subdomains in the C-terminal region. (**B**) ASB proteins function as a substrate recognition module in a putative Elongin BC-Cullin-SOCS-box (ECS) type E3 ubiquitin ligase complex. Adapt from Sartori da Silva et al 2010 (50).

All representatives of the ASB family have two functional domains: an ankyrin repeat region where specific protein-protein interactions occur and a SOCS box region which serves as a generic adapter directing the degradation of targeted proteins. The ankyrin repeat consensus is approximately 33 amino acids in length usually encountered in variable number of copies. Each ankyrin repeat comprises a V-shaped helix-turn-helix motif linked together by loops. Studies have shown that some loops serve as sites of protein-protein interactions, while the ankyrin repeats provide a stabilizing platform [18]. As a functional specific domain, the

ankyrin repeat has been found in proteins with a wide range of cellular functions [19, 20].

The C-terminal domain, SOCS box, has approximately 40 to 60 amino acids. It was first identified in the SOCS proteins and has since been found in more than 70 proteins across a range of species. The SOCS box serves as a generic adapter site for the Elongin BC components [21-23]. Members of SOCS box families (e.g. SOCS proteins, WSBs and ASBs) were reported to bind Elongin C, which in turn associates with Elongin B, a scaffold protein known as cullin and a RING (Really Interesting New Gene) finger protein called Rbx [15]. Together, these elements form the Elongin C-cullin-SOCS box (ECS) complex [14] (Fig. 3B).

The SOCS box is divided into two sub-domains, the BC box and the cullin box. The BC box binds to Elongin C that links SOCS box proteins to the Cullin-Rbx module. The cullin box, located immediately downstream of the BC box, is proposed to determine whether a given SOCS box protein assembles into either a Cul2-Rbx1 or a Cul5-Rbx2 module [24].

In cooperation with an ubiquitin activating enzyme (E1) and an ubiquitin-conjugating enzyme (E2), the ECS complex, formed by E3 ubiquitin ligases, facilitates the polyubiquitylation and proteasomal degradation of targeted proteins [25, 26]. Other reports suggest that the interaction between SOCS box and Elongin-BC may stabilize SOCS proteins, thereby protecting them from degradation [27].

So far very little is known about the function of the ASB members as a substrate-recognition component of the ECS complex. Some studies have proposed that ASBs perform an analogous role to the SOCS proteins, regulating cellular functions via interaction of their SOCS box motif and the Elongin-BC complex leading targeted proteins to destruction [14, 28]. While SOCS proteins use the SH2 domain to recruit substrates with phospho-tyrosine motifs, ASB proteins are expected to use the ankyrin repeats to recruit substrates. The specificities of the substrates are determined by E3 ubiquitin ligases. It recognizes its substrate and catalyzes the binding between the C-terminal of ubiquitin and the targeted protein, thereby allowing proteolytic degradation by the 26S proteasome. Hence, E3

ubiquitin ligases are key molecules in the regulation of Ub-dependent proteolysis [29].

To date, very few proteins have been described as potential substrates of specific ASB family members. However, the SOCS box motifs of ASB1, ASB2, ASB3, ASB4, ASB6, ASB7, ASB8, ASB9, ASB11 and ASB12 have been shown to directly interact with one or more components of the ECS complex. Moreover, in most of the cases, ASB proteins were dependent on the presence of an integral SOCS box domain to exert their function properly. These findings demonstrate the importance of this group in mediating cellular responses by ubiquitylation and degradation of proteins.

The many faces of ASB proteins

While Skp-Cullin-F-box (SCF) complexes have been well established to control cell growth through degradation of critical regulators (e.g. cyclins, CDK inhibitors and transcription factors) [17], the function of ASBs as integrants of the ECS complex, remains poorly understood. At the present time, approximately 40 papers (http://www.ncbi.nlm.nih.gov) have reported on ASB protein action in different biological processes, generally related to cell proliferation and differentiation. Numerous cases, but not all, showed the effects of ASB to be dependent on the presence of its SOCS box domain and to bind to components of the ECS complex (e.g. Elongin C), confirming the ubiquitylating properties of ASB proteins. Other studies focus on the action and function of ASB proteins in metabolism and cancer. Below we summarize the current state with respect to knowledge of the ASB family of proteins.

ASB1

The function of ASB1 was studied by utilizing genetically modified mice. Transgenic mice ubiquitously overexpressing ASB1 had no obvious effect on normal mouse development while *Asb1* knock-out mice displayed subtle defects in spermatogenesis in some seminiferous tubules. The lack of an

apparent phenotype in transgenic mice raises the possibility of overlapping or shared functions between individual members of the ASB family [30].

ASB2

ASB2 expression was activated by all-*trans* retinoic acid (ATRA) during differentiation of human myelocytic leukemia HL-60 cells. The activation of *ASB2* occurred through the binding of a retinoic receptor alpha (RARα) to the retinoid receptor or retinoid X receptor (RARE/RXRE) element present in the *ASB2* promoter. Increase of ASB2 was accompanied by growth inhibition, chromatin condensation and granulocytic maturation in the cells [31, 32]. In agreement, an ASB2 isoform, ASB2β, was induced during myogenic differentiation of C2C12 and primary myoblasts. The inhibition of ASB2β blocked myoblasts fusion and myotube formation, crucial processes in the later phase of muscle development. In addition, ASB2β triggered ubiquitin-mediated degradation of the actin filamin B (FLNb) by assembling with elongin B, elongin C, Cullin 5 and Rbx2 to reconstitute an active E3 ubiquitin ligase complex [33]. Other studies also showed ASB1, ASB2, ASB6, ASB7 and ASB12 interacting with Cul5–Rbx2 but neither Cul2 nor Rbx1 in HEK293 cells [14]. However in a study using insect cells the ASB2-Elongin BC complex presented E3 ligase activity by assembling with Cul5–Rbx1 [15].

Alternatively, in a recent study ASB2 promoted the ubiquitylation of Notch targets such as E2A and Janus kinase (Jak) 2 by forming non-canonical E3 ligase complexes. ASB2 likely bound Jak2 directly but associated with E2A through the F-box-containing protein, Skp2, which is known to associate with Skp1 and Cul1 [34]. Moreover, ASB2 was transcriptionally activated by Notch signalling, which fits well with the role established for other ASB proteins as regulators of Notch signalling [13].

Although these findings imply an important function of ASB2 in degrading key proteins involved in cell proliferation and differentiation, more studies are required to understand the variations occurred in the ASB2-mediated ubiquitylation complexes.

ASB3

ASB3 has been identified as a negative regulator of tumor necrosis factor receptor type 2 (TNF-R2) signalling in response to TNF-α. By recruiting ElonginC through its SOCS box domain, ASB3 might mediate the TNF-R2 ubiquitylation and degradation [35]. ASB3 may be involved in the negative feedback on inflammatory responses as TNF-R2 plays a coordinating role in host defence and functional studies in knock out animal exposed to microbiological infection models may provide further insight here.

ASB4

Studies have shown that ASB4 expression was down-regulated in homeostasis-related brain areas of fasted rat and obese Zucker rat, both models of energy disequilibrium. Transgenic mice expressing *Asb4* in specific neurons had reduced fat mass and increased lean mass in addition to lower levels of blood Leptin. They were also resistant to high-fat diet-induced obesity [36, 37]. Furthermore, ASB4 interacted and reduced G-protein pathway suppressor 1 (GPS1 or CSN1) levels. The inhibitory effect was independent of the SOCS box domain and did not involve polyubiquitination, suggesting that ASB proteins may act by additional degradation pathways. Expression of GPS1 stimulated c-Jun NH_2-terminal kinase (JNK) activity. JNK has been reported to provide negative feedback with respect to insulin signalling. By interacting with GPS1, ASB4 inhibits JNK activity, providing a mechanism by which cellular insulin responses are regulated. Thus, it is assumed that ASB4 has a role in the regulation of energy homeostasis, involved in the control of feeding behaviour and metabolic rate [38].

Other studies have proposed that ASB4 promoted endothelial differentiation and/or maturation in response to increasing oxygen levels during early vascular development of mouse embryos. ASB4 interacted with the factor inhibiting HIF1α (FIH) and is a substrate for FIH-mediated hydroxylation via an oxygen-dependent mechanism. Additionally, ASB4 co-immunoprecipitated with endogenously expressed elonginB, Cul5, Roc1 (Rbx1), and to a lesser extent with Cul2 [39], all consistent with a role of ASB4 in ubiquitylating target proteins, including ASB4 itself. The target

substrate and the molecular mechanisms for endothelial cell fate, however, remain to be established.

ASB5

Asb5 is involved in the initiation of arteriogenesis in rabbit. mRNA and protein levels are significantly upregulated in growing collateral arteries. The infusion of doxorubicin, which inhibits angiogenesis, led to a significant decrease of *asb5* mRNA [40]. Furthermore, expression of ASB5 identified in differential genetic screens suggested a function in cardiovascular development [41] and myogenesis [42]. However, with lack of further information, ASB5 function in physiology and especially in vascular and muscle development remains open to speculation.

ASB6

ASB6 was described as an adipocyte-specific protein that interacts with the adaptor protein containing PH and SH2 domains (APS), which is involved in the insulin signalling for glucose transportation. Activation of the insulin receptor was required for ASB6 recruitment of Elongin BC. Prolonged insulin stimulation resulted in the degradation of APS when ASB6 was co-expressed but not in the absence of ASB6 [28]. Thus ASB6 seems implicated in the regulation of metabolic control through signalling of the insulin receptor in adipose tissue, linking this protein to diabetes.

Another study described that ASB6 was abundantly expressed in oral squamous cell carcinoma (OSCC) with relatively low expression in adjacent normal tissue. In oral cancer patients, increased ASB6 expression was positively correlated with the use of areca nut extract (ANE), the major component of the betel quit. Betel quit chewing is a popular habit, especially in southern and south-eastern Asia. The result corresponded to upregulation of ASB6 in normal keratinocytes and oral cancer cells by ANE treatment. In addition, survival analysis showed that ASB6 upregulation was highly associated with a worse prognosis of OSCC [43]. These results suggest that ASB6 may be involved in carcinogenesis and could act as a

prognostic marker for oral cancer; however more data of ASB6 mechanism of action is necessary.

ASB8

ASB8 transcripts are widely expressed in different tissues, as skeletal muscle, heart, brain, placenta, liver, kidney, and pancreas. Although no expression has been found in normal lung, ASB8 was present in a variety of lung cancer cell lines. Furthermore, analysis of lung tumor xenografts in nude mice revealed high ASB8 expression in the malignant lung cancer compartment, while lower or no expression was detected in noncancerous stromal area. Thus, ASB8 may be up-regulated in lung carcinoma, suggesting regulatory effects on the cell growth of lung cancer cells. Consistently, inhibition of cancer growth was evident when a mutant of ASB8 lacking the SOCS box domain was employed, the authors explained this effect from an action of the truncated ASB8 protein as a dominant negative regulator. Further evidence for a role of ASB8 as a component of the ubiquitylation complex was provided by the demonstration of its interaction with Elongin BC [44, 45]. Together, these results support the concept that ASB proteins act in cell proliferation through the ubiquitin pathway, although the targets involved remain unknown.

Support for roles of ASB proteins in the control of compartment size come from studies suggesting that ASB8 is important for spermatogenesis, at the differentiation stage. ASB8 was downregulated in the testes of a senescence-accelerated mouse (SAMP1) strain. SAMP1 mice undergo sexual maturation at earlier age; however, they present a functional decline in spermatogenesis more rapidly and at a younger age. In normal testes, ASB8 was abundantly expressed, mainly in spermatocytes and spermatids [46].

ASB9

Human and murine ASB9 were identified as specific binding partners of the ubiquitous mitochondrial creatine kinase (uMtCK) and the creatine kinase B (CKB), respectively, in human embryonic kidney (293T) cells.

Overexpression of ASB9 dramatically reduced endogenous uMtCK and CKB proteins. Although ASB9 and ASB9 lacking the SOCS box domain (ASB9ΔSOCS) could interact with uMtCK and CKB independently of the SOCS box domain, only the interaction of full length ASB9 led to a SOCS box-dependent polyubiquitylation and a decline in cellular protein levels. Furthermore, the creatine kinase activities and cell growth were significantly reduced by ASB9 but not by ASB9ΔSOCS [47, 48].

Recent studies analyzed the ASB9 expression in paired cases of colorectal cancer (CRC) and non-cancerous regions. The analysis demonstrated that ASB9 was higher expressed in CRC tissue than corresponding normal tissue. An immunohistochemical study revealed that ASB9 was predominantly expressed in cancer cells and a multivariate analysis showed that ASB9 expression status was an independent prognostic factor of overall survival. These results suggest a general role of ASB9 in cell proliferation and a specific function as an indicator of prognosis in CRC [49].

Asb11

The *Danio rerio* Asb11 (d-Asb11) was found to regulate neuronal progenitor compartment size by maintaining the neural precursors in the proliferating state via SOCS-dependent ubiquitylation of the Notch ligand DeltaA and thereby leading to the activation of Notch signaling. Knock down of the *d-Asb11* led to a reduction of the neuronal compartment of the embryos, whereas its forced expression led to a massive expansion of the central nervous system [10, 13].

A recent study showed that zebrafish carrying a mutant allele in the cullin box subdomain of the SOCS box were defective in Notch signalling and had severely affected cell fate specification within the neurogenic regions of the embryos. This report revealed the first organism harboring a mutated cullin box and suggested an *in vivo* importance of the cullin box for SOCS-box proteins [50]. Further studies demonstrated that these effects were due to a positive role of Asb11 in canonical Notch signalling in progenitor cells.

ASB13

ASB13 was first referred in the results of a gene-expression data set of diffuse large B-cell lymphoma (DLBCL). DLBCL is the most frequent B cell Non-Hodgkin's lymphoma. The experiment aimed to find key genes differentially expressed in different groups of patients, improving prognosis and survival predictions of patients with medium survival time.
The results revealed that ASB13 was overexpressed in activated B cell-like (ABC) group when compared to germinated centre B cell-like (GCB) group. The ABC group has a more aggressive behaviour and a lower overall survival rate compared to the GCB group [51]. Although ASB13 seems to be upregulated in more malignant cancer cells, functional data on this effect have not been provided as yet.

ASB15

ASB15 promoted muscle growth both *in vivo* and cell culture experiments. ASB15 overexpression is associated with increased protein synthesis and greater myofiber area in mice skeletal muscle. In mouse C2C12 myoblasts, ASB15 overexpression produced a delay in differentiation. Results from *ASB15* gene with removed SOCS box motif, support the hypothesis that ASB15 might interact with appropriate target proteins through the ankyrin repeat region targeting them for ubiquitylation and proteasomal degradation. Expression of ASB15 also altered phosphorylation of the PI3K/PKB pathway, as $ASB15^{+}$ and $ASB15^{-}$ cells have decreased and increased Akt phosphorylation, respectively [52, 53]. These data are consistent with the concept that PI3K/PKB pathway controls skeletal muscle growth and point to ASB15 exerting its control on skeletal compartment size through a negative control of the PI3K/PKB pathway.

ASB17

Analysis of mouse and human tissues revealed that ASB17 is expressed exclusively in testes, with the highest expression in round spermatids, but no expression in Leydig cell and epididymis [54, 55]. These results suggest a role of ASB17 in testes development and spermatogenesis.

Others

Studies about ASB7, ASB10, ASB12, ASB14, ASB16 and ASB18 have not been reported hitherto and data on these proteins are urgently required to obtain full understanding of this protein family in the control of cell physiology.

ASB proteins and cancer

E3 ubiquitin ligases mediate the ubiquitylation of a variety of significant substrates for targeted degradation, being important in the regulation of many biological processes. ASBs together with elongin BC, cullin and RING proteins, constitute a well established group of E3 ubiquitin ligases [21]. Increasing amounts of evidence suggest that the abnormal regulation of some E3 ligases or aberrant proteolysis of their substrates contribute significantly to development of various diseases including cancer [56]. Furthermore, some E3 ubiquitin ligases are frequently overexpressed in human cancers [57], which correlate well with findings by which ASB proteins were up-regulated in cancerous cells of patients with oral (ASB6) and colorectal (ASB9) carcinoma and B cell Non-Hodgkin's lymphoma (ASB13) (Table1).

In addition, ASB8 was present in lung cancer cell lines and lung tumor of nude mouse while lower or no expression was detected in human and mouse normal lung tissues. Besides, mutated ASB proteins were found in some cancer tissues: as kidney carcinoma (ASB3, ASB8 and ASB16), glioma (ASB4), breast and skin cancer (ASB11) and lung cancer (ASB15). Mutation in ASB11 presented 2 incidences in breast cancer; both were placed in the SOCS box region (http://www.sanger.ac.uk/genetics/CGP/cosmic/). This is in agreement with SOCS box being essential for assembling the ubiquitylation complex, thus, allowing ASB proteins to exert their proper function in targeting proteins for degradation. Furthermore, ASB proteins play essential roles in cell proliferation and differentiation of several tissues (e.g. spermatogenesis, myogenesis, arteriogenesis and neurogenesis) (Table1). Considering that the processes underlying tumor and normal cell

proliferation are very similar, further studies of ASB proteins and their target substrates may help to elucidate regulatory mechanisms in normal and tumor proliferating cells, improving cancer diagnosis, risk prognosis as well as development of potential anticancer therapies.

ASB protein	Biological function	Negative regulation	E3 activity	Disease-related
ASB1	Spermatogenesis	n/a	n/a	n/a
ASB2	Hematopoiesis	n/a	n/a	n/a
	Myogenesis	FLNb	yes	n/a
ASB2β	Notch signalling	E2A/Jak2	yes[1]	n/a
ASB3	Inflammatory responses	TNF-α	yes	n/a
ASB4	Insulin signalling	GPS1 (CSN1)	no	diabetes[2]
	Vascular development	FIH[3]	yes	n/a
ASB5	Vascular development, Myogenesis	n/a	n/a	n/a
ASB6	Insulin signalling	APS	yes	diabetes[2]
	n/a	n/a	n/a	oral carcinoma
ASB8	n/a	n/a	yes	lung carcinoma
	Spermatogenesis	n/a	n/a	n/a
ASB9	n/a	uMtCK/CKB	yes	n/a
ASB9	n/a	n/a		colonrectal cancer
ASB11	Neurogenesis, Notch signalling	DeltaA	yes	n/a
ASB13	n/a	n/a	n/a	Non-Hodgkin's lymphoma
ASB15	Myogenesis, PI3K/PKB pathway	n/a	yes	n/a
ASB17	Spermatogenesis	n/a	n/a	n/a

Table 1. Summary of the ASB proteins functions. ASB proteins (first column) were found to negatively regulate key proteins (third column) involved in different biological functions (second column) by targeting them to the ubiquitin-proteasome pathway (forth column). Deregulation of cellular protein levels results in the development of different human pathologies (fifth column). [1]non-canonical

ECS complex, [2]Predicted pathology, [3]In this specific case, FIH acts as a negative regulator of ASB4.

Conclusions and perspectives

Despite the large size of the ASB family, its strong genetic conservation and the demonstrated potency in regulation of compartment sizes, very little is known about few single ASB proteins. The information combined in the present review provides a general view of the family as well as shared and particular functions of its members.

Analysis of ASB transcripts levels revealed a tissue-specific expression pattern. Based on the highest mRNA levels, ASBs may be divided into 3 main groups: ASBs most strongly expressed in testis (ASB1, ASB3, ASB4, ASB9 and ASB17), in muscle (ASB2, ASB5, ASB10 and ASB11) and widely expressed in different levels in many tissues, including muscle and testis (ASB8, ASB13). These expression patterns indicate potential tissue-specific functions as well as overlapping or shared functions among individuals of the ASB family.

ASB association with components of Cullin-based ubiquitylation complexes via the SOCS box domain is well established [21]. However, at least one study showed that the inhibitory effect of ASB4 on a protein expression (GPS1) was independent of the SOCS box domain and did not involve polyubiquitination [58], suggesting that ASB proteins may act by additional regulation pathways. Conversely, in another study the authors demonstrated that ASB4 had ubiquitin ligase activity and co-precipitate with E3 ligases components [39]. They also provided evidences on ASB4 auto-ubiquitylation, indicating that ASB proteins may present a mechanism of self-regulation. This is in agreement with the findings that many RING finger E3 ubiquitin ligases exhibited self-ubiquitination activity *in vitro*, and that F-box proteins underwent self-ubiquitination in the absence of substrates [58], although upon overexpression of myc-tagged asb11 we ourselves were not able to detect such an event.

The precise binding between ASB proteins and their E3 ligase partners have diverged and, sometimes, counteracted among studies. Sequence motif analysis showed that all the ASB proteins share the consensus sequence of

Cul5 box but not Cul2 box. Thus, it is highly likely that ASB proteins associate with the Cul5–Rbx2 but not the Cul5–Rbx1 module in cells forming ECS complexes [14, 24]. In fact, studies described ASB2 and ASB4 associating with Rbx1 [15, 38] and, more surprisingly, a recent report showed a previous unrecognized association of ASB2 with Skp2, a protein of the SCF complex, forming a non-canonical E3 ligase complex [34]. These data provide evidence that ASB proteins may vary to form ubiquitylation complexes and it could be related with substrate specificity, proteins availability and biological functions. Therefore, more studies are necessary to investigate ASB protein interactions required for ubiquitylation complexes formation and to define specific substrates by which ASBs interact with and regulate either by the ubiquitin pathway or by alternative vias. Besides, ankyrin repeats are known to mediate protein interactions, however, no studies provide strong evidence of how the binding between an ASB protein and its substrate occurs and this represents an important question in the field.

ASB proteins are firmly implicated in the regulation of cell proliferation and differentiation. These processes are important to maintain controlled cell growth and prevent aberrant cell accumulation in the tissue which would lead to tumor formation. Consistently, abnormal ASB expression was found in different cancer types. Researchers have begun to understand how defective or overactive protein degradation contributes to tumor development. More investigation is needed to address crucial protein substrates that play a major role in tumorigenesis and are not yet linked to their specific ubiquitin ligases. Targeting ubiquitin proteasome components, such as E3 ubiquitin ligases, is an emerging concept for anticancer therapies [56], thus, a comprehensive understanding of ASB proteins function in the biology of stem and tumor cells will provide valuable knowledge for developing potential stem cell and cancer therapies and provide important information as the control of normal development by this class of proteins.

References

1. Vincent, J.P. and D. Irons. Curr Biol, 2009. 19(22): p. R1028-30.
2. Lawrence, P.A. and G. Struhl. Cell, 1996. 85(7): p. 951-61.
3. Irvine, K.D. and C. Rauskolb. Annu Rev Cell Dev Biol, 2001. 17: p. 189-214.
4. Blair, S.S. Curr Biol, 2003. 13(14): p. R548-51.
5. Kiecker, C. and A. Lumsden. Nat Rev Neurosci, 2005. 6(7): p. 553-64.
6. Wildwater, M., I. The, and S. van den Heuvel. Dev Cell, 2007. 12(6): p. 841-2.
7. Parker, J. Curr Biol, 2006. 16(20): p. 2058-65.
8. Muller-Sieburg, C.E., et al. Blood, 2000. 95(7): p. 2446-8.
9. Muller-Sieburg, C.E. and H.B. Sieburg. Curr Opin Hematol, 2006. 13(4): p. 243-8.
10. Diks, S.H., et al. J Cell Biol, 2006. 174(4): p. 581-92.
11. Hilton, D.J., et al. Proc Natl Acad Sci U S A, 1998. 95(1): p. 114-9.
12. Alexander, W.S. Nat Rev Immunol, 2002. 2(6): p. 410-6.
13. Diks, S.H., et al. Nat Cell Biol, 2008. 10(10): p. 1190-8.
14. Kohroki, J., et al. FEBS Lett, 2005. 579(30): p. 6796-802.
15. Heuze, M.L., et al. J Biol Chem, 2005. 280(7): p. 5468-74.
16. Morris, L.G., S. Veeriah, and T.A. Chan. Oncogene, 2010. 29(24): p. 3453-64.
17. Guardavaccaro, D. and M. Pagano. Oncogene, 2004. 23(11): p. 2037-49.
18. Li, J., A. Mahajan, and M.D. Tsai. Biochemistry, 2006. 45(51): p. 15168-78.
19. Tee, J.M. and M.P. Peppelenbosch. Crit Rev Biochem Mol Biol, 2010. 45(4): p. 318-30.
20. Mosavi, L.K., et al. Protein Sci, 2004. 13(6): p. 1435-48.
21. Kamura, T., et al. Genes Dev, 1998. 12(24): p. 3872-81.
22. Larsen, L. and C. Ropke, *Suppressors.* APMIS, 2002. 110(12): p. 833-44.
23. Kile, B.T. and W.S. Alexander, *The suppressors of cytokine signalling (SOCS).* Cell Mol Life Sci, 2001. 58(11): p. 1627-35.
24. Mahrour, N., et al. J Biol Chem, 2008. 283(12): p. 8005-13.
25. Weissman, A.M. Immunol Today, 1997. 18(4): p. 189-98.
26. Finley, D. and V. Chau. Annu Rev Cell Biol, 1991. 7: p. 25-69.
27. Piessevaux, J., et al. Cytokine Growth Factor Rev, 2008. 19(5-6): p. 371-81.
28. Wilcox, A., et al. J Biol Chem, 2004. 279(37): p. 38881-8.
29. Ardley, H.C. and P.A. Robinson, *E3 ubiquitin ligases.* Essays Biochem, 2005. 41: p. 15-30.
30. Kile, B.T., et al. Mol Cell Biol, 2001. 21(18): p. 6189-97.
31. Kohroki, J., et al. FEBS Lett, 2001. 505(2): p. 223-8.
32. Guibal, F.C., et al. J Biol Chem, 2002. 277(1): p. 218-24.
33. Bello, N.F., et al. Cell Death Differ, 2009. 16(6): p. 921-32.
34. Nie, L., et al. Cell Res, 2010.
35. Chung, A.S., et al. Mol Cell Biol, 2005. 25(11): p. 4716-26.
36. Li, J.Y., et al. Endocrinology, 2010. 151(1): p. 134-42.
37. Li, J.Y., et al.. J Neuroendocrinol, 2005. 17(6): p. 394-404.
38. Li, J.Y., et al. Cell Signal, 2007. 19(6): p. 1185-92.
39. Ferguson, J.E., 3rd, et al. Mol Cell Biol, 2007. 27(18): p. 6407-19.
40. Boengler, K., et al. Biochem Biophys Res Commun, 2003. 302(1): p. 17-22.
41. Zhang, S.X., et al. J Biol Chem, 2005. 280(19): p. 19115-26.
42. Seale, P., et al. Dev Biol, 2004. 275(2): p. 287-300.
43. Hung, K.F., et al. Oral Oncol, 2009. 45(6): p. 543-8.
44. Liu, Y., et al. Biochem Biophys Res Commun, 2003. 300(4): p. 972-9.
45. Liu, Y.Z., et al.. Sheng Wu Hua Xue Yu Sheng Wu Wu Li Xue Bao (Shanghai), 2003. 35(6): p. 548-53.
46. Chiba, T., et al. Mamm Genome, 2007. 18(2): p. 105-12.

47. Kwon, S., et al. BMC Biol, 2010. 8: p. 23.
48. Debrincat, M.A., et al. J Biol Chem, 2007. 282(7): p. 4728-37.
49. Tokuoka, M., et al. Int J Oncol, 2010. 37(5): p. 1105-11.
50. Sartori da Silva, M.A., et al. PLoS One, 2010. 5(11): p. e14023.
51. Blenk, S., et al. Cancer Inform, 2007. 3: p. 399-420.
52. McDaneld, T.G., K. Hannon, and D.E. Moody. Am J Physiol Regul Integr Comp Physiol, 2006. 290(6): p. R1672-82.
53. McDaneld, T.G. and D.M. Spurlock. J Anim Sci, 2008. 86(11): p. 2897-902.
54. Kim, K.S., et al. Zygote, 2004. 12(2): p. 151-6.
55. Guo, J.H., et al. Arch Androl, 2004. 50(3): p. 155-61.
56. Sun, Y. Neoplasia, 2006. 8(8): p. 645-54.
57. Sun, Y. Cancer Biol Ther, 2003. 2(6): p. 623-9.
58. Glickman, M.H. and A. Ciechanover. Physiol Rev, 2002. 82(2): p. 373-428.

CHAPTER 3

d-Asb11 is an essential mediator of canonical Delta-Notch signaling

Sander H. Diks[1*], Maria A. Sartori da Silva[1,2*], Jan-Luuk Hillebrands[1], Robert J. Bink[2], Henri H. Versteeg[1], Carina van Rooijen[2], Anke Brouwers[2], Ajay B. Chitnis[3], Maikel P. Peppelenbosch[1] and Danica Zivkovic[2]

[1]Department of Cell Biology, University Medical Center Groningen, University of Groningen, Groningen, The Netherlands

[2]Hubrecht Institute-KNAW & University Medical Center Utrecht, Utrecht, The Netherlands

[3]Section on Neural Developmental Dynamics, Laboratory of Molecular Genetics, NICHD, NIH, Bethesda, USA

*These authors contributed equally.

Nat Cell Biol.

2008 Oct;10(10):1190-8

Abstract

In canonical Delta-Notch signaling, expression of Delta activates Notch in neighboring cells, leading to downregulation of Delta in these cells[1]. This process of lateral inhibition results in selection of either Delta-signaling cells or Notch-signaling cells. Here we show that d-Asb11 is an important mediator of this lateral inhibition. In zebrafish embryos, morpholino oligonucleotide (MO)-mediated knockdown of *d-asb11* caused repression of specific Delta-Notch elements and their transcriptional targets, whereas these were induced when d-Asb11 was misexpressed. d-Asb11 also activated legitimate Notch reporters cell-non-autonomously *in vitro* and *in vivo* when co-expressed with a Notch reporter. However, it repressed Notch reporters when expressed in Delta-expressing cells. Consistent with these results, d-Asb11 was able to specifically ubiquitylate and degrade DeltaA both *in vitro* and *in vivo*. We conclude that d-Asb11 is a component in the regulation of Delta-Notch signaling, important in fine-tuning the lateral inhibition gradients between DeltaA and Notch through a cell non-autonomous mechanism.

Introduction

The Notch signaling pathway is essential in the spatio-temporal regulation of cell fate[1,2,3]. Expression of transmembrane ligands of the DSL family (Delta, Serrate, Lag-2) initiates Notch signaling in one cell, activating the Notch receptor in neighboring cells[1]. This canonical Notch signal involves proteolytic cleavage of the Notch receptor to generate an intracellular fragment (Notch-ICD) that replaces a nuclear repressor, forming an activating complex. This complex may cause downregulation of DSL-family ligands in the Notch signaling cell and, as a consequence, adjacent cells acquire different cell fates because of differences in Notch signaling activity[4,5]. The precise molecular mechanisms underlying establishment of lateral inhibitory Delta bioactivity gradients, and especially the original bias

in relative DSL ligand activity in neighboring cells, remains only partially understood.

The final outcome of the Delta-Notch communication, with respect to cell fate, is subject to intricate regulation by a multitude of factors[6,7]. Proteins that modulate signaling through post-translational modification, such as ubiquitylation, seem to be important[1,2,8]. The ubiquitin ligases Sel-10, Itch and Suppressor of Deltex negatively regulate Delta-Notch signaling either by ubiquitylation of Notch itself or by influencing post-endocytic sorting[9,10,11]. Conversely, for the ubiquitylation of the DSL ligands, mono-ubiquitylating enzymes that positively regulate Notch signaling have been described[12,13,14,15]. In a recent zebrafish screen, designed to identify genes involved in maintaining proliferation in the progenitor compartment, we identified d-Asb11, a member of the family of SOCS box-containing proteins, and showed that this protein is an essential regulator of the neural progenitor compartment size[16].

Results and Discussion

We first investigated whether common pathways involved in neural precursor fate were affected by knockdown of d-Asb11 (Supplementary Information, Fig.S1) to determine what molecular mechanisms might be involved. Next, we investigated the expression of d-Asb11 protein, relative to expression of Delta-Notch cascade components. Single-cell FACS experiments on dissociated embryos combined with *in situ* hybridization for such signaling elements, and immunohistochemistry for d-Asb11 unequivocally showed co-expression of d-Asb11 and components of the Delta-Notch cascade in the same cells (Supplementary Information, Fig.S2). This suggests that various domains of the developing embryo support interactions between d-Asb11 and Delta-Notch components. Furthermore, whole-mount *in situ* hybridization (WISH) and quantitative RT-PCR (qRT-PCR) of whole embryos showed that MO-mediated knockdown of *d-asb11* resulted in reduced expression of *deltaA*, *notch3* and the Delta-Notch target *her4.1* (Fig.1a-d). However, *deltaA* and *deltaD* showed only marginal

differences between control and morphants (Fig.1b,d). These data suggest that *d-asb11* knockdown causes a reduction in specific Delta-Notch signaling elements in relevant areas of the embryo. To examine whether forced Notch signaling also influences d-Asb11 expression, we injected zebrafish embryos with tagged *deltaA* mRNA and evaluated *d-asb11* mRNA expression. WISH and qRT-PCR showed that *d-asb11* mRNA was induced in the injected half of the embryo (Fig.1e)[17]. Together, these experiments establish a positive-feedback loop between activity of the Delta-Notch pathway and *d-asb11* expression.

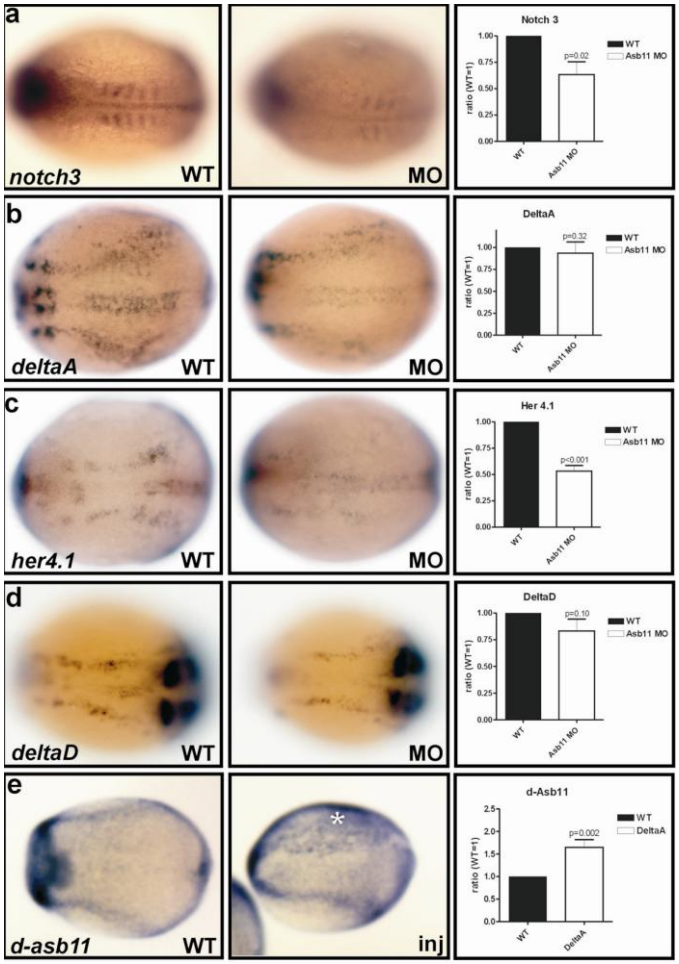

Figure 1: Delta-Notch and d-Asb11 function in a positive-feedback loop.

(a-d) MO-mediated knockdown of *d-asb11* leads to deficient Delta–Notch signaling, as shown by reduced expression of *notch3* (**a**), *deltaA* (**b**) and *her4.1* (**c**). *deltaD* expression remained largely unaffected (**d**). Wild-type embryos (WT, left panels) and morphants (MO) (middle panels) at about 6 somites are shown. qRT-PCR (right panels) was used to quantify the respective expressions. (**e**) Expression of *d-asb11* was upregulated by the DeltaA. Zebrafish embryos were injected with 300 pg *MT-deltaA* mRNA at the two-cell stage in one of the two blastomeres and analysed by *in situ* hybridization and qRT-PCR for *d-asb11*. qRT-PCRs represent average results of two independent experiments performed in triplicate, each consisting of 50 *d-asb11* morphants (**a-d**) or DeltaA-overexpressing wild-type, compared with wild types (**e**). Significance was determined using a one-tailed heteroscedastic t-test (n= 3). Scale bars are 100 μm.

In addition, a Notch-responsive luciferase reporter (HES1) was also activated in the presence of a Myc-tagged *d-asb11* expression construct (MT-d-asb11) but not with control DNA (Myc-tag (MT) only) (Fig.2a)[18,19]. We observed no synergism when Notch-ICD and d-Asb11 were co-expressed (Fig.2c), suggesting that d-Asb11 signals within the Delta-Notch pathway and not in parallel to or independently of it. However, quenching of transcription machinery components by Notch-ICD, or suboptimal molecular performance of the zebrafish proteins in mammalian cells, may also be involved. Importantly, a *d-asb11* construct lacking the carboxy-terminal domain, including the SOCS-box (d-Asb11ΔC), did not transactivate the HES1 reporter. We successfully repeated this experiment with a pluripotent cell line (nTera2-d1) (Fig.2b). To confirm Notch-specificity of this transactivation, we performed experiments using a HES1 reporter lacking proper CSL-binding sites (Hes1-RBP) or using DAPT to inhibit γ-secretase[18] (Supplementary Information, Fig.S3). The lower induction and higher basal level of HES1 activation in nTera2-d1 cells, compared with HeLa, may be attributed to their pluripotent nature. d-Asb11 acts specifically on the Delta-Notch pathway, as judged by its inability to transactivate a panel of other reporters (Fig.2d). These data show that d-Asb11 acts through the canonical Notch pathway.

As SOCS-box proteins downregulate signaling pathways through ubiquitylation, and effects of cellular d-Asb11 enhance Notch activity, d-Asb11 may degrade negative regulators of Notch, such as Nrarp[20,21].

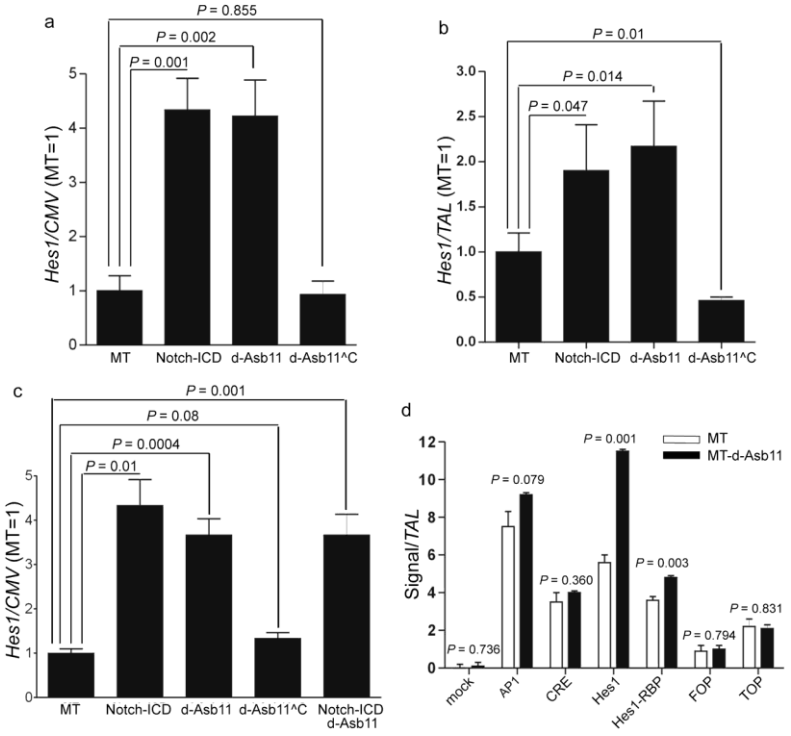

Figure 2: d-Asb11 transactivates specific Notch dependent reporters.
(**a**) Transactivation of the mammalian Notch reporter HES1 by different expression constructs in combination with HES1-luciferase or CMV-luciferase. Myc-tag only (MT) was used as a control and its activity under unstimulated conditions was set to 1. The relative activity was determined by normalizing HES1-luciferase counts over control CMV-luciferase counts. (**b**) The HeLa experiment was repeated in nTera2-d1 cells with HES1 normalized with a TAL reporter. (**c**). When co-transfected in HeLa cells, synergism between Notch-ICD and d-Asb11 on HES1 reporter activity was not observed, demonstrating that both signals act in the same pathway. (**d**) Control or d-Asb11 was transfected in these cells and a reporter was co-transfected simultaneously: AP1 (fos-jun dependent), CRE (CREB dependent), HES1 (Notch-dependent), HES1–RBP (Notch-independent), TOP (β-catenin dependent) and FOP (β-catenin independent). CSL mutant HES1 reporter was used to determine Notch dependent transactivation and TOP-luc or FOP-luc were used to determine β-catenin dependent transactivation. Significance was determined using a one-tailed heteroscedastic t-test (n = 4).

However, Myc-tagged Nrarp (MT-Nrarp) not only co-immunoprecipitated with d-Asb11 but also with the inactive d-Asb11ΔC and d-Asb11ΔSOCS

(Fig.3a). Furthermore, Nrarp knockdown embryos have diminished Wnt responses[22], but this was not observed in d-Asb11 morphants (Supplementary Information, Fig.S1), thus eliminating the possibility that Nrarp is a target of d-Asb11. It is also possible that d-Asb11 enhances Notch activity by regulating the availability of Notch ligands. In a loss-of-function context, proteins such as Neuralized and Mind bomb show a neurogenic phenotype similar to that produced by *d-asb11* knockdown, albeit more pronounced. Hence, we also evaluated whether d-Asb11 could bind the Notch ligand DeltaA[12,13,23]. Indeed, DeltaA was immunoprecipitated by d-Asb11 (Fig.3b). When DeltaA was co-expressed with d-Asb11ΔC or d-Asb11ΔSOCS, no DeltaA could be detected, demonstrating that for interaction with DeltaA, full-length d-Asb11 is required (Fig.3b).

To investigate whether d-Asb11 exerts its effects on the Delta-Notch pathway by targeting DeltaA for ubiquitylation, we injected zebrafish embryos with Myc-tagged *deltaA* (MT-deltaA), HA-tagged *ubiquitin* (HA-ub) and *d-asb11* mRNAs. We precipitated the HA-tagged ubiquitylated proteins from the lysates and verified the presence of Myc-tagged DeltaA in the precipitate. Indeed, ubiquitylated MT-DeltaA was present in the lysates when both MT-DeltaA and d-Asb11 were misexpressed in embryos (Fig.3c; no proteosome inhibitor was present hence no poly-ubiquitylation was detected). However, when Nrarp was misexpressed instead of DeltaA, no ubiquitylation of Nrarp could be detected (Fig.3c). As a control, we investigated the ubiquitylation of Notch-ICD in zebrafish embryos, but none was observed.

These observations suggest that positive regulation of the Notch signal may be mediated through ubiquitylation of DeltaA. To determine whether d-Asb11 degrades DeltaA in the developing embryo, we misexpressed both MT-d-Asb11 and MT-DeltaA and observed degradation of MT-DeltaA on a western blot (Fig.4a). MT-DeltaA protein expression was rescued in the morphants, indicating that endogenous d-Asb11 was capable of degrading MT-DeltaA (note that in Fig.3b, c, d-Asb11 and DeltaA were expressed outside their normal range and thus we were unable to determine the molecular ratio at which d-Asb11 degrades DeltaA *in vivo*). When we

studied the effects of MT-d-Asb11 misexpression on co-expressed HA-tagged DeltaD protein, we found that there was no d-Asb11-dependent degradation of DeltaD. Thus, d-Asb11 is highly specific for DeltaA.

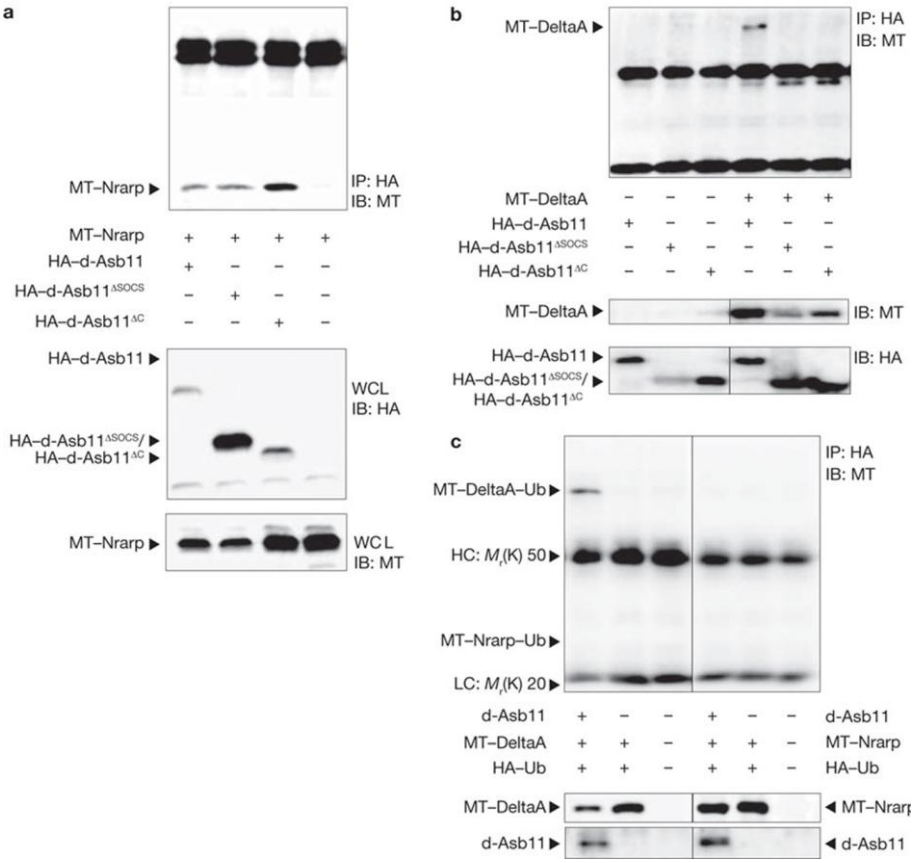

Figure 3: d-Asb11 binds to the Notch regulator Nrarp and the Notch ligand DeltaA.

(**a**) Myc-tagged Nrarp (MT-Nrarp) or DeltaA (MT-DeltaA) was overexpressed in combination with HA-tagged d-Asb11 (HA-d-Asb11), d-Asb11 lacking the complete C-terminal tail (HA-d-ASB11$^{\Delta C}$) or the SOCS-box (HA-d-ASB11$^{\Delta SOCS}$). Nrarp could be precipitated out of the lysates by d-Asb11 in a SOCS-box independent manner. (**b**) DeltaA could only be precipitated out of the lysate when it was overexpressed in combination with full-length d-Asb11. This binding is SOCS-box dependent. (**c**) MT-DeltaA was mono-ubiquitylated when d-Asb11 and MT-DeltaA were both misexpressed in the embryo. Nrarp, however, was not ubiquitylated when it was misexpressed in embryos in combination with d-Asb11.

Moreover, precocious activation of *her4.1::GFP* upon mosaic expression of antimorphic DeltaA was observed (Supplementary Information, Fig.S4a)[24]. To determine whether a feedback loop operates between DeltaA and d-Asb11, we generated morphants for *deltaA*, *deltaD* or both. In *deltaA*, but not *deltaD* morphants, d-Asb11 was markedly downregulated (Fig.4b) and *her4.1* expression reduced (Fig.4c). Misexpression of *MT-d-asb11* mRNA in one-cell stage embryos caused induction of *her4.1* in its endogenous expression domain (Fig.4c, upper right). When MT-d-asb11 was misexpressed in *deltaA* morphants *her4.1* could not be upregulated (Fig.4c, lower right), suggesting that d-Asb11-mediated upregulation of the Notch output signal operates specifically through DeltaA (Fig.4c).

As the Delta-Notch mechanism of lateral signaling requires at least two cells to establish different cell fates, we developed a model (mix-and-match) in which we specifically expressed d-Asb11 in the signal-sending or the signal-receiving cell and monitored activation of the reporter signal in the other cell in molecular terms[25]. When d-Asb11 was transfected in the same cell as the HES1 reporter, the reporter was activated (Fig.5a, left graph). In contrast, when d-Asb11 was overexpressed in cells not containing the HES1 reporter, d-Asb11 abolished HES1 reporter activity (Fig.5a, right graph). Thus d-Asb11 transactivates the HES1 reporter and activates Notch in one cell, thereby repressing Notch activity in the neighboring cell while amplifying Notch activity in the Notch-signaling cell. In these experiments, complete confluence of the cell cultures was a prerequisite for induction of the HES1 promoter. *HA-d-asb11* and *MT-deltaA* DNAs were co-injected into *her4.1::gfp* reporter embryos and mosaic activation of the reporter was assessed at the single-cell level[26]. We did not detect a GFP signal in MT-DeltaA-expressing cells, but there was a strong signal in the HA-d-Asb11-expressing neighboring cell (Fig.5b). We repeated mix-and-match experiments in a cell line stably producing Delta-like 1 (OP9-Dl1) or GFP (OP9-GFP) with the *MT-d-asb11* construct or a control construct, and mixed it with nTera2-d1 cells independently transfected with HES1 reporter[27]. We observed that the OP9-Dl1 cells but not the OP9-GFP cells were able to activate the HES1 reporter (Fig.5c, left panel). When the OP9-Dl1 cells were

transfected with *MT-d-asb11* and added to nTera2-d1 cells transfected with the HES1 reporter, the activity of the reporter was decreased to background levels (Fig.5c, right panel). The data are consistent with a model in which d-Asb11 autonomously activates Notch signaling while non-autonomously inhibiting Notch activity, possibly by ubiquitylation and degradation of DeltaA. By inhibiting γ-secretase with DAPT, we further tested the prediction that d-Asb11 operates through a cell-to-cell interaction. Co-transfection of d-Asb11 and a HES1 reporter in the same cell did not induce activation of the reporter in the presence of DAPT (Fig.5d, left panel), showing that induction of the HES1 reporter requires stimulation with Delta from an adjacent cell. Conversely, when d-Asb11 was transfected in adjacent cells and not in the Notch reporter cells, the reduction of the HES1 reporter was abrogated (Fig.5d, right panel). We verified these findings in embryos by injecting a *her4* reporter DNA construct, co-expressing HA-d-Asb11 and measuring transactivation by quantifying the GFP signal obtained on exposure to DAPT or control. HA-d-Asb11 misexpression significantly induced the reporter. When injected alone, DAPT did not affect GFP expression. However, when applied after co-injection of *her4::gfp* with HA-d-asb11, DAPT caused a significant reduction in GFP expression (Fig.5e). Consistent with the previous data, these results suggest that a feedback loop operates between DeltaA-Notch and d-Asb11, as DAPT treatment also caused downregulation of misexpressed HA-d-Asb11 (Fig.5f). Apparently, d-Asb11 functions through lateral cell-to-cell signaling.

The fundamental role of Notch signaling in the expansion of the neural progenitor compartment suggests that d-Asb11 exerts its regulatory influence on the size of this compartment by affecting Notch signaling, presumably through SOCS-box dependent ubiquitylation of as yet unidentified substrate.

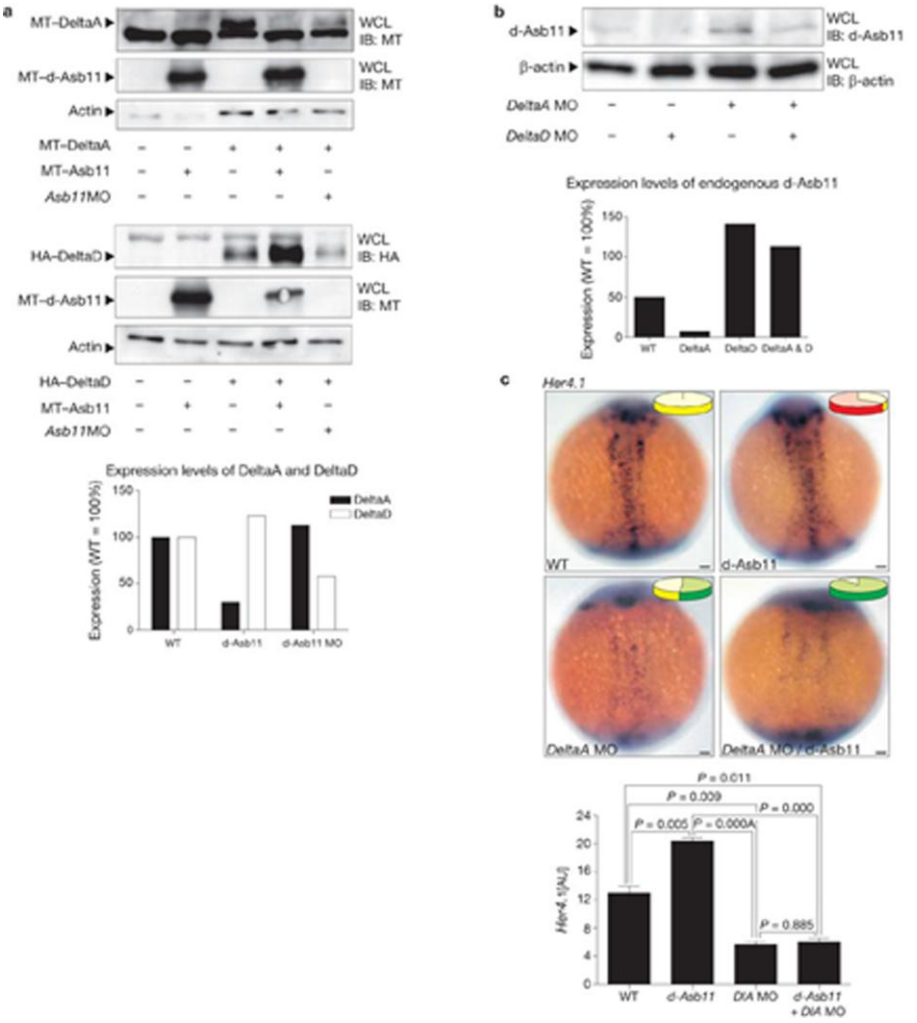

Figure 4: d-Asb11 acts upstream of DeltaA.

(**a**) Misexpression of *d-asb11* combined with misexpression of *MT-deltaA* caused degradation of MT-DeltaA. When MT-DeltaA was misexpressed, knockdown of *d-asb11* rescued this degradation (upper panel). When this was repeated with DeltaD, the opposite effects were observed (middle panel). The lower panel shows quantification of this effect. (**b**) d-Asb11 levels in morphants for DeltaA, for DeltaD or for a combination of both MOs. In DeltaA, but not in DeltaD morphants, d-Asb11 was markedly downregulated. (**c**) Experiments in embryos show that d-Asb11 acts upstream of DeltaA, as d-Asb11 cannot overcome DeltaA knockdown, as assessed by *her4.1* expression (graph). DeltaA was required for d-Asb11 activity. Representative embryos of the different treatments are shown. Pie chart in the upper right corner shows the percentage change in *her4.1* phenotype (yellow,

unchanged; red, increased; green, decreased). Intensity of *her4.1* in at least 6 embryos in each group was quantified and significance was determined using a one-tailed heteroscedastic t-test. Scale bars are 50 µm.

Indication for a role for d-Asb11 in Delta-Notch signaling was supported by co-localization of *d-asb11* and *deltaA* and this notion was confirmed by loss of transcriptional targets of Delta-Notch and their signaling intermediates upon knockdown of d-Asb11, as well as by the induction of these transcriptional targets after misexpression of d-Asb11. The sensitivity of both *in vivo* and *in vitro* assays to the γ-secretase inhibitor DAPT indicates that positive regulation of Notch-dependent transcription by d-Asb11 requires interaction with Delta from adjacent cells. The experiments with DAPT strongly suggest that upregulation of Notch reporter activity by d-Asb11 is cell non-autonomous, which was confirmed by the mix-and-match experiments.

To test the hypothesis that downregulation of DeltaA in the Notch signaling cell may allow upregulation of Delta on the membrane of neighbouring cells, enhancing Notch activity in the first cell (Fig. 2; Supplementary Information, Fig. S4b), we performed experiments analogous to those described in previous studies[12,25]. When d-Asb11 was transfected in the same cell as the HES1 reporter, the reporter in that cell was activated. In contrast, when d-Asb11 was overexpressed in cells not containing the HES1 reporter, the opposite results were obtained (Fig.5). We confirmed these data using a cell line that stably expresses the Notch ligand Dl1. On a molecular level, d-Asb11 acts as a direct binding partner for DeltaA and is capable of ubiquitylating as well as degrading DeltaA but not DeltaD. Our results provide further biochemical evidence that SOCS-box containing proteins can target binding partners for ubiquitylation. The initial event in lateral signaling within an equivalent group of cells entails stochastic determination of the signal-sending Delta-positive cell versus the signal-receiving Notch-positive cell. Several Delta- and Notch-modifying genes involved in fine-tuning the Delta-Notch pathway, such as d-Asb11, have already been described, showing the importance of a finely but tightly regulated communication between Delta-Notch proteins.

The spatio-temporal expression pattern of Delta and Notch products as well as their co-localization at the single cell level suggests that there are opportunities for interaction. Indeed, the mix-and-match experiments suggest that d-Asb11 is an upstream regulator of the Notch pathway and to control cell fate within an equivalent group of cells, it has to act during inductive phases in setting up the patterns of lateral signaling. Consequently, during mid-somitogenesis, when d-Asb11 is still expressed, cells at the prospective mid-hindbrain boundary and in some domains of the neural plate margins express d-Asb11 and show active Notch signaling (equivalent to cells that co-express d-Asb11 and HES1). In contrast, DeltaA is expressed and Notch signaling downregulated in cells of the proneural domain, which abut the margin (equivalent to cell population with only HES1 but without d-Asb11). The finding that expression of *notch3* mRNA is reduced in the morphants suggests that d-Asb11 functions upstream of Delta-Notch to initially amplify the differences between signal-sending and signal-receiving cells, rather than in maintenance of the lateral signaling. Our experiments suggest that the consequence of setting up initial cell differences during lateral signaling seems to be establishment of a feedback loop between the Delta-Notch pathway and d-Asb11. Misexpression of d-Asb11 in embryos transactivates the Notch reporter *her4*, whereas blocking Delta-Notch signaling with DAPT feeds back to downregulate d-Asb11. Accordingly, loss of d-Asb11 function in morphants leads to upregulation of DeltaA protein. In agreement, DeltaA is required for d-Asb11 expression as in DeltaA morphants endogenous d-Asb11 is reduced.

Thus, the present study has shown that d-Asb11 is a positive regulator of Notch signaling, probably acting at the level of DeltaA ubiquitylation and thereby regulating Notch signaling activity in a non cell-autonomous manner. A new speculative co-regulatory mechanism emerges from our results suggesting that DeltaD behaves as a downstream target of the DeltaA-Notch signaling cascade, perhaps through d-Asb11.

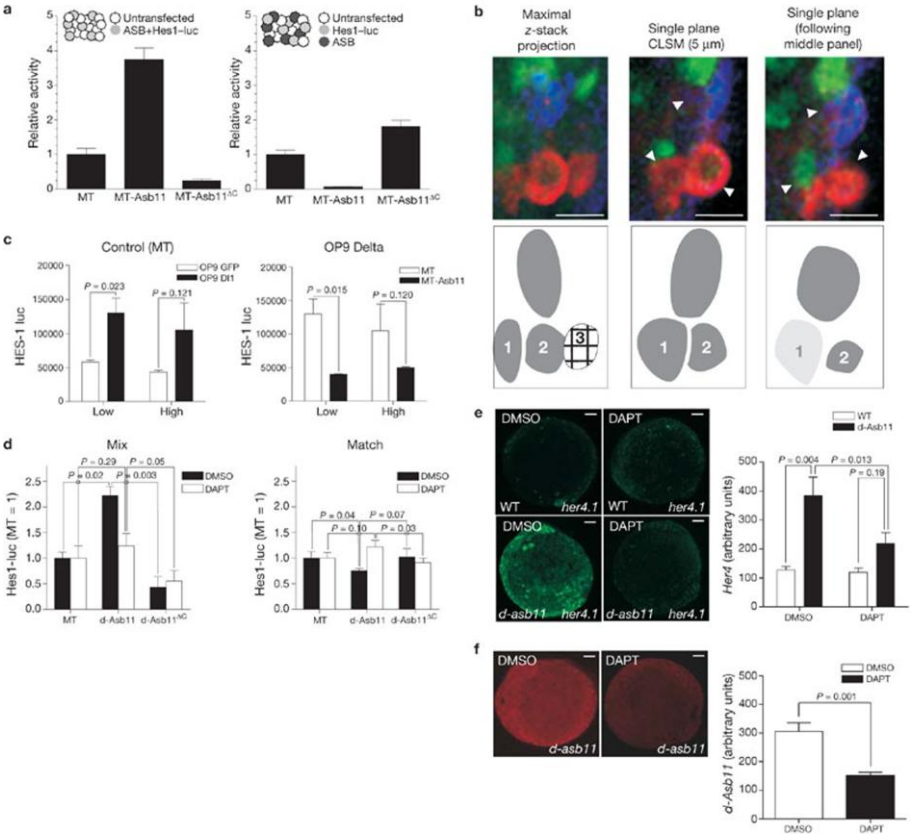

Figure 5: Activation of Notch reporters by d-Asb11 requires other cells.

(**a**) When d-Asb11 was overexpressed in the same cell as the Notch reporter, HES1 activity was elevated (left panel).

However, when d-Asb11 was expressed in cells adjacent to cells transfected with the Notch reporter, d-Asb11 abrogated HES1-dependent Notch activity (right panel). This effect was also dependent on the SOCS-box, as d-Asb11 lacking the C-terminal part of the protein did not have this effect. (**b**) Confocal images showing mosaic expression of co-injected *MT-deltaA* cDNA (MT-tagged protein in red) and *HA-d-asb11* cDNA (HA-tagged protein in blue) in stably transgenic *her4.1::gfp* embryo (green). Notch pathway activation was observed in HA-d-Asb11-expressing cells (overlap green-blue) and absence of Notch activity in the adjacent MT-DeltaA expressing cells (no overlap red-green). Left panel: maximal projection of all the CLSM planes encompassing the embryo showing 3 MT+ cells and 1 HA+ cell (diagram below). To show the signal belonging to individual cells, two consecutive optical sections of 5 µm each are shown where MT+ cells 1 and 2 are depicted in the diagram (middle and right panels). (**c**) Similar effects were observed when the Dl1-overexpressing cell line (OP9-Dl1) was used. When MT-transfected OP9-Dl1

cells were added to HES1 reporter cells, the activity of the HES1 reporter was enhanced, compared with OP9–GFP (left graph). However when d-Asb11 was transfected into OP9-Dl1 cells, HES1 reporter activity was inhibited (right graph). (**d**) Effect of DAPT on mix-and-match experiments. DAPT treatment in the 'mix' resulted in abrogation of HES1 induction in the d-Asb11 overexpressing group but not in the two control groups. In the 'match' experiment, however, the inhibition of HES1 in the d-Asb11-overexpressing group was abrogated by DAPT treatment. (**e**) Effect of DAPT (100 µM for 1.5-11 hpf) on HA-d-Asb11-mediated induction of the *her4.1* reporter in injected embryos. The induction of the *her4.1* reporter was abrogated by DAPT treatment. (**f**) Expression of injected HA-d-Asb11 was also decreased in DAPT treated embryos. Significance was determined using one-tailed heteroscedastic t-tests (n = 3). Scale bars are 20 µm (a–c) and 100 µm (d–f).

Material and Methods

Fish and embryos

Zebrafish were kept at 27.5°C. Embryos were obtained by natural mating, cultured in embryo medium and staged according to methods described previously[28,29]. Heterozygous *her4.1::gfp* (provided by S. Yeo, Kyungpook National University, Korea) transgenic fish embryos were used where indicated[26].

Cell cultures

HeLa and nTera2-d1 cells were maintained in Dulbecco's modified Eagle's medium (DMEM) containing 10% fetal calf serum (FCS). OP9–GFP and OP9–Dl1 cells were maintained in alpha-MEM containing 10% FCS[27]. The culture medium was supplemented with 5 mM glutamine and antibiotics-antimycotics. Cells were incubated at 5% CO^2 in a humidified incubator at 37°C.

Plasmid construction

Plasmids, containing *d-asb11* sequences, were constructed as described previously[16]. A partial cDNA fragment of *d-asb11* in pBluescript was used as a template to generate a riboprobe for *in situ* hybridizations. The pCS2$^+$MT-deltaA construct was provided by B. Appel (Vanderbilt University, Nashville TN), the pCS2$^+$HA-deltaD by M. Itoh (Nagoya University, Japan) and MT-

notch1a ICD by the late J. A. Campos-Ortega (Institut für Entwicklungsbiologie, Köln, Germany). *her4.1::gfp* was provided by S. Yeo. For MT-Nrarp, zebrafish *nrarp* (AI957982) was cloned into the EcoRI and XbaI sites of pCS2^{+}MT.

mRNA synthesis, mRNA and DNA microinjections

Capped mRNAs were synthesized using the mMESSAGE mMACHINE kit (Ambion). For Fig.3, embryos were injected with the following mRNAs: 350pg *d-asb11*, 500pg *HA-ubiquitin*, 600pg *MT-deltaA* and 100pg *MT-nrarp* or a combination. The total volume of the injection was set at 1.5 nL. For Fig.4a embryos were injected with the following mRNAs: 300pg *d-asb11*, 400pg *MT-deltaA*, 400pg *deltaD-HA*. DNAs for dominant-negative Xdelta^{stu} (ref. 24), *delta-MT* or *d-asb11-HA* were injected at 10pg or *her4.1::gfp* at 5pg in a final injection volume of 1 nL.

Morpholino oligonucleotides (MOs)

d-asb11 antisense MOs were used as described previously[16]. MOs against *deltaA* and *deltaD* (approximately 3.25 and 10ng nL^{-1}, respectively) were also injected at the 1-cell stage[30, 31].

DAPT treatment

Embryos were injected with 5pg *her4.1::gfp* DNA or 5pg *her4.1::gfp* + 10pg *d-asb11-HA DNA* (Fig.6b). Half of each group was incubated in 100 µM DAPT in embryo-medium (5mM NaCl, 0.17mM KCl, 0.33mM CaCl2, 0.33mM MgSO4, 0.00005% methylene blue). The other half was incubated in 1% DMSO in embryo-medium. The embryos were incubated from 1.5-11.5 hours post fertilization (hpf), fixed with 4% paraformaldehyde overnight at 4°C and used for immunohistochemistry. Transgenic heterozygous *her4.1::gfp* embryos were treated with DAPT (200 µM) from two-cell stage until fixation at 12 hpf as described above.

In situ hybridization

Whole-mount *in situ* hybridizations were performed according methods described previously[32, 33]. Probes for *deltaA* and *her4.1* were provided by B. Appel (Vanderbilt University, Nashville TN). M. Lardelli (University of Adelaide, Australia) provided the probe for *notch3*. C. Haddon (Imperial Cancer Research Fund, London, United Kingdom) provided *deltaD*.

Whole-mount immunolabelling

Whole-mount immunohistochemistry was performed as described earlier[16]. The primary antibodies were diluted in PBS containing 1% BSA (anti-MT (9E10), 1:500, Santa Cruz Biotechnology; anti-GFP, 1:4000, provided by E. Cuppen, Hubrecht Institute; anti-HA (12CA5), 1:200, Abcam; anti-d-Asb11 antibody, 1:250)[16].

Preparation of zebrafish embryos for immunoblotting and immunoprecipitation

At 7 hfp, the chorion was removed and the yolk was separated from the embryos in calcium-free medium[29], and 50-60 embryos were lysed and ground in 100µl cell lysis buffer (50mM HEPES pH 7.5, 150mM NaCl, 1.5mM MgCl2, 1mM EGTA, 10% glycerol, 1% Triton X-100).

Immunoprecipitation

Zebrafish lysate immunoprecipitation was performed using a 1:100 dilution of the anti-HA (12A5) or anti-MT (9E10 or Cell Signalling 2272) antibody and the lysates were incubated overnight at 4°C. The next, day protein-A-sepharose (Sigma) beads were added and lysates were incubated for 3 hours at 4°C. After 3h, the beads were washed twice in lysis buffer, taken up in Laemmli sample buffer and analysed by western blotting. For the determination of DeltaA binding to d-Asb11, HeLa cells were transfected using Effectene (Qiagen) with the mentioned plasmids. After 24h the cells were lysed (Cell Signalling Technologies 9803) and immunoprecipitated overnight at 4°C. After washing, the immunoprecipitates were taken up in Laemmli sample buffer and analysed by western blotting.

Luciferase reporter assay

HeLa cells were seeded in a 24-well plate at a density of 25%. The next day, cells were transfected with the expression construct (0.1µg) and the reporters (0.1 µg HES1-luc and 0.01 µg pRL) using Effectene (Qiagen) with the standard protocol. After 24h the cells were lysed in passive cell lysis buffer (dual-luciferase reporter assay). The amount of luciferase was measured using a dual-luciferase reporter assay (Promega). The values were normalized with the Renilla luciferase and the averages were from triplicate data points from three different experiments.

NTera2-d1 cells were seeded in a 96-well plate and transfected using IBAfect and MA-enhancer (IBA Biosciences, GmbH) using the suppliers protocol. Luciferase was measured on a Packard TOPCOUNT Microplate Scintillation Counter (Packard). The experiments were performed at least twice, in quadruplicate. Values were normalized with TAL-luc (nTera2-d1).

Mix-and-Match luciferase reporter assay

HeLa cells were seeded in a 24-well plate. The cells were transfected in triplicate using Effectene (Qiagen) at a density of 50%. After 12h, the fourth well was washed with PBS and cells were removed from the bottom using only EDTA. These cells were then added to triplicate transfected cells containing the HES1 or the CMV reporter (Supplemental Information, Fig. S4b). After 24h, the cells were lysed in Triton lysis buffer (1% Triton X-100, 25mM glycylglycine, 15mM MgSO4, 4mM EGTA, 1mM dithiothreitol, pH 7.8) and measured as described earlier. The values are means of triplicate data points from two different experiments. nTera2-d1, OP9–GFP and OP9–Dl1 cells were seeded in 6-well plates and transfected using IBAfect and MA-enhancer (IBA Biosciences, GmbH) using the suppliers protocol. The next day, the cell populations were collected, counted and reseeded at a density of 30k cells per well in a 96-well plate. The next day, OP9 cell populations were collected, counted and added to the nTera2-d1 cells at different densities. After 72h, the cells were washed and luciferase was measured as described in the previous section. The values are means of quadruplicate data points from two different experiments.

Microscopy and image quantification

Pictures were obtained using a Carl Zeiss Axioplan with a 10x 0.30 plan neofluar. Images were digitized with a Leica DFC480 camera and processed with Leica IM500 Image Manager. Pictures of sections were made using a Nikon Eclipse E 600 microscope, with a 10x 0.33, 20x 0.50 or a 40x 0.75 objective and a Nikon DXM1200 camera. Software used for these pictures was Nikon ACT-1 version 2.63.

For analysis of fluorescent stainings, Leica Confocal TCS SPE was used. To quantify the intensity of d-Asb11-HA signal and/or Her4.1::GFP, a z-stack (z of 7µM) were made, scanning the whole embryo. Leica software (Application Suite 1.8.0) was used to create a maximum projection of the z-stack. Quantification was performed as described earlier[16].

RNA isolation and qRT–PCR

Embryos were injected with 5ng d-asb11-MO-2. At 11.5 hpf, the chorion was removed and 50 embryos were collected. Total RNA extraction and purification was performed by using standard Trizol and isopropanol precipitation. cDNA synthesis was performed using hexamer primers and M-MLV Reverse Transcriptase. Transcript levels of *notch3*, *deltaA*, *her4.1*, *deltaD* and *actin* were quantified by real-time PCR using ABsolute QPCR SYBR Green Fluorescein Mix (Westburg) on an iCycler iQ Real-Time PCR detection system (Bio-Rad). Results are expressed as a relative ratio to the housekeeping gene *actin*, according to a mathematical method described previously[34]. Primer sequences are listed in Supplemental Table S1.

Statistical testing

All statistical tests were performed using heteroscedastic one-tailed t-tests. Mean ± s.e.m. are shown.

Acknowledgements

We wish to thank J. A. Campos-Ortega for providing the *MT-notch1aICD* construct, B. Appel for the *MT-deltaA* construct and A. Israel for the different *HES1-luciferase* reporter constructs. We thank R. Dorsky, C.

Houart, P. Ingham, J.P. Concordet for the riboprobes. We thank J. Lewis for DeltaD antibody, G. Strous for *HA-Ubiquitin*, U. Strähle for XDelta^{stu}. We are indebted to R. Dorsky and R. Moon for providing TOPdGFP fish. We thank Y.J. Jiang for advice. We also wish to thank K. Österreicher and D. Kolmer (TissueGnostics, GmbH) for their help in the quantification of the co-localization studies described in Supplementary Information, Fig.S2. NWO Casimir, NWO Genomics, NWO ALW, TIPharma and the IAG program of the province of Groningen and the European Commission are thanked for financial support. We are especially grateful to S. van de Water, S. van den Brink, A. Visser and L. Glazenburg for technical assistance and to the animal facility of the Hubrecht Institute for care of zebrafish.

References

1. Louvi, A. & Artavanis-Tsakonas, S. Nature Rev. Neurosci. 7, 93–102 (2006).
2. Lai, E. C. Development 131, 965–973 (2004).
3. Mumm, J. S. & Kopan, R. Dev. Biol. 228, 151–165 (2000).
4. Crowe, R., Henrique, D., Ish-Horowicz, D., & Niswander, L. Development 125, 767–775 (1998).
5. Kopan, R. & Turner, D. L. Curr. Opin. Neurobiol. 6, 594–601 (1996).
6. Le Borgne, R. Curr. Opin. Cell Biol. 18, 213–222 (2006).
7. Chitnis, A. Dev. Dyn. 235, 886–894 (2006).
8. Baron, M. et al. Mol. Membr. Biol. 19, 27–38 (2002).
9.Wilkin, M. B. et al. Curr. Biol. 14, 2237–2244 (2004).
10. Gupta-Rossi, N. et al. J. Cell Biol. 166, 73–83 (2004).
11. Wu, G. et al. Mol. Cell Biol. 21, 7403–7415 (2001).
12. Itoh, M. et al. Dev. Cell 4, 67–82 (2003).
13. Lai, E. C., Deblandre, G. A., Kintner, C., & Rubin, G. M. Dev. Cell 1, 783–794 (2001).
14. Pitsouli, C. & Delidakis, C. Development 132, 4041–4050 (2005).
15. Wang, W. & Struhl, G. Development 132, 2883–2894 (2005).
16. Diks, S. H. et al. J. Cell Biol. 174, 581–592 (2006).
17. Appel, B. & Eisen, J. S. Development 125, 371–380 (1998).
18. Jarriault, S. et al. Signalling downstream of activated mammalian Notch. Nature 377, 355–358 (1995).
19. Nishimura, M. et al. Genomics 49, 69–75 (1998).
20. Krebs, L. T., Deftos, M. L., Bevan, M. J., & Gridley, T. Dev. Biol. 238, 110–119 (2001).
21. Lamar, E. et al. Genes Dev. 15, 1885–1899 (2001).
22. Ishitani, T., Matsumoto, K., Chitnis, A. B., & Itoh, M. Nature Cell Biol. 7, 1106–1112 (2005).
23. Deblandre, G. A., Lai, E. C., & Kintner, C. Dev. Cell 1, 795–806 (2001).
24. Chitnis, A., Henrique, D., Lewis, J., Ishhorowicz, D., & Kintner, C. Nature 375, 761–766 (1995).
25. Bijlsma, M. F. et al. PLoS. Biol. 4, e232 (2006).

26. Yeo, S. Y., Kim, M., Kim, H. S., Huh, T. L., & Chitnis, A. B. Dev. Biol. 301, 555–567 (2007).
27. Schmitt, T. M. & Zuniga-Pflucker, J. C. Immunity. 17, 749–756 (2002).
28. Kimmel, C. B., Ballard, W. W., Kimmel, S. R., Ullmann, B., & Schilling, T. F. Dev. Dynam. 203, 253–310 (1995).
29. Westerfield, M. The Zebrafish Book (Eugene: University of Oregon Press, 1994).
30. Holley, S. A., Julich, D., Rauch, G. J., Geisler, R., & Nusslein-Volhard, C. Development 129, 1175–1183 (2002).
31. Latimer, A. J., Dong, X. H., Markov, Y., & Appel, B. Development 129, 2555–2563 (2002).
32. Joore, J. et al. Mech. Dev. 46, 137–150 (1994).
33. Cunliffe, V. T. & Casaccia-Bonnefil, P. Mech. Dev. 123, 24–30 (2006).
34. Pfaffl, M. W. Nucleic Acids Res. 29, e45 (2001).

Supplementary Information

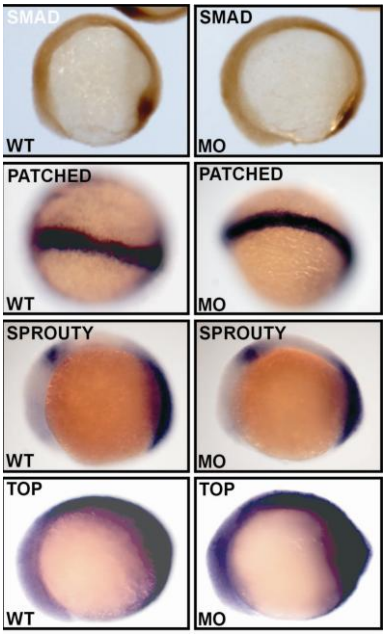

Figure S1
Morpholino-mediated knock-down of *d-asb11* does not affect pathways involved in neural precursor fate such as Bmp (SMAD), hedgehog (PATCHED), Fgf8 (SPROUTY) or Wnt (TOP). Scale bar: 100µm.

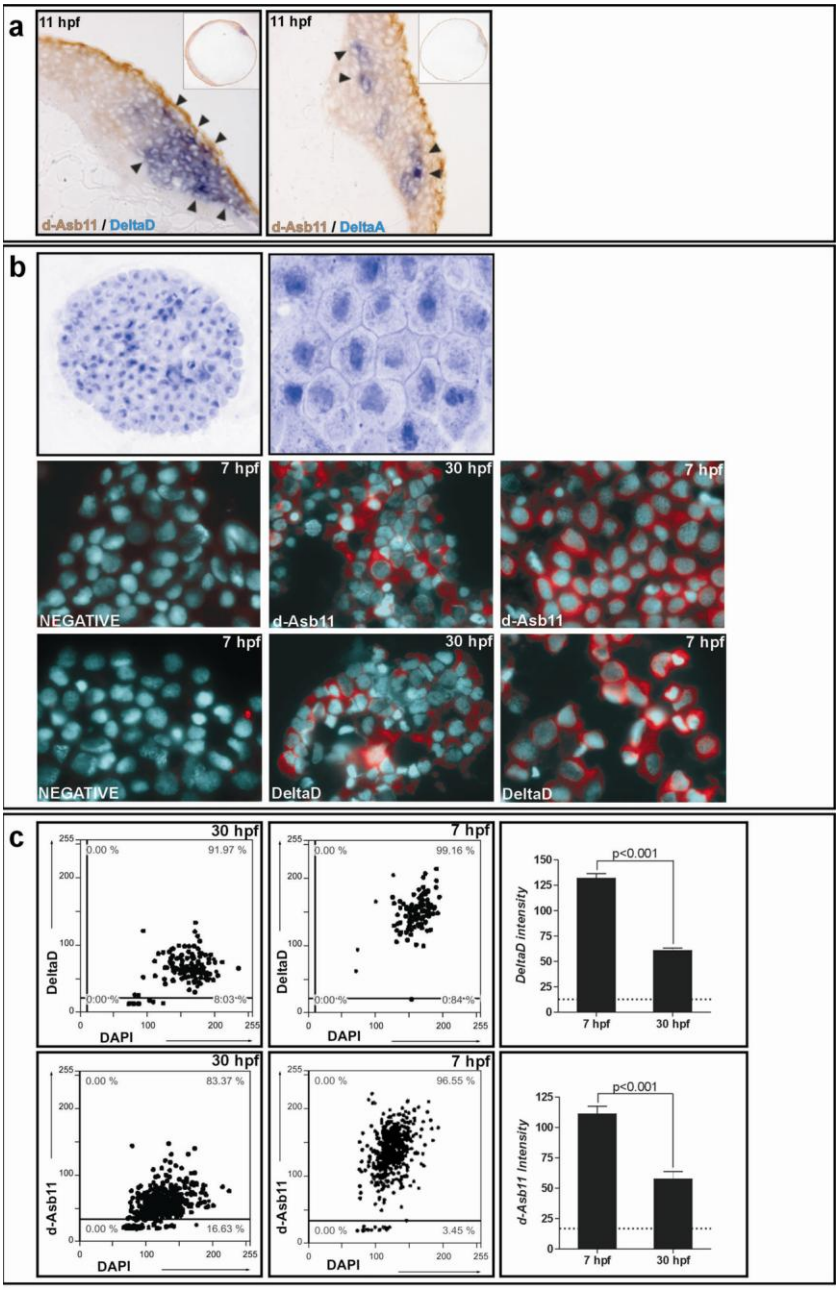

Figure S2 Co-localization of d-Asb11 and Delta-Notch signaling elements.
To ascertain that d-Asb11 is in the position to alter Delta-Notch signaling, we checked whether d-Asb11 is co-expressed in cells that are Delta-positive. (**a**) The

upper two panels show an antibody staining of d-Asb11 combined with an *in situ* staining of *deltaA* or *deltaD*. Sections of 11hpf double-whole mount stained embryos were used. Large co-localization domains of *d-asb11* with *deltaD* (left panel) and minor co-localization with *deltaA* (right panel) are observed. (**b**) Single cell isolates of 7 and 30hpf embryos were prepared and a nuclear counterstain with hematoxilin was performed to verify morphology of the single cell suspensions (upper panels). Next, these cells were fluorescently stained for DAPI and d-Asb11 or DeltaD. Cells from older embryos were used as a negative d-Asb11 control as these embryos contain only low amounts of d-Asb11 (Diks et al, JCB 2006). Clearly a high percentage is positively stained in 7hpf cells compared to the 30hpf cells. (**c**) Quantification of the staining of d-Asb11 and DeltaD generated by TissueFAXS system (TissueGnostics GmbH Vienna), shows a high level of positive staining with both antibodies. Dot plots also reveal distinct populations of high and low expressing cells. Quantification of more than 1500 individual cells from d-Asb11 and DeltaD stainings show a clear decrease in staining levels in older embryos ($p<0.001$). Moreover the percentage of overlap between the high and low populations is well below 50%, meaning that double positive cells (d-Asb11 and DeltaD) are present. Scale bar: 20µm, (b) blow up 5µm.

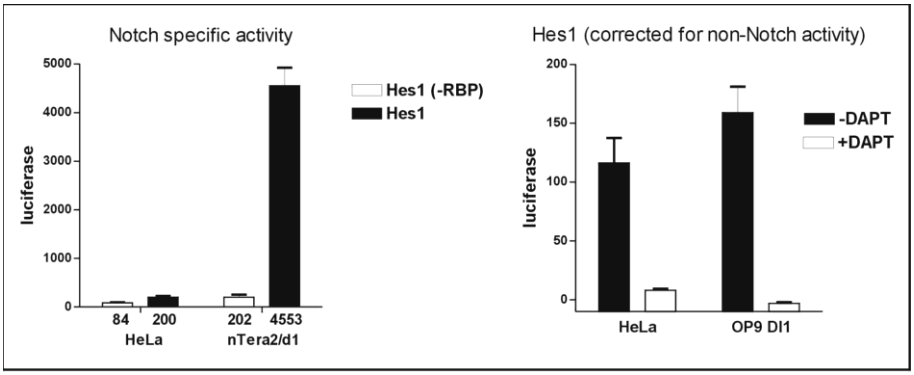

Figure S3 Notch-specific activity in HeLa and nTera2/d1 cells.
Cells transfected with HES1-reporter and HES1-reporter lacking the RBP binding domains were used to determine the presence of Notch-specific HES1 activity. The left panel shows a clear Notch (RBP)-specific activity in HeLa and nTera2/d1 cells. However, the amount of this activity is much larger in nTera2 cells. The right panel shows that this Notch specific activity can be inhibited with DAPT.

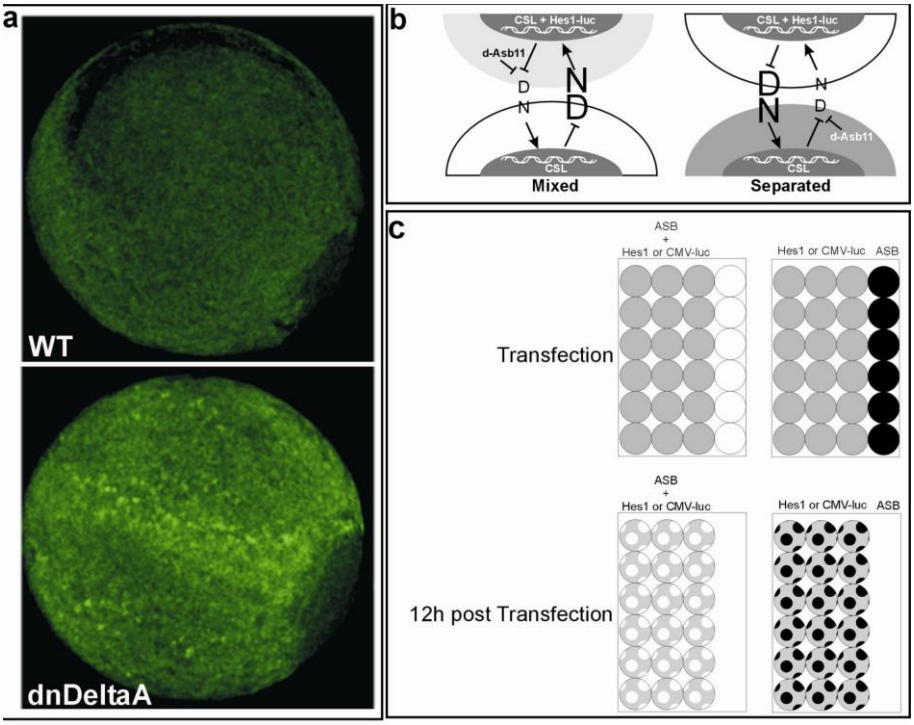

Figure S4

(**a**) Zygotes were injected with 10pg XDelta1^{stu} (dnXDelta) DNA into *her4.1::gfp* stably transgenic zygotes. Mosaic expression of delta inhibition by dnDelta induces precocious activation of Notch signaling as shown by GFP^{+} cells that are observed already at 70-80% epiboly while Notch activation is at that time not activated in the uninjected transgenic embryos. (**b**) Schematic representation of the molecular mechanism by which d-Asb11 could influence Delta-Notch signaling. When d-Asb11 is active, it ubiquitylates DeltaA thereby inhibiting the activation of Notch in the neighboring cells. The repression of DeltaA is released in the neighboring cell, increasing Delta levels on its membrane resulting in increased Notch activity in the cell with active d-Asb11. Thus, when a Notch reporter is expressed in the same cell as d-Asb11, it will show an elevated Notch activity (left panel), but when the reporter is expressed in an adjacent cell, Notch activity will be diminished (right panel). (**c**) Graphic representation of the experiments performed in figure 5A and 6A. Cells were transfected with the Notch reporter in combination with d-Asb11 or a control plasmid containing only a myc-tag and a batch of cells are transfected separately with d-Asb11 or control plasmid. After 12 hours, the cells transfected with only d-Asb11 or control plasmid are removed using only EDTA (not trypsin

since it cleaves all membrane-bound proteins) and added to the cells containing the Notch reporter. Activity is measured after 24 hours. Scale bar: 100µm.

Materials and methods

Figure S1

Whole mount *in situ* hybridizations were performed according to Joore[1], or according to Cunliffe and Casaccia-Bonnefil[2].TopdGFP was provided by R. Dorsky (University of Utah, Salt Lake City UT, USA), *sprouty4* was provided by C. Houart (MRC Centre for Developmental Neurobiology, London, UK). P Ingham (Ingham Singapore lab, Singapore, Singapore) provided *patched1*. Immunohistochemistry using SMAD 1,5,8-antibody was started by dehydration of fixed embryos, incubation in 100% MeOH overnight at -20°C. After rehydration and several washes in PBS+0.1% Tween-20, the embryos were digested with proteinase K (10µg/ml) for 1 minute at room temperature (RT). Several washes were performed and embryos were incubated in block solution (PBS+10% Goat serum + 1% DMSO+10% Tween-20). First antibody incubation (anti-phosphosmad 1/5/8, #9511 Cell Signaling Technology) 1:200 was done overnight at 4°C in block solution. After several washes with PBS+0.1% Tween-20 and incubation in block solution for at least 1hr, incubation in pre-incubated secondary antibody was done overnight, 4°C (goat anti-rabbit biotin labelled, 1:200 in block solution). After several washes, incubation in ABComplex and DAB-staining were performed as described.

Figure S2

Whole-mount immuno and *in situ* staining

Detection of d-Asb11 protein after *in situ* hybridization with *deltaA* or *deltaD* riboprobes, according to Diks et al.[4], was done by immunohistochemistry using polyclonal rabbit anti-d-Asb11 serum containing polyclonal antibody directed against d-Asb11[4]. After staining of the *in situ* hybridization, the embryos were fixed with 4% PFA for 30 minutes. Embryos were digested with proteinase K (10 µg/ml) for 1 minute at RT and washed 5x 5min with PBS+0.1% Tween-20. Embryos were

incubated in block solution (PBS+10% goat serum + 1% DMSO +10% Tween-20). First antibody incubation (d-Asb11 1:250) in block solution was done overnight, at 4°C. After extensive washing and incubation in block solution for 1hr, the embryos were incubated in pre-incubated secondary antibody, (swine-anti-rabbit-biotin), 1:200 in block solution, overnight at 4°C. Embryos were washed, 4x30 min in PBS+0.1% Tween-20 and incubated in ABComplex (Dakocytomation) for 45 min. After several washes, embryos were incubated in DAB-solution+0.0006% H_2O_2. Staining was stopped by rinsing several times with PBS+0.1% Tween-20 and fixing 30 min with 4% PFA. Embryos were washed again, dehydrated, embedded in plastic and sectioned.

Single cell suspension

Single cells suspensions were made from 7 and 30 hours old embryos according to the following protocol (adapted from Covassin et al.)[5]. In short, embryos were treated with pronase to remove the chorion. The embryos were then moved to +chorion solution to separate the chorion from the embryos (using a glass pipet). The embryos were then tranferred to deyolking buffer (PBS+ 5mM KCl and 10mM D-glucose) until the yolk was dissolved (through resuspension). Subsequently the suspension was treated with trypsin and EDTA (0.25% trypsin and 3mM EDTA) at 28°C to obtain single cell suspensions. After about 20 minutes or when the clumps were dissolved $CaCl_2$ and serum were added (final concentration 3mM and 10%, respectively). Cells were spun down (3', 1500rpm) and washed in deyolking buffer. Subsequently the suspension was filtered with a 40µm filter and fixed o/n in 4% PFA or cytospots (Shandon Cytospin4, Thermo Electran Corporation) were made from aliquots of 50000 cells/cytospot. Cytospots were air dried for 30 minutes.

Staining (Histofine) and FAXS quantification

Slides were air dried for 30 minutes and fixed for 2hr (fix & perm, eBiosciences). Subsequently the slides were washed (PBS+0.1% Tween20) and permeabilised with permeabilisation buffer (eBiosciences) for 30

minutes after which endogenous peroxidase was blocked with PBS+0.03% H_2O_2 and 1% BSA. Next the slides were washed and primary antibody (d-Asb11 8160, 1:25, DeltaD 1:25 diluted) in permeabilisation buffer solution was added. After 1 hr incubation at RT, the slides were washed 3x and the proper secondary antibody containing horseradish peroxidase was added (Histofine). After 1 hr the slides were washed again 3x and a TSA amplification kit (Cy3, Invitrogen) was used according to the supplier's protocol to boost the low fluorescent intensity. To visualize the nuclei, 10 minute incubation with DAPI was added with the proper washing steps. Finally, the slides were sealed with AF1 citifluor (Citifluor). Images were produced on a Leica fluorescent microscope (Leica Microsystems). The images shown were taken with the same magnification and exposure. The quantification data is generated using a TissueFAXS system and the analysis was performed with the TissueQuest Software (TissueGnostics GmbH Vienna).

Figure S3

Luciferase experiments were performed as described in the Material and Methods section in the article.

Figure S4

DNAs for dominant negative Xdelta^{stu} were injected at 10pg in a final injection volume of 1nL^{3}.

The luciferase experiments were performed as described in the Material and Methods section in the article.

Table S1: Primers sequences used for qRT-PCR.

Hairy related 4.1

Forward: TGGATCAATCAGCAGCAGAG

Reverse: TGAGCCAGAAGAGTCTTGAGC

Notch 3

Forward: GCAACCAAGACATGGATGAA

Reverse: GCATGGACAGACACTCGT

DeltaA

Forward: GGCTCTTCTGCAACCAAGAT

Reverse: ACAGCTGGCTCCTGAGAATC

DeltaD

Forward: AGGGAAGCTACACCTGCTCA

Reverse: GAAACCAGGAGGACAAGTGC

Actin

Forward: CGTCTGGATCTAGCTGGTCGTGA

Reverse: CAATTTCTCTTTCGGCTGTGGTG

References

1. Joore,J. et al. Mechanisms of Development 46, 137-150 (1994).
2. Cunliffe,V.T. & Casaccia-Bonnefil,P. Mech. Dev.123, 24-30 (2006).
3. Chitnis,A., Henrique,D., Lewis,J., Ishhorowicz,D., & Kintner,C. Nature 375, 761-766 (1995).
4. Diks,S.H. et al. J. Cell Biol. 174, 581-592 (2006).
5. Covassin,L. et al. Dev. Biol. 299, 551-562 (2006).

CHAPTER 4

Essential role for the d-Asb11 *cul5* Box Domain for Proper Notch Signaling and Neural Cell Fate Decisions *in vivo*

Maria A. Sartori da Silva[1,3], Jin-Ming Tee[1], Judith Paridaen[1], Anke Brouwers[1], Sander H. Diks[2], Vincent Runtuwene[1], Danica Zivkovic[1], Sander H. Diks[2], Daniele Guardavaccaro[1] and Maikel P. Peppelenbosch[3]

[1]Hubrecht Institute-KNAW & University Medical Center Utrecht, Utrecht, The Netherlands.

[2]Departement of Cell Biology, University Medical Center Groningen, University of Groningen, Groningen, The Netherlands

[3]Department of Gastroenterology and Hepatology, Erasmus MC-University Medical Center Rotterdam, Rotterdam, The Netherlands.

PLoS One

2010 Nov 19;5(11):e14023

Abstract

ECS (Elongin BC-Cul2/Cul5-SOCS-box protein) ubiquitin ligases recruit substrates to E2 ubiquitin-conjugating enzymes through a SOCS-box protein substrate receptor, an Elongin BC adaptor and a cullin (Cul2 or Cul5) scaffold which interacts with the RING protein. *In vitro* studies have shown that the conserved amino acid sequence of the cullin box in SOCS-box proteins is required for complex formation and function. However, the *in vivo* importance of cullin boxes has not been addressed. To explore the biological functions of the cullin box domain of ankyrin repeat and SOCS-box containing protein 11 (d-Asb11), a key mediator of canonical Delta-Notch signaling, we isolated a zebrafish mutant lacking the Cul5 box (Asb11^{Cul}). We found that homozygous zebrafish mutants for this allele were defective in Notch signaling as indicated by the impaired expression of Notch target genes. Importantly, asb11^{Cul} fish were not capable to degrade the Notch ligand DeltaA during embryogenesis, a process essential for the initiation of Notch signaling during neurogenesis. Accordingly, proper cell fate specification within the neurogenic regions of the zebrafish embryo was impaired. In addition, *asb11^{Cul}* mRNA was defective in the ability to transactivate a *her4::gfp* reporter DNA when injected in embryos. Thus, our study reporting the generation and the characterization of a metazoan organism mutant in the conserved cullin binding domain of the SOCS-box demonstrates a hitherto unrecognized importance of the SOCS-box domain for the function of this class of cullin-RING ubiquitin ligases and establishes that the d-Asb11 cullin box is required for both canonical Notch signaling and proper neurogenesis.

Introduction

The ubiquitin-proteasome system plays a fundamental role in the control of numerous cellular processes, including cell cycle progression, gene transcription, signal transduction, proliferation and differentiation [1]. In this system, ubiquitin is first activated by an E1 ubiquitin-activating enzyme. Activated ubiquitin is then transferred to the active-site cysteine of an E2

ubiquitin-conjugating enzyme. Subsequently, an E3 ubiquitin ligase mediates the transfer of ubiquitin from E2 to a lysine residue on the protein substrate. Multiple rounds of these reactions lead to the formation of polyubiquitylated substrates that are targeted to the 26S proteasome [2]. There are two major classes of E3 ubiquitin ligases, proteins with a HECT (homologous to E6-AP carboxyl terminus) domain and proteins with a RING (Really Interesting New Gene)–like motif. Within this class, cullin-RING E3s are multisubunit ubiquitin ligases composed of a scaffold protein known as cullin, a RING finger protein, which mediates the interaction with the E2, a variable substrate-recognition subunit and an adaptor that links the cullin-RING complex to the substrate recognition subunit [3]. Among the cullin-RING E3s, the group collectively denominated as ECS (Elongin BC-Cul2/Cul5-SOCS-box protein) ubiquitin ligases has recently attracted special attention [4]. This group of E3 ligases has been implicated in transduction of extracellular cues to altered gene transcription. Many details of its modus operandi remain, however, obscure. Specifically, there is remarkably little insight into the *in vivo* relevance of the different components of ECS ubiquitin ligases. *In vitro* studies have shown that in ECS ubiquitin ligases the SOCS-box protein works as the substrate recognition subunit. SOCS-box proteins are composed of two distinct protein-protein interaction domains, a substrate binding domain and a SOCS-box domain. The SOCS-box motif is found at the C-terminus of over 70 human proteins in nine different families. *In vitro* studies show that SOCS boxes act as substrate recognition modules of the ECS type E3 ubiquitin ligase complex (Fig. 1A) [2]. The SOCS-box domain is divided into two sub-domains: the BC box, which links SOCS-box proteins to the cullin-Rbx module and a motif termed cullin box, located immediately downstream of the BC box. The cullin box is proposed to determine whether a given SOCS-box protein assembles into either a Cul2-Rbx1 or a Cul5-Rbx2 module to recruit and activate the E2 ubiquitin-conjugating enzymes for substrates ubiquitylation [5]–[8]. *In vivo* evidence that the cullin box is involved in mediating the biological action of any SOCS-box protein has not been provided hitherto.

Ankyrin repeat and SOCS-box containing proteins (ASB) constitute the largest subclass of the SOCS-box protein family. ASB members (ASB1-ASB18) are structurally characterized by a variable number of N-terminal ankyrin repeats, which mediate the association with the substrate [9]. ASB proteins in general participate in various important biological processes [10]–[17], but like the superfamily of SOCS-box proteins *in toto*, their role *in vivo* remains largely unknown. We have recently showed that *Danio rerio* Asb11 (d-Asb11) regulates compartment size in the endodermal and neuronal lineages [10] via ubiquitylation of DeltaA, leading to the activation of the canonical Notch pathway [11]. Thus, d-Asb11 is an attractive protein to assess the elusive functions of the cullin box motif in the SOCS-box holodomain. All ASB proteins share, with slight divergences, the consensus sequences of BC box and Cul5 box in their C-terminal (Fig. 1B)[5], [6], [8]. Thus elucidation of the *in vivo* mode of action of d-Asb11 should also provide important clues for this family in its entirety. Together, these considerations prompted us to explore the function of Asb11 cullin box *in vivo*.

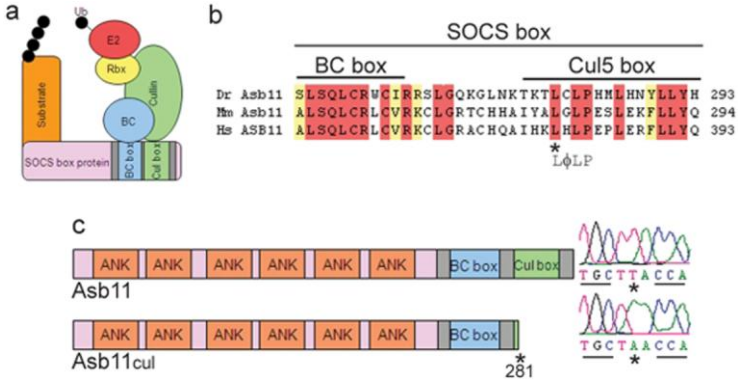

Figure 1. Schematic representation of Asb11 proteins.
(**a**), Asb11 functions as a substrate recognition module in a putative Elongin BC-Cullin-SOCS-box (ECS) type E3 ubiquitin ligase complex. (**b**), Sequence alignment of conserved Asb11 SOCS-box domain in different species. The cul5-box consensus sequence is indicated below the alignment. Identical amino acids are highlighted in red and similar ones in yellow. Dr: *Danio rerio*; Mm: *Mus musculus*; Hs: *Homo sapiens*. (**c**), (left) Illustration of the wild type and mutant *d-asb11* gene products. Mutated protein is represented as Asb11^{cul} showing the predicted residual

fragment and the position of the identified mutation. The different domains are indicated. (right) The T→A mutation changes a leucine into a stop codon.

Here, we describe the isolation of a zebrafish carrying a mutant allele in the conserved LPϕP sequence of the d-Asb11 cullin box. This mutant represents the first metazoan harboring a mutated cullin box. Asb11^{Cul} fish are defective in Notch signaling and have severely affected cell fate specification within the neurogenic regions of zebrafish embryos. Thus, our results establish a previously unrecognised *in vivo* importance of the cullin box for SOCS-box proteins in general and for Asb11 SOCS-box protein function in particular.

Results and Discussion

Generation and characterization of d-asb11 mutants

The consensus sequence ϕXXLPϕPXXϕXX(Y/F) corresponds to the Cul5-box in the C-terminal portion of the canonical SOCS-box proteins, and is highly conserved in vertebrates [5], [9] (Fig. 1B). We performed a TILLING screen on an F1 N-ethyl-N-nitrosurea (ENU)-mutagenized zebrafish library for *d-asb11* mutations mapping to the putative consensus sequence [18]. A premature stop codon corresponding to amino acid 281 in the conserved LPϕP sequence of the d-Asb11 was identified (Fig. 1C), and the homozygous allele was designated asb11^{cul}. To our knowledge, this is the first report of a metazoan mutant presenting a mutation in the consensus sequence of any SOCS-box protein, allowing for the first assessment of the *in vivo* function of the cullin box.

Morphological analysis of asb11^{cul} revealed a slight hyperpericardium at 48 and 72 hours post-fertilization (hpf) (Fig. 2A). This corresponds to the Asb11 knockdown morphant phenotype we described previously, although with less severity [10].

Next, to further identify the functional consequences of the mutated allele, we performed whole-mount *in situ* hybridization (WISH) with *d-asb11* probe on 10 hpf embryos. Strikingly, *d-asb11* transcripts were enhanced in asb11^{cul} mutants compared to wild type, showing expanded expression in the polster, a U-shaped structure surrounds the head [19], and along the margins of the neural plate (Fig. 2B). Quantitative RT-PCR (qPCR), confirmed the increase of mRNA transcripts in asb11^{cul}. Accordingly, higher protein expression levels were detected by immunoblotting on 12 hpf lysates from asb11^{cul} embryos (Fig. 2C). No significant quantitative differences between wild type and heterozygous embryos confirmed the recessive nature of the mutation. The higher mRNA transcripts and protein levels suggest a compensatory effect of a hypomorphic mutation in the asb11^{cul} embryo (we can exclude that this works through reduced Notch signaling as DAPT treatment reduces d-Asb11 and forced Notch signaling increases d-Asb11 expression [11]), implying that the cullin box mutation has consequences for d-Asb11 function.

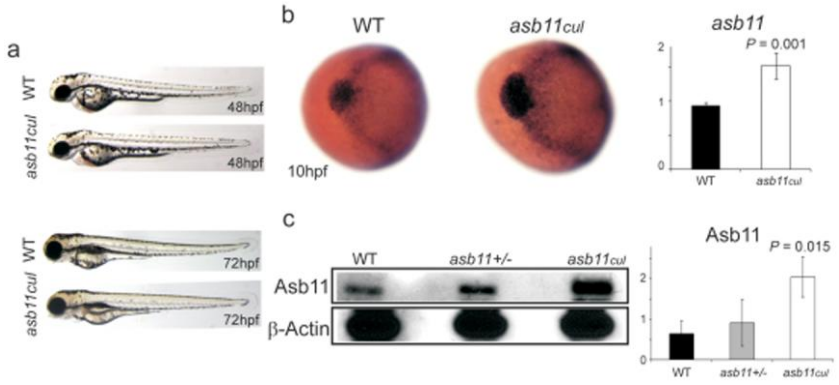

Figure 2. Phenotypic assays on wild type and asb11^{cul} embryos.
(**a**), Morphological analysis of wild type and mutant embryos at 48 and 72hpf. (**b**), (left) Anterior view of wild type and mutant embryos at 10hpf after whole mount *in situ* hybridization, using probe against *d-asb11*. (right) Graph shows the quantification of the respective expressions using qPCR. (**c**), (left) Endogenous d-Asb11 in wild type (WT), heterozygous (asb11+/−) and mutant (asb11cul) embryos at 12 hpf was detected by immunoblotting using anti-d-Asb11 antibody. (right) Graph quantifies 3 individual experiments, with 30 embryos/genotype/experiment.

Cullin box is required for correct expression of Notch target genes

Morpholino-mediated knockdown of *d-asb11* causes repression of specific Delta-Notch elements and their transcriptional targets, whereas misexpression of *d-asb11* induces Delta-Notch activity [11]. To test whether the cullin box mutation has comparable consequences for d-Asb11 function in regulating Delta-Notch signaling pathway, we first explored the capacity of the cullin box-deleted protein to activate, upon its overexpression, Notch-dependent transcription *in vitro*. We observed that overexpression of wild type d-Asb11 in human neuronal precursor cell line, NTera2 [20] led to a strong activation of the Notch target gene *HES1*, however, overexpression of the mutant protein was not capable of doing so (Fig. 3). Because Notch signaling induces activation of *HES1* gene through the CSL transcriptional complex [21], we used a *HES1* reporter lacking the conserved CSL-binding site (hes1-RBP) to confirm Notch-specificity for this transactivation. However, neither d-Asb11 nor Asb11^{Cul} were capable of transactivating hes1-RBP. These results showed that the Cul5 box of d-Asb11 is essential for its function to activate the Notch target gene *HES1* through Notch pathway.

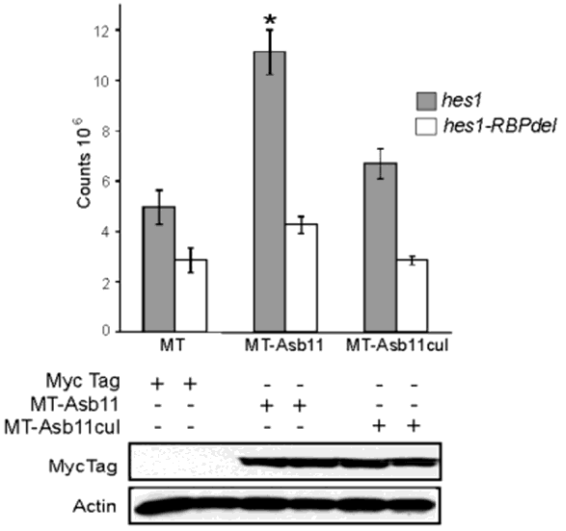

Figure 3. Cullin box domain promotes induction of *HES1* gene *in vitro*.

nTera-d1 cells were co-transfected with *HES1-luciferase* (hes1) or *HES1-luciferase* lacking the conserved CSL-binding site (hes1-RBPdel) and myc-tag (MT) as a control, or myc-tagged *d-asb11* full length (MT-Asb11) or myc-tagged *asb11^{Cul}* (MT-Asb11cul) cDNA. HES1-dependent Notch activity was analyzed by luciferase measurement.

Next, we investigated the expression of Notch target genes *in vivo* by performing WISH for the Hairy/E(spl)-related transcription factors, *her1*, *her4* and *her5* on 12 hpf asb11^{Cul} and wild type embryos. At this time point, the expression of *her1* and *her4* was considerably reduced in asb11^{Cul} embryos (Fig. 4A–B). As *her1* and *her4* are known to be activated by the Notch signaling [22], this result suggests that the Notch signaling pathway is disrupted in embryos lacking the cullin box domain of Asb11.

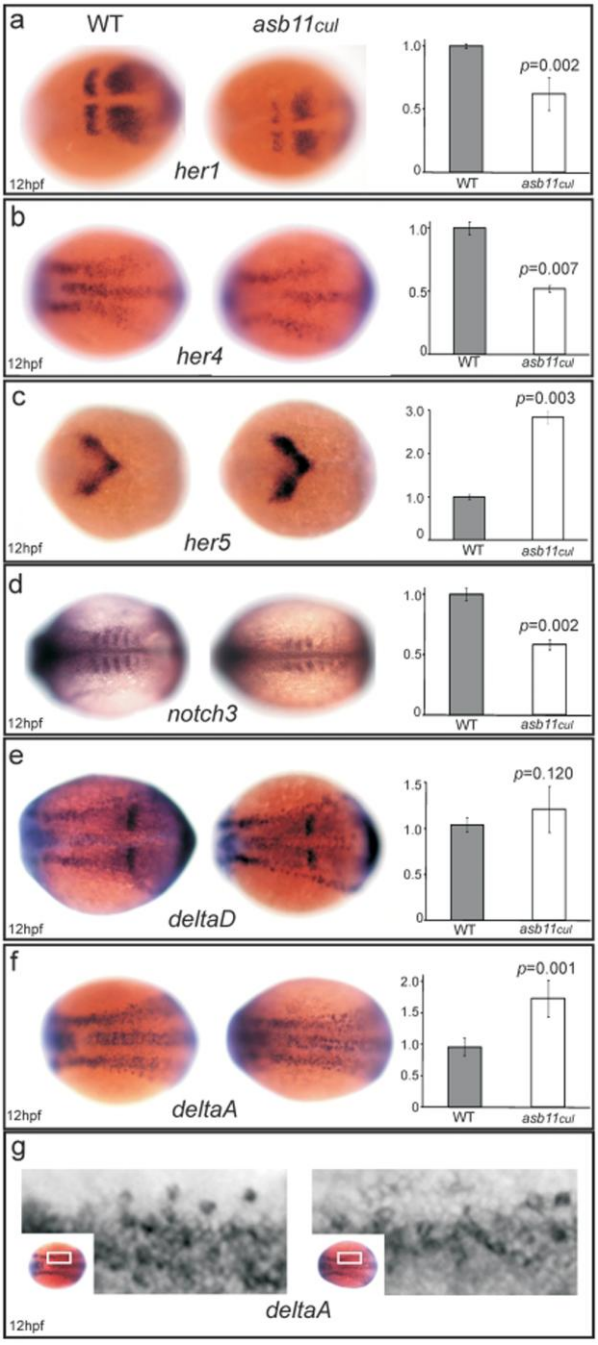

Figure 4. asb11^{cul} presented altered expression of Delta-Notch pathway components.
Wild type (left panel) and mutant (middle panel) embryos at 12 hpf were analyzed for WISH using probes against *her1*, **a**; *her4*, **b**; *her5*, **c**; *notch3*, **c**; *deltaD*, **e**; and deltaA, **f**. (**g**), Higher magnification shows detailed analysis of *deltaA* expression. (left) Graphs quantify the mRNA expression levels.

In contrast, asb11^{Cul} showed a significant increase in the expression of *her5* (Fig. 4C), which is known to be downregulated by the Notch1A-intracellular domain [23]. Consistently, we observed downregulation of *notch3* (Fig. 4D), which has been shown to repress *HES5*, a mammalian homologue of zebrafish *her5* [24] (although Notch inhibition does not expand the *her5* expression domain per se [25], and thus the exact status of *her5* as a Notch target gene remains uncertain). The other Notch genes have not been reported to change expression of *her5* at this stage of zebrafish embryogenesis, thus we did not attempt to assess their expression levels in the context of the analysis of *her5* expression patterns. Next, we analyzed expression of the Notch ligands DeltaA and DeltaD in asb11cul embryos. *deltaA* transcripts showed increased expression in asb11^{Cul} embryos (Fig. 4F), whereas *deltaD* remained unaffected (Fig. 4E). Detailed examination of the WISH expression patterns of *deltaA* revealed a change in distribution of mRNA in the neural plate (Fig. 4G). Wild type embryos exhibit a distinct "salt and pepper" aspect of *deltaA* mRNA distribution whereby some cells have stronger expression than their neighbors, consistent with the notion of Delta-Notch lateral signaling [26]. In contrast, asb11^{Cul} embryos showed a smear of *deltaA* mRNA transcripts across the neural plate, indicating an impaired Notch-mediated lateral inhibition. Thus, the mutation in the *d-asb11* cullin box results in the disruption of canonical Delta-Notch signaling.

The cullin box domain of Asb11 is a bona-fide promoter of Notch-mediated *her4* induction expression

It was reported that Hairy/E(Spl) expression and activity can be independent of Notch signaling *in vivo* [27]. Hence, to determine whether the altered regulation of Hairy/E(spl)-related transcription factors in asb11^{Cul} embryos was mediated by Notch activity, we co-injected *her4::gfp* reporter DNA with *d-asb11* or *asb11^{Cul}* mRNA in zebrafish embryos, which were then treated with DAPT, a γ-secretase inhibitor that blocks Notch signaling [28]. *her4* transactivation was determined as a summation of all green fluorescent protein (GFP) present in the embryo. Confocal microscopy was used to trinomially classify transactivation of the *her4*

promoter as weak, medium or strong (Fig. 5A). When *her4::gfp* was injected with myc tag (MT) mRNA as a control, embryos presented 80%, 12% and 8% of weak, medium and strong GFP signals, respectively. Upon DAPT treatment, the number of medium and strong signal expressing embryos decreased to 8% and 4%, respectively, showing that Notch signaling was disrupted in response to DAPT treatment. Misexpression of *MT-d-asb11* mRNA resulted in an increase in embryos expressing medium GFP signals (52%, c.f. 12% in MT-injected embryos; $p<0.05$), and strong GFP signals (24% c.f. 8% in MT-injected embryos; $p<0.05$). In agreement with previous data, MT-dAsb11 was unable to induce *her4:gfp* upon exposure of DAPT [11], showing the hierarchical upstream function of d-Asb11 in canonical Notch activation.

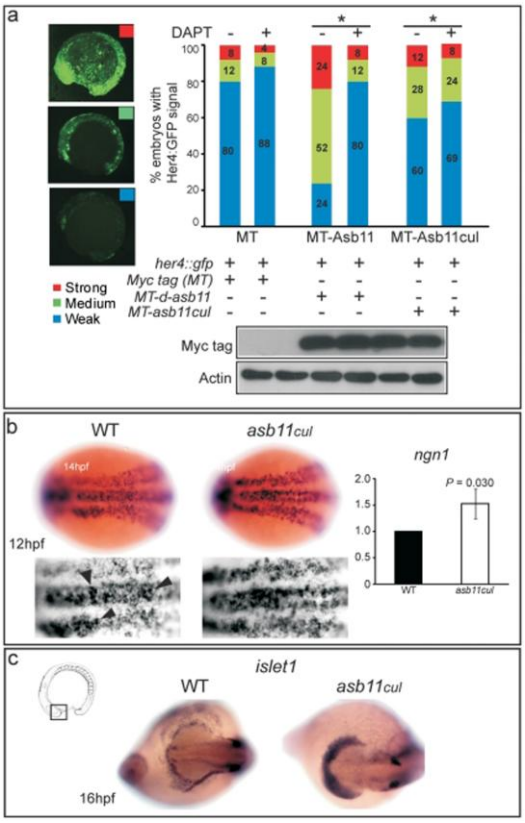

Figure 5. *her4::gfp* transactivation and premature differentiation of neural cells in asb11^{Cul}.

(**a**), the *her4::gfp* reporter was co-injected with myc-tag (MT) mRNA as a control, myc-tagged *d-asb11* full length (MT-Asb11) or myc-tagged *asb11^{Cul}* (MT-Asb11cul) mRNA in zebrafish embryos. Injected embryos were treated with (+) (n= 25) or without (−) (n= 25) DAPT, from 1.5 hpf. At 14 hpf, embryos were analyzed for *her4* transactivation based on the intensity of the GFP signal. Positive embryos were counted and percentages of embryos presenting weak (blue), medium (green) or strong (red) signal were given. (**b**), Wild type (left panel) and mutant (middle panel) embryos at 12 hpf were analyzed for WISH using probe against *ngn1*. (right)

Graph quantifies expression of *ngn1* using qPCR. (**c**) Wild type (left panel) and mutant (right panel) polster of embryos at 16 hpf were analyzed for WISH using probe against *islet1*.

Interestingly, injection of *MT-asb11cul* mRNA caused an increase in the number of embryos expressing medium signals, whereas the number of embryos with strong *her4::gfp* expression was slightly increased compared with control MT-injected embryos. However this effect was observed in both DAPT treated and untreated embryos (24% and 28%, respectively), suggesting that d-Asb11 lacking the cullin box domain ($Asb11^{Cul}$) is much less efficient in inducing the *her4* reporter than wild type d-Asb11 and its function is independent of Notch signaling. These data are consistent with studies showing that *her4* may be expressed in a Notch-independent manner in specific regions of the nervous system [27]. Although during early neurogenesis *her4* expression requires Notch activation, during late neuronal development the *her4* induction in sensory neurons is independent of Notch signaling and dependent on proneural genes, as *neurogenin1* (ngn1) and *zath3* [29].

We performed WISH to investigate the expression of *ngn1*, a bHLH transcription factor, which is expressed in neuronal precursors and differentiated neural cells [30] and is negatively regulated by Notch signaling [31]. As expected, wild type embryos at 12 hpf displayed the typical clustered expression of *ngn1* (Fig. 5B). However, $asb11^{Cul}$ embryos expressed *ngn1* at a uniform high level with less evidence of clustering. The increase in *ngn1* mRNA expression was confirmed by qPCR. d-Asb11 morphants showed a similar phenotype [10], confirming that the higher expression of *ngn1* is caused by loss of d-Asb11 function in the mutant.

Some studies have shown that *her4* is also expressed in Islet1/2-positive sensory neurons and its expression is not involved in canonical Notch signaling [29]. Consistently, *islet1*, detected by WISH, was also increased in zebrafish mutants at 16 hpf. Interestingly, *islet1* expression was higher in the polster region where $asb11^{Cul}$ were significantly increased in mutants (Fig. 5C).

All together our data suggest that the cullin box domain of d-Asb11 is essential to regulate Notch targets genes although d-Asb11 lacking the cullin box may yet affect protein expression independently of Notch, via proneural genes.

The cullin box is essential for DeltaA degradation and regulation of neural committed cells

We have previously shown that d-Asb11 affects Delta-Notch signaling by targeting DeltaA for ubiquitylation and subsequent degradation. This effect, strictly dependent on the presence of the SOCS-box [11], establishes the lateral inhibition gradients between DeltaA and Notch facilitating canonical Notch signaling. To study the role of the cullin box domain in d-Asb11-mediated degradation of DeltaA, we injected zebrafish embryos with Myc-tagged *deltaA* (MT-dlA) and *d-asb11* or *asb11*^{Cul} mRNA at one-cell stage. Embryos were analyzed for the presence of MT-DeltaA protein at 12 hpf. Wild type embryos injected with full-length *d-asb11* displayed substantial DeltaA degradation. In contrast, injected *asb11*^{Cul} was not capable of degrading DeltaA when compared to control (Fig. 6A; $p<0.05$).

Thus, we show that the cullin box domain of d-Asb11 is essential for degradation of Notch ligand DeltaA in zebrafish embryos, providing the first *in vivo* (but not *in vitro*, e.g. [32]) evidence that absence of a cullin box interferes with a protein degradation function of a SOCS-box protein. Moreover, the expression of *deltaA* in the three longitudinal domains of zebrafish neural plate corresponds to regions that express elevated levels of *ngn1* and in which the earliest neurons are born [33]. As Asb11^{Cul} was unable to degrade DeltaA and acted as a dominant negative increasing the quantity of DeltaA protein in mutant embryos, we propose that the premature neuronal commitment in asb11^{Cul} embryos, assessed by the increased expression of the proneural gene *ngn1*, is a consequence of DeltaA accumulation in the neural plate.

Absence of the cullin box alters proliferation patterns

As Notch signaling drives (or maintain) precursor cell proliferation within the neurogenic regions of the embryo, a prediction from our findings would be that the loss of d-Asb11 cullin box would impair such proliferation. Indeed, fluorescent whole-mount antibody labeling with the mitotic marker anti-phosphohistone-3 (PH3) antibody showed a significant decrease in the rate of cellular proliferation of asb11^{Cul} embryos at 24 hpf (Fig. 6B, green label), indicating that the d-Asb11 cullin box is necessary for proper cell proliferation. Alternatively, the premature differentiation of precursor cells in d-asb11 mutants led to diminished number of proliferating cells.

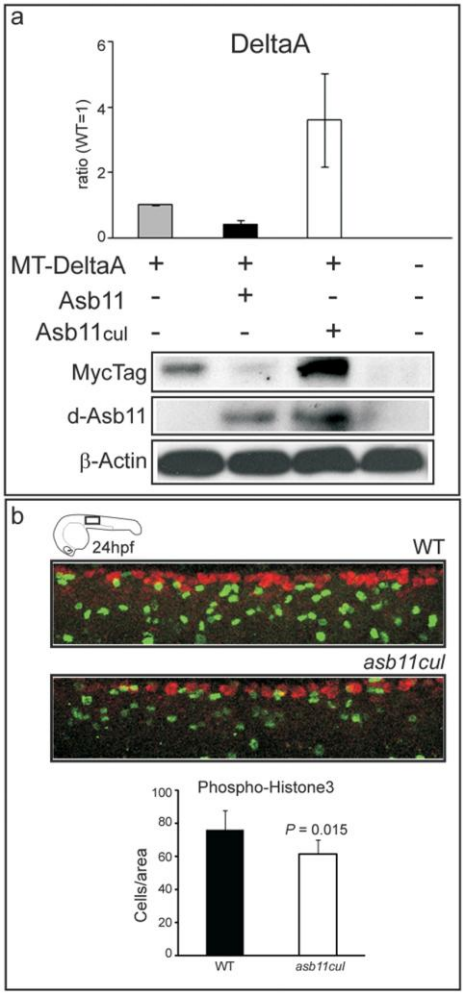

Figure 6. Cullin box is essential for DeltaA degradation and for maintaining a cell proliferating state *in vivo*.
(**a**) Zebrafish embryos were injected with Myc-tagged *deltaA* (MT-DeltaA) and *d-asb11* (Asb11) or *asb11*^{Cul} (Asb11cul) mRNA at one-cell stage. (lower panel) Lysates of 12 hpf embryos were analyzed by immunoblotting for the presence of DeltaA. (higher panel) Graph quantifies 2 individual experiments, each with 30 injected embryos/ group. (**b**), Fluorescent whole-mount antibody labeling of wild type (WT) and asb11^{Cul} embryos at 24 hpf for the mitotic marker anti-phosphohistone-3 (PH3) antibody (green) and the neuronal marker Hu(C). Graph shows the number of positive cells per area (5 somites from beginning of yolk extension) of 5 embryos for each genotype.

In summary, here we show that the Cul5 domain of d-Asb11 is necessary for proper Notch signaling *in vitro* and *in vivo*. Zebrafish embryos lacking the cullin box of d-Asb11 displayed alterations in the expression of Notch pathway components and defective neurogenesis. Thus, our *in vivo* study reveals a novel role of cullin boxes previously unrecognized in *in vitro* experiments.

Materials and Methods

Fish and embryos

Zebrafish were kept at 27.5°C. Embryos were obtained by natural matings, cultured in embryo medium and staged according to methods previously described [34].

Plasmid construction

Plasmids were constructed and/or provided as previously described [10], [11]. The pCS2^{+}MT-d*eltaA* construct was provided by B. Appel (Vanderbilt University, Nashville TN) [35]. The *her4::gfp* reporter was provided by S. Yeo (Kyungpook National University, Korea) [2]. For asb11^{Cul}, mutant zebrafish cDNA was isolated and cloned into the EcoRI and XhoI sites of pCS2^{+}MT and pCS2^{+}.

mRNA synthesis, mRNA and DNA microinjections

Capped mRNAs were synthesized using the mMESSAGE mMACHINE kit (Ambion). Fig. 6A, embryos were injected with 600pg *MT-deltaA* and 350pg *d-asb11* or 350pg *asb11^{Cul}* mRNAs. Fig. 5A, embryos were injected with 5pg *her4::gfp* DNA or 5pg *her4::gfp* + 300pg *d-asb11* or *asb11^{Cul}* mRNA. Total volume of the injection was set at 1 nL.

DAPT treatment

Half of each injected group (n= 50) (Fig. 5A) was incubated in 100µM DAPT diluted in 1% DMSO in embryo-medium (5mM NaCl, 0.17mM KCl, 0.33 mM CaCl2, 0.33mM $MgSO_4$, 0.00005% Meth Blue). The other half was incubated

in 1% DMSO in embryo-medium. The embryos were incubated from 1.5hpf till 14hpf, fixed with 4% PFA overnight at 4°C and analyzed for GFP expression.

***In situ* hybridization**

Whole mount *in situ* hybridizations were performed according to methods previously described [36]. All probes used in this study are previously described [10], [11].

Immunoblotting

Whole mount *in situ* hybridizations were performed according to methods previously described [36]. At 12hfp, chorion and yolk were removed. Embryos were lysed in cell lyses buffer (50mM Tris-Cl pH 7.5, 150mM NaCl, 1mM EDTA, 0.1% Na-deoxycholate, 1% NP-40, 10u, 1% protease inhibitor (ROCHE), 2 µl/embryo. Primary antibodies were diluted in PBS containing 5% milk (fig. 2: rabbit anti-asb11 1:100, fig. 5: rabbit anti-MT 1:1000, Bioke) and used for immunoblotting as previously described [37]. As loading control an anti-actin body was used in addition to coomassie staining of the membrane. For densitometric analysis all bands were measured with a GS-800 Densitometer (Biorad), and total area counts (OD x mm2) were corrected for back ground (equivalent area on a non-relevant place on the blot). Subsequently samples were corrected for loading using the control band and finally values were expressed relative, defining the intensity of the wild type sample as 1.

RNA isolation and qRT-PCR

Total RNA was extracted from whole wild type and mutant embryos at 10 or 12 hpf. Total RNA extraction, cDNA synthesis and qPCR quantification were performed according to previously described methods [38].

Whole mount immunolabelling, microscopy and image quantification

Whole-mount immunohistochemistry and picture capture and analysis were performed as described [13], [39]. For figure 6B anti-HuC (red) and

anti-PH3 (green) antibodies (Upstate Biotechnology) were used. For the analysis of fluorescent stainings, Leica Confocal TCS SPE was used. To quantify the intensity of signal, a z-stack (z-slices of 7 µM) was made, scanning the whole embryo. Leica software (Application Suite 1.8.0) was used to create a maximum projection of the z-stack.

Luciferase reporter assay

nTera2/d1 cells were maintained in DMEM containing 10% FCS. The culture media were supplemented with 5mM glutamine and antibiotics/antimycotics. Cells were incubated at 5% CO_2 in a humidified incubator at 37°C. NTera2/d1 cells were seeded in a 96-well plate and transfected using IBAfect and MA-enhancer (IBA Biosciences, GmbH) using the suppliers protocol. Luciferase was measured on a Packard TOPCOUNT Microplate Scintillation Counter (Packard). The experiments were performed two times in triplicate. Values were normalised with TAL-luc [11].

Statistical testing

Each value with a standard deviation is the average of at least two independent experiments performed in triplicate. Statistical tests were performed using two-tailed t-test. All bars in graphs depict mean values with error bars depicting standard deviations. Statistical $\chi 2$-test was performed for Fig. 5A.

Acknowledgments

We thank Dr. Paula van Tijn for helpful discussions.

References

1.Gao M, Karin M (2005). Mol Cell 19: 581–931.
2.Kile BT, Schulman BA, Alexander WS, Nicola NA, Martin HM, et al. (2002). Trends Biochem Sci 27: 235–241.
3.Deshaies RJ, Joazeiro CA (2009). Annu Rev Biochem 78: 399–434.
4.Piessevaux J, Lavens D, Peelman F, Tavernier J (2008). Cytokine Growth Factor Rev 19: 371–81.
5.Kamura T, Maenaka K, Kotoshiba S, Matsumoto M, Kohda D, et al. (2004). Genes Dev 18: 3055–3065.

6.Kohroki J, Nishiyama T, Nakamura T, Masuho Y (2005). FEBS Lett 579: 6796–6802.
7.Krebs DL, Hilton DJ (2000). J Cell Sci 113: 2813–2819.
8.Mahrour N, Redwine WB, Florens L, Swanson SK, Martin-Brown S, et al. (2008). J Biol Chem 283: 8005–8013.
9.Hilton DJ, Richardson RT, Alexander WS, Viney EM, Willson TA, et al. (1998). Proc Natl Acad Sci U S A 95: 114–119.
10. Diks SH, Bink RJ, van de Water S, Joore J, van Rooijen C, et al. (2006). J Cell Biol 174: 581–592.
11. Diks SH, Sartori da Silva MA, Hillebrands JL, Bink RJ, Versteeg HH, et al. (2008). Nat Cell Biol 10: 1190–1198.
12. Boengler K, Pipp F, Fernandez B, Richter A, Schaper W, et al. (2003). Biochem Biophys Res Commun 302: 17–22.
13. Ferguson JE 3rd, Wu Y, Smith K, Charles P, Powers K, et al. (2007). Mol Cell Biol 27: 6407–6419.
14. Kile BT, Metcalf D, Mifsud S, DiRago L, Nicola NA, et al. (2001). Mol Cell Biol 21: 6189–6197.
15. Kim KS, Kim MS, Kim SK, Baek KH (2004). Zygote 12(2): 151–15.
16. McDaneld TG, Hannon K, Moody DE (2006). Am J Physiol Regul Integr Comp Physiol 290: R1672–1682.
17. McDaneld TG, Spurlock DM (2008). J Anim Sci 86: 2897–290.
18. Wienholds E, van Eeden F, Kosters M, Mudde J, Plasterk RH, et al. (2003). Genome Res 13: 2700–2707.
19. Kimmel CB, Ballard WW, Kimmel SR, Ullmann B, Schilling TF (1995). Dev Dyn 203(3): 253–310.
20. Pleasure SJ, Lee VM (1993). J Neurosci Res 35: 585–602.
21. Katoh M, Katoh M (2007). Int J Oncol 31(2): 461–6.
22. Takke C, Campos-Ortega JA (1999). Development 126: 3005–14.
23. Hans S, Scheer N, Riedl I, v Weizsacker E, Blader P, et al. (2004). Development 131: 2957–2969.
24. Beatus P, Lundkvist J, Oberg C, Lendahl U (1999). Development 126: 3925–3935.
25. Geling A, Plessy C, Rastegar S, Strähle U, Bally-Cuif L (2004). Development 31: 1993–2006.
26. Skeath JB, Thor S (2003). Curr Opin Neurobiol 13: 8–15.
27. Yeo SY, Kim M, Kim HS, Huh TL, Chitnis AB (2007. Dev Biol 301: 555–567.
28. Geling A, Steiner H, Willem M, Bally-Cuif L, Haass C (2002). EMBO Rep 3: 688–694.
29. So JH, Chun HS, Bae YK, Kim HS, Park YM, et al. (2008). Biochem Biophys Res Commun 379: 22–26.
30. Ma Q, Chen Z, del Barco Barrantes I, de la Pompa JL, Anderson DJ (1998). Neuron 20: 469–482.
31. Blader P, Fischer N, Gradwohl G, Guillemot F, Strahle U (1997). Development 124(22): 4557–4569.
32. Chung AS, Guan YJ, Yuan ZL, Albina JE, Chin YE (2005). Mol Cell Biol 25: 4716–4726.
33. Appel B, Eisen JS (1998). Development 125: 371–380.
34. Kimmel CB, Ballard WW, Kimmel SR, Ullmann B, Schilling TF (1995). Dev Dyn 203(3): 253–310.
35. Appel B, Fritz A, Westerfield M, Grunwald DJ, Eisen JS, et al. (1999). Curr Biol 11: 247–56.
36. Oxtoby E, Jowett T (1993). Nucleic Acids Res 21: 1087–109.
37. Versteeg HH, Sørensen BB, Slofstra SH, Van den Brande JH, Stam JC, et al. (2002). J Biol Chem 277: 27065–72.
38. Braat H, Stokkers P, Hommes T, Cohn D, Vogels E, et al. (2005). J Mol Med 83: 601–9.
39. Peppelenbosch M, Boone E, Jones GE, van Deventer SJ, Haegeman G, et al. (1999). J Immunol 162: 837–45.

CHAPTER 5

d-Asb11 is a novel regulator of embryonic and adult regenerative myogenesis

Maria A. Sartori da Silva[1,2*], Jin-Ming Tee[1*], Agnieszka M. Rygiel[2], Vanesa Muncan[3], Anke Brouwers[1], Robert Bink[1], Gijs R. van den Brink[3], Paula van Tijn[1], Danica Zivkovic[1], Liudmila L. Kodach[2], Sander H. Diks[4], Daniele Guardavaccaro[1], and Maikel P. Peppelenbosch[2]

[1]Hubrecht Institute-KNAW and University Medical Center Utrecht, Utrecht, The Netherlands.

[2]Department of Gastroenterology and Hepatology, Erasmus MC-University Medical Center Rotterdam, Rotterdam, The Netherlands.

[3]Tytgat Institute for Liver and Intestinal Research, Amsterdam, The Netherlands

[4]Department of Pediatric Oncology, University Medical Center Groningen, Groningen, The Netherlands.

*These authors contributed equally.

(Submitted)

Abstract

The specific molecular determinants that govern progenitor expansion and final compartment size in the myogenic lineage, either during gestation or during regenerative myogenesis, remain largely obscure. Recently, we retrieved *d-asb11* from a zebrafish screen designed to identify gene products that are down regulated during embryogenesis upon terminal differentiation and identified it as a potential regulator of compartment size. Here we report highly specific d-Asb11 expression in the label-retaining Pax7^{+} muscle satellite cell compartment. Forced expression of *d-asb11* impaired terminal differentiation and caused hyperproliferation in the myogenic progenitor compartment both *in vivo* and *in vitro* model systems, whereas either knock down of *d-asb11* or introduction of a germline hypomorphic mutation in the zebrafish *d-asb11* gene produced premature differentiation of the muscle progenitors and delayed regenerative responses in adult injured muscle. Hence, we provide evidence that *d-asb11* is a principal regulator of embryonic as well as adult regenerative myogenesis.

Introduction

The establishment of the relative sizes of the various compartments in the vertebrate body is one of the most important and defining processes of developmental biology. During embryonic development, tissue-specific progenitor compartments must undergo massive cell expansion before to achieve further differentiation ensues. The increase and diversification of vertebrate compartments played a crucial factor in the terms of evolution and enabled organisms to cope with different environmental conditions (1). Furthermore, aberrant compartment regulation is implicated in many serious pathologies (e.g. cancer) (2). Knowledge of the factors that determine and regulate cell proliferation, thus, defining compartment size, remains poorly understood and elucidation of the underlying molecular

mechanisms driving expansion of progenitor compartments represents an important scientific question.

Likewise, little is known with respect to biological events triggering muscle compartment expansion. In vertebrates the skeletal muscle arises from an embryonic compartment called myotome, originated from a transient epithelial structure, the dermomyotome, which in turn is derived from somites. Somites are formed sequentially, as paired segments of the paraxial mesoderm on either side of the neural tube, from anterior to posterior, at regular time intervals. The somites are transient structures patterned by signals from the surrounding tissue into compartments that later differentiate into different types of tissues that will give rise to several trunk structures: sclerotome (precursor of the bones, cartilages and tendons), myotome (precursor of the muscle) and dermatome (precursor of the dermis) (3,4,5).

The primary myotome is formed as the first differentiated muscle from the dermomyotome between E11.5 and E15.5 in the mouse. There, some myoblasts irreversibly exit the cell cycle, align with each other, and fuse, forming multinucleated myotubes. After primary myogenesis, secondary myoblasts in the dermomyotome use the primary myotome as a scaffold to attach to and fuse with each other, giving rise to secondary myotubes. A similar molecular process of myogenesis occurs postnatally, to recruit adult muscle precursors into new myofibers during skeletal muscle damage (6,7). Enhanced knowledge of the molecular determinants in the formation of muscular tissue, both in embryos and adult organisms, will help to elucidate important processes involved in developmental biology and give a better understanding of degenerative diseases such as muscular dystrophy as well as the process of repair, reproduction or replacement of lost or injured cells, possibly leading to new ways of treatment.

Earlier we reported on efforts to discover the participants involved in progenitor compartment size regulation by isolating genes that are differently expressed during terminal differentiation as well as genes responsible for the proliferation of the stem cell compartment. To this end, transcripts from zebrafish embryos treated with 0.5 μM all-trans retinoic

acid (RA) (which terminates progenitor expansion and induces full terminal differentiation) were isolated and compared to untreated embryos. Differential fragments were tested using whole mount *in situ* hybridization at different developmental stages. Finally, one fragment was singled out for detailed characterization based on its restricted spatio-temporal expression pattern during late gastrulation and early somitogenesis (8). The full-length sequence of the down-regulated fragment revealed that the gene is homologous to the mammalian ankyrin repeat and suppressor of cytokine signaling (SOCS) box-containing protein 11 (*ASB11*) and it was further referred to as *d-asb11*. The amino acid sequence of zebrafish d-Asb11 has 293 residues, composed of a series of six ankyrin repeats at the N-terminus, and a C-terminal SOCS box domain (8).

The ASB family constitutes a chordate-unique gene family whose members are characterized by variable numbers of N-terminal ankyrin repeats and a C-terminal SOCS box (9). ASB proteins act as substrate receptor subunits of E3 ligases, enzymes that mediate ubiquitylation and degradation of target proteins (10,11). Although the zebrafish d-Asb11 has the most functional homology with human ASB11, sequence analysis also showed high homology of d-Asb11 with other members of the ASB family, most markedly with ASB9. Considering the fact that *ASB9* and *11* are also located close to each other on the genome (which seems to have arisen as the result of a recent gene duplication event), we proposed that these genes are both mammalian homologues of d-Asb11 (8). Furthermore, ASB proteins show very high pan-chordate conservation, *Homo sapiens* ASB1 and its orthologue in the urochordate *Ciona intestinalis* sharing 50% overall similarity on an amino acid basis, which points to very fundamental functions in chordate physiology.

Consistently, forced expression of d-Asb11 in the presumptive nervous system of zebrafish embryos maintained cell progenitor proliferation and increased the neuronal compartment size, whereas in the absence of d-Asb11 premature terminal differentiation was induced resulting in a reduced compartment size. The molecular mechanisms by which d-Asb11 sustain progenitor expansion, likely involve Notch activation as we

established that d-Asb11 is a positive regulator of canonical Notch signalling (8,12).

However, d-Asb11 function in embryogenesis and adult organisms has not been fully explored, and thus, it is possible that d-Asb11 is relevant for compartment definition outside the neuronal system, prompting more comprehensive analysis of its *in vivo* expression. Indeed, d-Asb11 was well capable of activating Notch signal transduction outside the neuronal system as heterologous expression of this gene activates Notch reporters in a variety of cell types (12).

In this context, muscle development may constitute an interesting target for d-Asb11 action as other ASB family members have been especially implicated in the regulation of this compartment. ASB2β was first identified in muscle cells during embryogenesis and in adult tissue, and was shown to regulate muscle differentiation by targeting actin filamin B (FLNb) for proteasomal degradation. Inhibition of ASB2β blocked myoblasts fusion and myotube formation, crucial processes in the later phase of muscle development (13). Additionally, ASB15 has emerged as a regulator of protein synthesis and muscle growth (14), possibly mediated by the PI3K/Akt signal transduction pathway (15). Besides, analysis of *asb11* transcripts showed that the expression of this gene in muscle tissue has a pan-vertebrate characteristic, presenting a particularly high expression in mammalian muscle (mouse and human). Hence, we decided to characterize the function of d-Asb11 during myogenesis. Further analysis showed that ASB11 expression is specifically restricted to pax7^{+} label-retaining compartment and may be important for progenitor maintenance. Downregulation of d-Asb11 interfered with myotome formation during embryogenesis and adult muscle regeneration, whereas forced expression led to expansion of the muscle compartment both *in vitro* and *in vivo*. We conclude that d-Asb11 constitutes a novel regulator of primary and regenerative myogenesis.

Results

Specific expression of d-Asb11 in the label-retaining Pax7^{+} muscle satellite cell

In an effort to determine possible extra-neuronal functions for d-Asb11, we explored the specific distribution of *d-asb11* transcripts in adult zebrafish tissues by reverse transcription-PCR (RT-PCR). *d-asb11* cDNA from total mRNA extracted from muscle, heart, eye, intestine, gills, testis, pancreas and brain was amplified. β-actin was used as a control. *d-asb11* is expressed in all the tissues we explored (Figure 1A), indicating functionality outside the nervous system, and possibly in muscle. This notion is reinforced by experiments attempting a pan-vertebrate comparison of d-Asb11 expression.

In mammals two orthologues of *d-asb11* are present, *ASB9* and *ASB11* which are highly homologous, both sharing approximately 70% sequence similarity to *d-asb11*. *ASB9* and *ASB11* lie adjacent to each other on the X-chromosome suggesting a *sarcopterygiic*-specific gene duplication event, not present in teleosts. We investigated specific-tissue expression of mice *m-Asb11* and *m-Asb9* and observed particularly prominent *m-Asb11* in skeletal and cardiac muscle and less, but significant, expression in brain (Figure 1B), whereas *m-asb9* was strongly expressed in testis and kidney (Figure 1C). This is in agreement with the earlier established function of *d-asb11* in regulating compartment size in the central nervous system of zebrafish embryos, but the expression of *m-Asb9* in testis and kidney shows that high expression of *d-asb11* orthologues in distinct mammalian tissues is a phenomenon observed in evolutionary highly divergent vertebrates and call for an investigation to the role for d-Asb11 in zebrafish compartment expansion in these tissues.

To analyze the endogenous expression of d-Asb11 during embryogenesis, we isolated total cell lysates of zebrafish embryos at 12, 14, 16 and 24 hours post-fertilization (hpf) and compared protein levels of d-Asb11 and muscle creatine kinase (MCK), a marker for terminal muscle differentiation whose onset of expression coincides with the end of progenitor expansion (16). Indeed, as expected, expression of MCK protein increases throughout somitogenesis (Figure 1D). Consistently with a role of *d-asb11* during

progenitor expansion in muscle development, the expression of d-Asb11 is high during early myogenesis and diminishes when the final stages in muscle differentiation ensue, being approximately complementary to the expression of MCK.

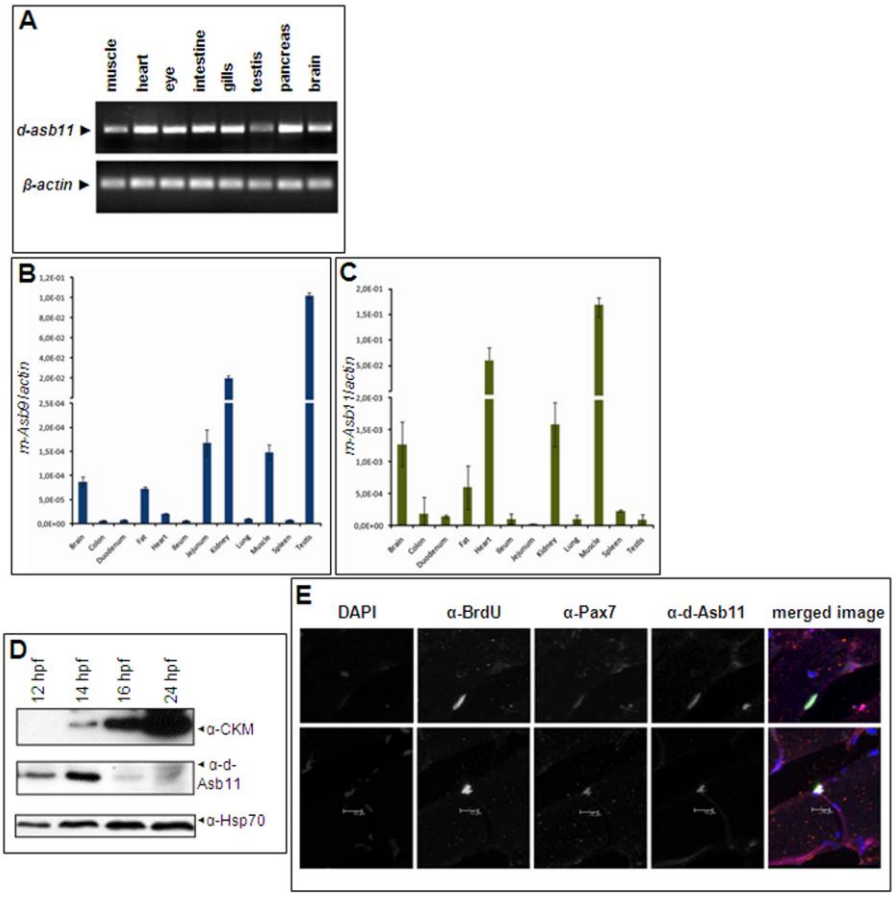

Figure 1. Expression of d-Asb11 in Pax7+ satellite cells and different tissues. (**A**) qRT-PCR analysis of zebrafish *asb11* (*d-asb11*) in mRNA samples isolated from muscle, heart, eye, intestine, gill, testis, pancreas and brain tissues of adult fish. Zebrafish *β-actin* was used as template control. Various tissue types isolated from adult mice were analyzed for expression of murine (**B**) *Asb9* (*m-Asb9*) and (**C**) *Asb11* (*m-Asb11*). The tissues are: brain, colon, duodenum, fat, heart, ileum, jejunum, kidney, lung, muscle, spleen and testis. Results were normalized by *β-actin expression.* (**D**) Analysis of protein levels of d-Asb11 and muscle creatine kinase (Mck), a marker of muscle terminal differentiation, in different stages during embryogenesis. Hsp70 expression is used as input control. (**E**) Adult muscles were

triple immunostained with anti-BrdU, anti-Pax7 and anti-Asb11 antibodies. Top panels show a representative of sarcolemma sagittal sections and bottom panels show a representative of transverse sections.

Next, we analyzed the histological localisation of *d-asb11* and its relationship with Pax7 label retention. Cross sections of skeletal muscle tissue of zebrafish were co-stained with an antibody specific for d-Asb11 and the well-established muscle satellite marker Pax7 (17). d-Asb11 staining displayed a distinct expression pattern on the sarcolemma where it co-localizes with a portion of the $Pax7^{+}$ compartment (Figure 1E). To confirm that these $Pax7^{+}$/d-$Asb11^{+}$ cells represent true muscle stem cells, we tested their long term BrdU label retention. Results in figure 1E confirmed that this double compartment truly represented slowly cycling satellite cells. Thus, the muscle stem cell compartment in adult muscle is characterized by highly specific d-Asb11 expression.

Forced expression of *d-asb11* inhibits muscle cell differentiation and supports progenitor expansion in the C2C12 model system

Heterologous expression of *d-asb11* has been shown to support progenitor expansion while simultaneously inhibiting terminal differentiation in the PC12 and N-Tera2 *in vitro* model systems for neurogenesis (8). Expression of d-Asb11 in the satellite cell compartment may suggest that d-Asb11 could also act in a similar manner in mesodermally-derived muscle formation. Mouse C2C12 myoblasts, upon application of diffentiation medium, synchronously withdraw from the cell cycle, elongate, adhere, and finally fuse together to form myotubes exhibiting most mechano-biochemical adaptations associated with fully differentiated muscle (18) (Figure 2A). Thus, this system represents a valuable model to study the effect of d-Asb11 on muscle cell differentiation.

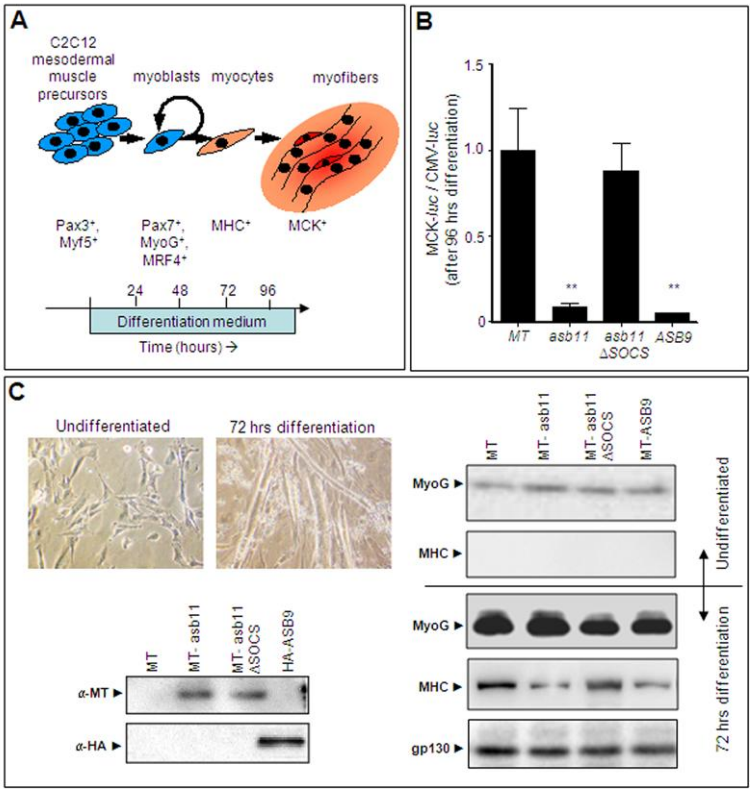

Figure 2. Heterologous expression of *d-asb11* or *h-Asb9* prevents terminal differentiation in the C2C12 model system of skeletal muscle differentiation. (**A**) Schematic depiction of the various stages of skeletal muscle differentiation as observed in the C2C12 model system and the associated expression of markers of muscle differentiation. (**B**) Following 96 hrs of exposure to differentiation medium, terminal differentiation of skeletal muscle was assayed by luciferase activity driven by the muscle creatine kinase (MCK) promoter in association with heterologous expression of either *d-asb11* or *h-Asb9*. Transfection of a vector expressing only myc-tag (MT) or a MT-SOCS box deficient d-Asb11 (MT-asb11ΔSOCS) was used as controls. As a control for transfection efficiency CMV promoter activity was used. (**C**) Following 72 hrs of exposure to differentiation medium (left side, top panel), C2C12 cells were transfected with a vector containing only the MT, MT-d-asb11, MT-asb11ΔSOCS, or MT-hAsb9. Expression of the transgenes is shown on the left side, bottom panel. Effects of these transgenes on the expression of Myogenin (MyoG; a myoblast marker) and Myosin heavy chain (MHC; a marker of terminal muscle cell differentiation) were tested either in undifferentiated cells or after 72 hours under differentiation medium treatment, right side.

Confirmation of the inhibitory effects of d-Asb11 on muscle cell differentiation was obtained from experiments in which C2C12 cells, upon differentiation medium, were transfected with different constructs in combination with MCK promoter-driven luciferase or a construct containing a CMV promoter-driven luciferase. Vectors containing either the Myc-tag (MT) or a SOCS-box deficient version of d-Asb11 (d-asb11ΔSOCS) were used as controls.

Differentiation induction of luciferase-mediated MCK promoter was significantly inhibited in the presence of *MT-d-asb11* or *MT-hASB9* (orthologue of *d-asb11* in the human genome, together with hASB11), while no significant effect was shown by co-expression with the *d-asb11* lacking the SOCS box domain (Figure 2B).

Subsequently, we tested the effect of MT-d-Asb11 as well as MT-hASB9 on the expression of the myogenic marker myogenin (MyoG) and the terminal myocyte marker myosin heavy chain (MHC) (Figure 2C). As expected, both genes were substantially induced under differentiation conditions in control cells. After verification that these transgenes were efficiently expressed (Figure 2C, left panel) we investigated the influence of such heterologous expression on *in vitro* muscle differentiation. Importantly, when cells were transfected with expressing *MT-d-asb11* or *MT-hASB9* constructs, differentiation no longer induced cellular levels of MHC (Figure 2C). However, induction of MyoG was unaffected by expression of either MT-d-Asb11 or MT-hASB9. Together, these observations showed that forced expression of d-Asb11 prevents terminal myocyte differentiation but not myoblast differentiation of muscle precursors, at least in the C2C12 model system, consistent with a possible role of *d-asb11* in maintaining progenitor proliferation in muscle.

Forced expression of d-Asb11 *in vivo* deregulates differentiation in the presumptive myotome and causes hyperplastic myotome formation

A prediction from the proposed role of *d-asb11* as a factor inhibiting differentiation and maintaining proliferation in the $Pax7^{+}$ muscle stem cell compartment would be that forced expression of *d-asb11* is associated with

impaired differentiation in zebrafish muscle. Thus, we injected *MT-d-asb11* mRNA into two cell stage blastomeres, and investigated the expression pattern of *d-myoD*, a bHLH transcription factor that is expressed in adaxial cells and in the posterior region of each developing somite (19), by using whole mount *in situ* hybridization. An anti-Myc tag antibody was used to confirm expression of injected mRNA and to identify the half of the embryo derived from the injected blastomere. Consistently, as compared to wild type embryos (Figure 3A) misexpression of *MT-d-asb11* resulted in loss of somitic *d-myoD* expression accompanied by variably reduced or absent expression in adaxial cells at 13-14 hpf (Figure 3B-D). Furthermore the expression pattern of *MT-d-asb11* in the embryo coincided with exclusion of *d-myoD* expression (Figure 3E-F). Additionally, when expressed in the whole embryo, d-Asb11 affected *d-myoD* in the entire myotome, showing a bended and/or displaced expression pattern at later stages (16 hpf) (Figure 3G-I). Hence, forced expression of *d-asb11* delays acquisition of d-myoD positivity in the presumptive axial myotome and deregulates important aspects of differentiation during zebrafish embryogenesis. In the *muscle creatine kinase* (*mck*), a marker for advanced muscle cell differentiation, *d-asb11* misexpression led to a substantially reduction (Figure 3J-L), whereas *myoG* was subtle affected by *d-asb11* expression (Figure 3M-O).

In an effort to confirm these effects at the protein level, zygotes were injected with *MT-d-asb11* and *MT-d-asb11ΔSOCS* mRNA. Uninjected embryos and embryos injected with MT only served as controls. Total cell lysates were isolated at 16hpf and analyzed using an anti-MCK antibody, while an anti-MT antibody was used to verify induced *d-asb11* variants (Figure 3T). Indeed, forced expression of *d-asb11* caused reduction of Mck, in agreement with its inhibitory function of cell differentiation.

Finally, to analyze the effects of forced d-asb11 expression in slow and fast muscle fiber formation, we injected of *MT-d-asb11* mRNA in zygotes which were then immunostained at 36 hpf. At this time point, aberrant expression of *d-asb11* caused gross abnormalities in both slow and fast muscle (Figure 3Q-S), accompanied of hyperplastic disruption of normal muscle architecture.

Together, these results indicate a role of *d-asb11* in muscle progenitor expansion.

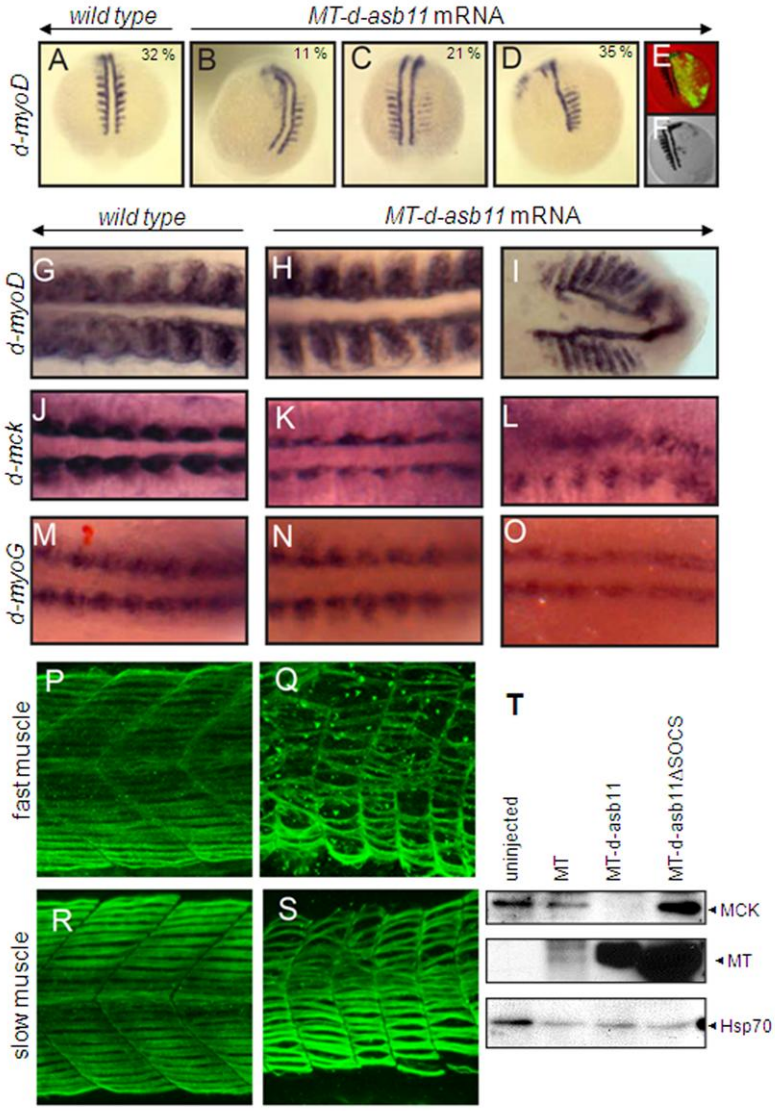

Figure 3. Forced expression of *d-asb11* mRNA interferes with muscle differentiation *in vivo*. (**A-D**) Zebrafish embryos were injected at the two-cell stage in one of the two blastomeres with encoding full-length MT-d-Asb11 mRNA (300pg). The numbers indicate the percentages of embryos displaying the particular phenotype (total n=85). (**E-F**) Immunolabelling of MT-d-Asb11 overlay with *d-myoD in situ* hybridisation. (**G-O**) Embryos were injected at one-cell stage

with d-*Asb11* mRNA and fixed at 16hpf. Whole mount *in situ* hybridization was performed using (**G-I**) *myo*D, (**J-L**) *muscle creatine kinase* (*mck)* and (**M-O**) *myogenin* (*myoG*) riboprobe. Expression was compared between uninjected (**G, J, M**) and injected embryos (**H, I, K, L, N, O**). (**P-S**) Abnormal axial muscle formation at 36 hpf in response to *d-asb11* mRNA injections. Fast and slow muscle fibers were stained by immunolabelling as described earlier (33). (**T**) Confirmation of *d-asb11* forced expression effects on *d-mck* at the protein levels. Zygotes were injected MT-*d-asb11* mRNA, MT only or MT-asb11ΔSOCS injected embryos serving as controls. Total cell lysates were isolated at 16hpf. The protein was analyzed using an anti-Mck antibody. Anti-MT antibody was used to verify induced expression of *d-asb11* variants, and as a control loading an anti-Hsp70 antibody was used.

Fish homozygous for a hypomorphic d-Asb11 mutation are impaired in muscle progenitor expansion and myotome formation

The expression of *d-asb11* in the muscle progenitor cell compartment and the inappropriate expansion of the myotome following its misexpression suggest that *d-asb11* is important for progenitor expansion. Thus, we decided to investigate the effect of moderate d-Asb11 deficiency during muscle development. To this end, we employed a mutant *d-asb11* zebrafish germline (*asb11*^{cul}) which lacks the cullin box, a SOCS box subdomain, resulting in a hypomorphic allele. We recently described the isolation of *asb11*^{cul} mutants in detail and demonstrated that these are defective in Notch signalling and have impaired cell fate specification within the neurogenic regions of the embryos (20). We did not analyse effects on muscle development, however. The *asb11*^{Cul} mutants survive until adulthood; however, they present a subtle shorter trunk and less well defined somites. Interestingly, when the developing myotome was analysed for the number of proliferating muscle progenitor cells, as defined by phospho-histone 3 (PH3) and Pax7 co-positivity, this number was significantly reduced in *d-asb11* mutants (Figure 4A). Furthermore, as judged by the expression of *mck,* muscle terminal differentiation in *asb11*^{cul} embryos is temporally enhanced (Figure 4B), whereas the cell proliferation in the myotome of these mutants is substantially reduced (Figure 4C-E).

Thus, we conclude that *d-asb11* is required for maintaining myogenic proliferation in the stem cell compartment during embryogenesis.

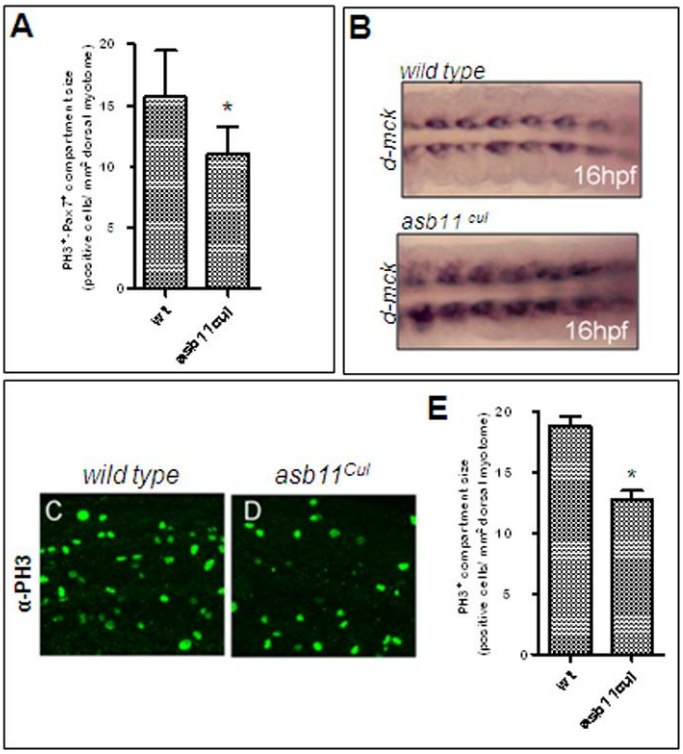

Figure 4. Hypomorphic *d-asb11* allele is associated with reduced pax7^{+} progenitor compartment and precocious terminal differentiation.
(**A**) The expanding muscle progenitor compartment of wild type and asb11^{cul} embryos at 24 hpf, was determined by double labelling with anti-PH3 antibody (a marker for proliferating cells) and anti-Pax7 antibody. Cells were counted at equivalent positions in the developing dorsal myotome. (**B**) Wild type and mutant embryos were fixed at 16 hpf and tested for advanced muscle differentiation using *mck* riboprobes. Proliferation in the presumptive myotome of wild type (**C**) and asb11^{cul} (**D**) embryos visualised by anti-PH3 staining at 48 hpf. (**E**) Quantification of total proliferative activity in zebrafish embryos using the number of PH3 positive cells as a surrogate measure. The results represent the average of 8 embryos.

Expression of d-Asb11 in proliferating satellite cells is important for adult regenerative myogenesis

Regenerative myogenesis is still a poorly understood process. To determine whether regenerative myogenesis like primary embryogenesis is regulated by d-Asb11, we induced mechanical injury with a 30G needle on the adult zebrafish body musculature, dorsal to the anus, and investigated the

number of BrdU$^+$, Pax7$^+$ and Asb11$^+$ cells in lesion-induced versus uninjured wild-type zebrafish at 7 days post-injury. Although this procedure does not produce significant changes in the number of BrdU$^+$ or Pax7$^+$ cells, the double positive d-Asb11$^+$/Pax7$^+$ compartment substantially increase in size following muscle injury, indicating that *d-ab11* may be involved in response to trauma in this tissue (Figure 5A).

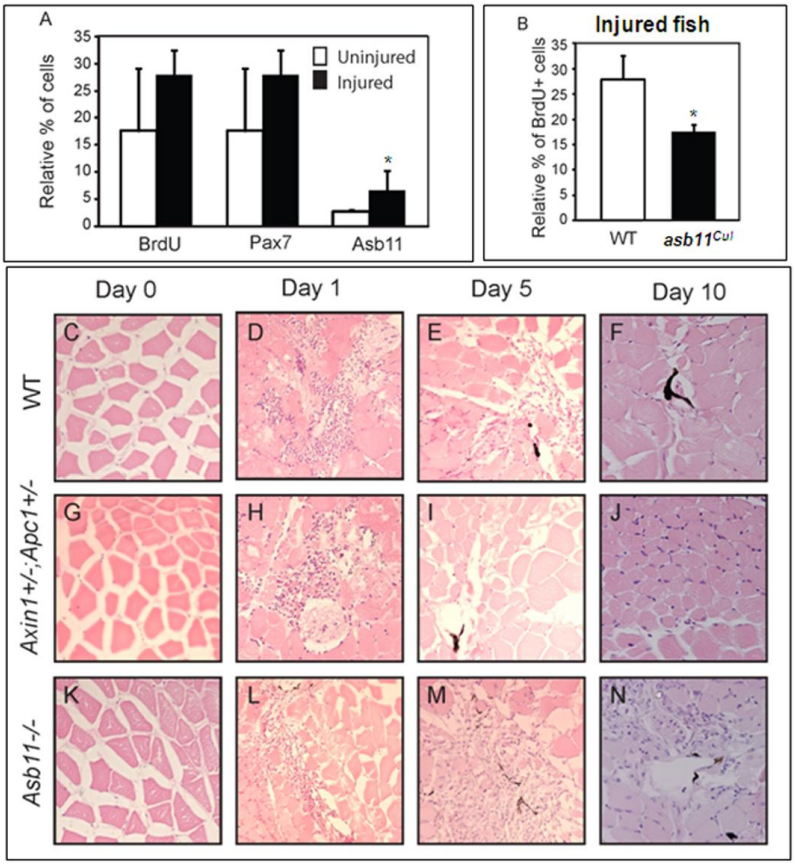

Figure 5. The hypomorphic *asb11^{cul}* allele is associated with impaired regenerative responses following mechanical injury.

(**A**) Zebrafish were fixed and frozen 7 days post-injury. Adult muscle tissues were cryosectioned and triple immunostaining with anti-BrdU, anti-Pax7 and anti-Asb11 was performed. (**B**) Wild-type and Asb11^{cul} zebrafish were fixed and frozen 7 days post-injury. Adult muscle tissues were cryosectioned and immunostaining with anti-BrdU was performed. (**C-N**) Zebrafish were fixed at (**C, G, K**) 0, (**D, H, L**) 1, (**E, I, M**) 5 and (**F, J, N**) 10 days post-injury. Evans Blue Dye was used as a marker to

identify the area of injury. The adult musculature was sectioned and counterstained with HE.

Subsequently, we compared the proliferation between injured *asb11*^{Cul} and wild-type zebrafish. Injured asb11^{Cul} mutants showed a significant diminished numbers of BrdU^{+} cells (Figure 5B), suggesting that regenerative proliferation is dependent on functional d-Asb11.

Next, we performed a muscle regeneration comparative analysis using injured tissues of wild-type, asb11^{cul} and *axin1/apc1* mutants. *axin1/apc1* double heterozygous mutants were used as a positive controls as Wnt signaling is shown to positively regulate satellite cell proliferation on adult muscle fibers during wound healing response in CD34^{+} cells (21) as well as cultured myofibers (22).

At Day 0, muscle fibers morphology was comparable in wild-type, *axin1/apc1* and asb11^{cul} zebrafish lines (Figures 5C, G, K). At Day 1 post-injury, there was a marked cellular invasion, and evident degeneration and necrosis of mature fibers of all tissues (Figure 5D, H, L). At Day 5 post-injury, *axin1/apc1* mutants showed remarkable recovery and numerous small diameter regenerating muscle fibers were observed (Figure 5I), whereas wild-type showed a slight recovery (Figure 5E) and in asb11^{cul} the muscle fibers were still necrotic (Figure 5M). At Day 10 post-injury, *axin1/apc1* showed a clear recovery and regeneration of the muscle fibers (Figure 5J), while the aspect of wild type fish appeared only moderately worse (Figure 5F). In asb11^{cul}, however, little improvement could be noted with small regenerating fibers emerging (Figure 5N). Altogether these results establish a crucial role of d-Asb11 in both embryonic and adult regenerative myogenesis.

Discussion

The determinants of the size of the muscle cell compartment remain poorly understood. During embryogenesis a group of Pax7^{+} stem cells arises and proliferates until the final compartment size is reached. In most precursor cells, a genomic programme, responsible for terminal differentiation, is

started resulting in functional muscle fiber, whereas a small subpopulation remains Pax7^{+} cells forming the satellite cell population from which regenerative myogenesis can start in response to injury. Our data presented here show that d-Asb11 is essential for maintaining muscle stem cell proliferation during zebrafish embryogenesis and is required for regenerative responses during injury as well. Importantly, we demonstrated that d-Asb11 is expressed beneath the basal lamina of adult zebrafish muscle fiber, and co-localized with a well-accepted muscle satellite cell specific marker Pax7. This, together with the co-expression of d-Asb11 with label retaining BrdU slow-cycling cells, suggested that the d-Asb11 positive cells are the muscle satellite cells themselves. Interestingly, there are significantly less d-Asb11^{+} cells compared with Pax7^{+} cells in the adult muscle fibers. It is tempting to speculate that the d-Asb11 cells are the primary stem cells, and thus, are activated and proliferate in response to muscle damage/injury.

The *d-asb11* gene has high homology to both mammalian *ASB9* and *ASB11,* however no obvious *asb9* homologue is present in fish. As *hASB9* and *hASB11* lie adjacent on the same chromosome (X), it seems to represent the result of an evolutionary relatively recent genetic duplication event. *In silico* analysis revealed that 46.6% of the ancestral chordate genes appear in duplicate in one or more of the vertebrate lineages, with 34.5% having at least one duplication before the divergence of fish from tetrapods and 23.5% having at least one duplication afterward (23). This suggests that zebrafish *d-asb11* functions similarly to both *hASB9* and *hASB11*, as it seems that Asb11, in zebrafish, bears a more varied number of functions, while in mammals the function of ASB proteins appear to be more specific. This hypothesis is supported by our results where zebrafish *d-asb11* transcripts were present in all tissues analyzed, whereas mice showed more tissue-specific expression for both *ASB9* (testis and kidney) and *ASB11* (muscle and heart) transcripts, although there is no information of the function of these genes in male germ cells compartment, urogenital system or muscle development. However ASB1 (24) and ASB17 (25), which are also high expressed in mice testis, have been implicated in mammalian

spermatogenesis. Moreover, human and murine ASB9 were reported to interact with the creatine kinase isoforms; brain creatine kinase (BCK) (26) and ubiquitous mitochondrial creatine kinase (uMtCK) (27), targeting them to proteosomal degradation. In agreement with the notion that zebrafish use ASB proteins in multiple compartments, whereas in mammals ASB proteins function in specific compartments, zebrafish present a lesser number of Asb proteins (14) compared to humans and mice (18). Clearly, more in depth analysis of expression and function of different ASBs in different tissues is required; however, it is tempting to speculate on a function of *d-asb11* in zebrafish spermatogenesis and kidney development.

Earlier, we have demonstrated that *d-asb11* maintains the neuronal progenitor compartment, implying a critical role in the ectodermal compartment size. In zebrafish, this function does not seem to be restricted to this germ layer, as we now show that it is important for mesodermal lineage as well and hence *d-asb11* appears a regulator of vertebrate compartment size of more general importance. The effects of *d-asb11* on embryonic myogenesis is remarkably similar to its effects on embryonic neural precursors (12), suggesting that *d-asb11* functions in a similar way in regulating both the neuroectodermal and mesodermal cell fates. Whether *d-asb11* is important for compartment size in the endodermal lineage, however, is questionable. Interestingly ASB9 expression has recently been linked to the maintenance of cell proliferation in colorectal cancer, thus, further investigations on how endodermal progenitor expansion is regulated and if they involve ASB like proteins should be warranted.

Recently we showed that the functions of d-Asb11 in neurogenesis are mediated by its potential to enable Notch signalling activity (12). Canonical Delta-Notch signaling plays a key role in satellite cell activation and muscle regeneration. There is a temporal switch between Notch and Wnt signaling, whereby, Notch signaling has to be downregulated for myogenesis to proceed (28). Consistently, our data showed that *d-asb11* expression in muscle satellite cells is required to maintain the muscle precursor pool and efficient muscle regeneration. It is important to note, that albeit slower, muscle regeneration is still evident in asb11^{Cul} zebrafish.

In conclusion, based on the evolutionary conservation of *d-asb11* with human *hASB9* and *hASB11*, it is tempting to hypothesize that the phenotypes we observed in the *d-asb11* mutants could be linked to human muscular diseases, prompting an investigation into the role of ASB11 in muscle pathology.

Experimental procedures

Fish and embryos

Embryos were obtained by natural matings, cultured in embryo medium and staged according to methods previously described (29). Zebrafish were kept at 27.5°C.

Cell culture

C2C12 mouse myoblasts were obtained from the ATCC and cultured in Dulbecco's modified Eagle's medium (DMEM) (Gibco, Paisley, Scotland) with 4.5 g/L glucose and L-glutamine and supplemented with penicillin (50U/mL), streptomycin (50µg/mL) and 10% fetal calf serum (FCS). Cells were grown in monolayers in a humidified atmosphere contaning 5% CO_2. The differentiation medium contained 2% horse serum instead of 10% FCS.

Plasmid construction

Plasmids, containing *d-asb11* sequences, were constructed as described previously (8). A partial cDNA fragment of *d-asb11* in pBluescript was used as a template to generate a riboprobe for *in situ* hybridizations.

mRNA synthesis, mRNA and cDNA microinjections

Capped mRNAs were synthesized using the mMESSAGE mMACHINE kit (Ambion). mRNAs were injected into one cell-stage embryos or in one-cell of the two-cell stage blastomere. cDNA and mRNA were injected by using a microinjector (World Precision Instruments). Three hundred pg of Asb11 mRNA or 10pg of cDNA was used unless otherwise indicated. Total volume of the injection was set at 1 nL.

RNA isolation and qRT–PCR

Total RNA extraction and purification was performed by using standard Trizol and isopropanol precipitation. cDNA synthesis was performed using hexamer primers and M-MLV Reverse Transcriptase. Transcript levels were quantified by real-time PCR using ABsolute QPCR SYBR Green Fluorescein Mix (Westburg) on an iCycler iQ Real-Time PCR detection system (Bio-Rad). Results are expressed as a relative ratio to the housekeeping gene *actin*.

Primers: Zebrafish: d- asb11-F: CTGCAAAGAGAGGTCACACG

d-asb11-R: TCCTTTTTGTCCCAGTGAGC

Mouse: m-Asb11-F: GTCAGAAGGCCTGGACCAT

m-Asb11-R: CTCATGGAGTGGGGATCG

m-Asb9-F: TCCTCTTCATGATGCTGCAA

m-Asb9-R: CACGTGATCTGCTGTGATGA

***In situ* hybridization**

Whole-mount in situ mRNA hybridization (WISH) was carried out as previously described (30). Embryos were fixed in 4% paraformaldehyde (PFA) overnight at 4˚C and digoxigenin-tagged probes to myoD, muscle creatine kinase (mck) and myogenin were made with Roche labelling mix (31). Images were obtained using a Zeiss Axioplan Stereomicroscope (Oberkochen, Germany) equipped with a Leica (Wetslar, Germany) digital camera.

Immunolabelling of zebrafish embryos

Embryos were fixed for antibody staining with 4% PFA and whole mount immunohistochemistry was performed according to Du et al. (32), using primary antibodies Pax7 1:20 (Developmental Studies Hybridoma Bank) and PH3 (Upstate Biotechnology #06570) 1:1000. Appropriate secondary antibodies were used at 1:200. Immunohistochemistry was analyzed at the level of yolk extension.

Immunolabeling of adult muscle

Short term (7 days) and long term (2 months) BrdU incorporation and labeling was performed by immersing and allowing the zebrafish to swim in BrdU (150mg/L for 4 hours per day) for 7 days. Fish were fixed at 2 months after the BrdU pulse. Adult muscle tissue was isolated and frozen in liquid nitrogen, post-fixed in 4% PFA, cryosectioned in 10 µm and dried overnight. Sections were post-fixed in acetone, washed and kept in 100% methanol overnight. Sections were permeabilized with 0.2% Triton X-100 and quenched with 100mM Glycine-NaOH pH 10. Sections were washed in PBS-Tween20 (PBS-T) and incubated in 2N Hydrochloric acid. To restore the pH, sections were washed in 0.1 M Sodium borate. After washing in PBS-T, sections were blocked (2% goat serum, 1% BSA, 1% DMSO in PBS-T) at room temperature for one hour. BrdU antibody (Abcam Ab6326) was incubated 1:200 in block overnight at 4°C.

After washing in PBS-T, sections were blocked again for 1 hour and anti-rat secondary antibody (Jackson Immunoresearch; 1:200) was incubated for 2 hours at RT. After washing, sections were blocked (20% Goat serum, 0.1% BSA in PBS) for 1 hour. Asb11 antibody (Diks et al., 2006) was pre-incubated in fish powder and subsequently incubated in block (10% goat serum, 0.1% BSA) overnight at 4°C.

After washing in PBS-T, sections were blocked for 1 hour and incubated in anti-rabbit secondary antibody (Jackson Immunoresearch) for 2 hours at RT. After washing, sections were blocked (10% goat serum, 0.1% BSA, 1% DMSO in PBST) for 1 hour at RT and incubated in Pax7 antibody (Developmental Studies Hybridoma Bank) 1:20 in block overnight at 4°C.

After washing in PBS-T sections were blocked and incubated in anti-mouse secondary antibody (Jackson Immunoresearch) for 2 hours at RT. After immunolabeling, sections were counterstained in DAPI (Sigma).

Tissue histology

For cryosections, adult muscle tissues were embedded in Jung Tissue Freezing Medium, and sectioned at 10µm. For plastic sections, adult muscle tissues was dehydrated and rehydrated in an ethanol gradient. Adult muscle tissues were embedded in Technovit 8100 (Kulzer) and sectioned at

7 µm. Sections were then counterstained with Mayer's haemotoxalin and eosin.

Zebrafish cell lysate for immunoblotting

Embryos were dechorionated at the appropriate stage and subsequently transferred to cell lysis buffer (50mM HEPES mH7.5, 150mM NaCl, 1.5mM $MgCl_2$, 1mM EGTA, 10% glycerol, 1% Triton-X 100) at 4˚C (2µl/embryo), and subsequently lysed by pippeting up and down and stored at - 20˚C. Before loading, 2X loading buffer was added and the sample was boiled for 5 min. A total of 7 embryos was loaded.

Immunoblotting

Cell lysates were sonicated and then centrifuged at 1200g for 10 minutes at 4ºC. The pellet was discarded and the protein concentration was measured with the BCA protein assay kit (Pierce chemical co. Rockford, IL, USA). Lysates were diluted 1:2 in protein sample buffer (125 mM Tris/HCl, pH 6,8; 4%SDS; 2% B-mercaptoethanol ; 20% glycerol; 1 mg bromphenol blue) and incubated at 95ºC for 5 minutes. Twenty five µg of protein per lane was loaded onto SDS-PAGE and subsequently transferred onto PVDF membrane (Millipore, Amsterdam, The Netherlands). The blots were blocked with 2% low fat milk in Tris Buffered Saline supplemented with 0.1% Tween-20 (TBST) for one hour at room temperature and washed in TBST before overnight incubation at 4ºC with primary antibody in 2% low fat milk in TBST. Blots were then washed with TBST and incubated for 1 hour at room temperature in 1:1000 Horse Radish Peroxidase (HRP) conjugated secondary antibody in 2% low fat milk in TBST. After a final wash with TBST, blots were incubated for 5 minutes in Lumilite plus (Boehringer-Mannheim, Mannheim, Germany) and then chemiluminescence detected using a Fuji LAS3000 illuminator (Fuji Film Medical Systems, Stamford, USA).

Lucciferase reporter assay

C2C12 cells were transiently co-transfected with a muscle creatine kinase (MCK) promoter-driven luciferase construct and one of the following

constructs: myc-tagged-d-Asb 11, myc-tagged-SOCS box deficient-d-Asb11, myc-tagged-h-Asb9 or myc-tag empty vector. To correct for transfection efficiency or dilution effects, cells were transfected as explained above but reporter vector was replaced with a cytomegalovirus (CMV) promoter-driven Renilla luciferase (Promega, Madison, Wisconsin, USA). Lipofectamine Plus (Invitrogen, Breda, the Netherlads) method was used according to manufacture's instruction. After 48 , 72 or 96 hours incubation in differentiation medium cells were lysed with passive lysis buffer as provided by Promega and luciferase acivity was assayed according to the Dual-Glo-Luciferase Assay System (Promega) protocol on a Lumat Berthold LB 9501 Luminometer (Berthold Technologies ,Bad Wildbad, Germany).

Imaging and Quantifications

Fluorescent labeling was imaged using a Leica TCS SPE confocal microscope. BrdU+, Pax7+ and Asb11+ cells in the adult muscle tissue were counted at comparable positions at the dorsal part of the myotome. For statistical analysis, two-tailed Student's t-test was performed using Microsoft Excel.

Acknowledgements

We would like to thank S Boj for the adult muscle tissue samples and ZY Gong for the m-*ck* construct. MAS da Silva and JM Tee are paid by ALW Grant #81702002 and #81502006, respectively; while SH Diks and P van Tijn are supported by the TI Pharma Grant T1-215 and Internationale Stichting Alzheimer Onderzoek #07508, respectively. All authors do not have any conflict of interests.

References

1. Cheung AF, Pollen AA, Tavare A, DeProto J, Molnár Z. Anat. 2007 Aug;211(2):164-76.
2. He X, Marchionni L, Hansel DE, Yu W, Sood A, Yang J, Parmigiani G, Matsui W, Berman DM. Stem Cells. 2009 Jul;27(7):1487-95.
3. Hollway G, Currie P. Birth Defects Res C Embryo Today. 2005 Sep;75(3):172-9.
4. Brand-Saberi B, Christ B. Curr Top Dev Biol. 2000;48:1-42.
5. N. Kahane, Y. Cinnamon and C. Kalcheim. *Mech Dev* 74 (1998), pp. 59–73.

6. N. Kahane, Y. Cinnamon and C. Kalcheim. *Development* 125 (1998), pp. 4259–4271.
7. Ava E. Brent and Clifford J. Tabin. Curr Opin Genet Dev. 2002 Oct;12(5):548-57. Review.
8. Diks, S.H., Bink, R.J., van de Water, S., Joore, J., van Rooijen, C., Verbeek, F.J., den Hertog, J., Peppelenbosch, M.P., and Zivkovic, D. (2006). J Cell Biol *174*, 581-592.
9. Hilton DJ, Richardson RT, Alexander WS, Viney EM, Willson TA, Sprigg NS, Starr R, Nicholson SE, Metcalf D, Nicola NA. Proc Natl Acad Sci U S A. 1998 Jan 6;95(1):114-9.
10. Debrincat MA, Zhang JG, Willson TA, Silke J, Connolly LM, Simpson RJ, Alexander WS, Nicola NA, Kile BT, Hilton DJ. J Biol Chem. 2007 Feb 16;282(7):4728-
11. Kohroki J, Nishiyama T, Nakamura T, Masuho Y. ASB proteins interact with Cullin5 and Rbx2 to form E3 ubiquitin ligase complexes.
12. Diks SH, Sartori da Silva MA, Hillebrands JL, Bink RJ, Versteeg HH, van Rooijen C, Brouwers A, Chitnis AB, Peppelenbosch MP, Zivkovic D. Nat Cell Biol. 2008 Oct;10(10):1190-8.
13. Bello NF, Lamsoul I, Heuzé ML, Métais A, Moreaux G, Calderwood DA, Duprez D, Moog-Lutz C, Lutz PG. Cell Death Differ. 2009 Jun;16(6):921-32.
14. McDaneld TG, Hannon K, Moody DE. Am J Physiol Regul Integr Comp Physiol. 2006 Jun;290(6):R1672-82.
15. McDaneld TG, Spurlock DM. J Anim Sci. 2008 Nov;86(11):2897-902.
16. Chamberlain JS, Jaynes JB, Hauschka SD. Mol Cell Biol. 1985 Mar;5(3):484-92.
17. Hawke TJ, Garry DJ. J Appl Physiol. 2001 Aug;91(2):534-51.
18. Lawson MA, Purslow PP. Cells Tissues Organs. 2000;167(2-3):130-7.
19. Buckingham M. C R Biol. 2007 Jun-Jul;330(6-7):530-3.
20. Sartori da Silva MA, Tee JM, Paridaen J, Brouwers A, Runtuwene V, Zivkovic D, Diks SH, Guardavaccaro D, Peppelenbosch MP. PLoS One. 2010 Nov 19;5(11):e14023.
21. Polesskaya, A., Seale, P., and Rudnicki, M.A. (2003). Cell *113*, 841-852.
22. Otto, A., Schmidt, C., Luke, G., Allen, S., Valasek, P., Muntoni, F., Lawrence-Watt, D., and Patel, K. (2008). J Cell Sci *121*, 2939-2950.
23. Dehal, P., and Boore, J.L. (2005). PLoS Biol *3*, e314.
24. Kile BT, Metcalf D, Mifsud S, DiRago L, Nicola NA, Hilton DJ, Alexander WS. Mol Cell Biol. 2001 Sep;21(18):6189-97.
25. Guo JH, Saiyin H, Wei YH, Chen S, Chen L, Bi G, Ma LJ, Zhou GJ, Huang CQ, Yu L, Dai L. Arch Androl. 2004 May-Jun;50(3):155-61.
26. Debrincat MA, Zhang JG, Willson TA, Silke J, Connolly LM, Simpson RJ, Alexander WS, Nicola NA, Kile BT, Hilton DJ. J Biol Chem. 2007 Feb 16;282(7):4728-37.
27. Kwon S, Kim D, Rhee JW, Park JA, Kim DW, Kim DS, Lee Y, Kwon HJ. BMC Biol. 2010 Mar 19;8:23.
28. Brack, A.S., Conboy, I.M., Conboy, M.J., Shen, J., and Rando, T.A. (2008). Cell Stem Cell *2*, 50-59.
29. Westerfield, M. (1995). The zebrafish book: a guide for the laboratory use of zebrafish (*Brachydanio rerio*). (Eugene, OR, University of Oregon Press)
30. Jowett, T. (2001). Methods *23*, 345-358.
31. Xu, Y., He, J., Wang, X., Lim, T.M., and Gong, Z. (2000). Dev Dyn *219*, 201-215.
32. Du, S.J., Devoto S.H., Westerfield, M., Moon R.T. (1997) J Cell Bio 139:145-156.
33. Tee, J.M., van Rooijen, C., Boonen, R., and Zivkovic, D. (2009). PLoS One *4*, e5880.

CHAPTER 6

Identification of novel interactors of ASB11 by mass spectrometry

Maria A. Sartori da Silva[1,2], Roberto Magliozzi[1], Teck Yew Low[3,4], Albert J.R. Heck[3,4], Maikel P. Peppelenbosch[2] and Daniele Guardavaccaro[1]

[1]Hubrecht Institute-KNAW & University Medical Center Utrecht, Utrecht, The Netherlands.

[2]Department of Gastroenterology and Hepatology, Erasmus MC-University Medical Center Rotterdam, Rotterdam, The Netherlands.

[3]Biomolecular Mass Spectrometry and Proteomics Group, Bijvoet Center for Biomolecular Research and Utrecht Institute for Pharmaceutical Sciences, Utrecht University, Utrecht, the Netherlands

[4]The Netherlands Proteomics Center, Utrecht, the Netherlands.

(in preparation)

Abstract

The Ankyrin repeat and SOCS-box containing protein 11 (ASB11) is a principal regulator of cell fate in vertebrate organisms through the activation of the canonical Notch signaling. Although studies employing zebrafish Asb11 mutants suggested that the cullin-box domain is required for the protein to exert its function properly, the molecular mechanisms of action of ASB11 remain poorly defined. Knowledge as to the molecular binding partners of ASB11 is, thus, urgently required to obtain better insight into its mode of action in cellular physiology. Here we report a comprehensive analysis of ASB11 interacting proteins using immunoaffinity chromatograpy followed by tandem mass spectrometry. These results revealed a role of ASB11 as a substrate recognition subunit of the canonical ECS ubiquitin ligase complex and also attempt to speculate a specific function of ASB11 in targeting membrane proteins for ubiquitylation and, possible, proteasomal degradation.

Introduction

The discovery of the ubiquitin-proteasome, a highly-specific energy-dependent system by which regulatory proteins are targeted for destruction, enabled the understanding of protein degradation at the molecular levels as well as its implication in many biological processes as diverse as cell cycle control, gene transcription, immune response, cell differentiation, apoptosis. Proteins are built-up to provide the structural and biochemical requirements of the cells. They are also broken-down by highly-regulated mechanisms important not only to dispose of misfolded or damaged proteins but also to fine-tune the concentration of essential proteins within the cell. Proteins have different half-lives; some are rapidly degraded, while others last longer. This rapid, highly specific proteolysis is achieved through the addition of several ubiquitin molecules to a target protein, a process called ubiquitylation. The ubiquitin tag will direct the

protein to the proteasome, a large protein complex, where proteins are degraded by enzymes called proteases.

Ubiquitylation consists of a post-translational modification carried out by the sequential action of E1, E2 and E3 enzymes. Ubiquitin is first activated by the E1 ubiquitin-activating enzyme. Ubiquitin is then transferred from the E1 to the E2 enzyme also known as ubiquitin-conjugating enzyme. Finally, the E3 ligase enzyme binds both the target substrate and the E2-ubiquitin complex and completes the transfer of ubiquitin to the substrate (1,2). Multiple rounds of ubiquitin conjugation lead to the formation of long chains of ubiquitin moieties. E3 ubiquitin ligases are primarily responsible for the recognition of specific substrates based on shared conserved recognition motifs within the target protein. Hence, E3 ubiquitin ligases are key proteins for controlling highly specific selection of the substrates to be targeted for ubiquitylation and degradation by the 26S proteasome (3).

The E3s are a large, diverse group of proteins, divided into different subgroups on the basis of specific structural motifs: the HECT (homologous to the E6-AP carboxyl terminus) domain, the RING (really interesting new gene)-finger domain and the U-box domain. Assembled on a Cullin scaffold, RING proteins form Cullin-RING multisubunit complexes that act as adaptor-like molecules, bringing the E2 and the substrate into close proximity, providing an optimal conformation for ubiquitin transfer (4,5). Cullin-RING complexes diverge in terms of their subunit composition and function.

One of the complexes that share a Cullin-RING module, the ECS (Elongin B/C-Cul2/Cul5-SOCS box protein) complex, recruits substrates through SOCS box proteins (6,7).

The suppressors of cytokine signaling (SOCS) box is a structural C-terminal domain that interacts with Elongin C by its B/C box conserved motif. In turn, Elongin C binds Elongin B forming a dimer that bridges the substrate bound by the SOCS box protein to a Cullin protein. This step is further supported by a conserved Cullin box motif, located downstream of the B/C box in the SOCS box. Cullin then recruits a RING-finger-containing protein Rbx1/2, completing the assembly of the ECS E3-type ubiquitn ligase complex (8,9). Therefore SOCS box proteins are the substrate recognition units of the ECS

complexes, regulating the turnover of a wide range of proteins by targeting them for polyubiquitylation and, subsequent, proteasomal degradation.
SOCS box proteins are classified into different families based on the protein motifs found N-terminally of the SOCS box (10). The ankyrin repeat and SOCS box (ASB) family represents the largest group of SOCS box proteins, with 18 human and murine ASB proteins identified so far.
We have recently showed that in zebrafish the ankyrin repeat and SOCS box-containing protein 11 (d-Asb11) regulated the levels of the Notch ligand DeltaA possibly by targeting it for degradation via the ECS complex (11). The altered expression of d-Asb11 disrupted normal cell fate specification during neurogenesis (12) and myogenesis (unpublished data). Moreover, a zebrafish carrying a mutant allele in the cullin box subdomain of the d-Asb11 SOCS box was defective in Notch signaling and had impaired neurogenesis during embryonic development (13). Despite of the high chordate conservation of ASB proteins in general, and ASB11 in particular, no evidence of binding partners and function of ASB11 have been reported in higher vertebrate organisms or mammalian cell lines.
Nevertheless, many findings have described ASB proteins to directly interact with one or more components of the ECS complex and, in most of the cases, ASBs proper function were dependent on an integral SOCS box domain. Although these findings demonstrated the importance of this family in mediating cellular responses by protein ubiquitylation and degradation, very few proteins were identified as potential substrates of specific ASB family integrants. These facts prompt us to study novel protein interactors of human ASB11, investigating its function as a component of the canonical ECS complex as well as unraveling new roles of ASB11 in biological processes into the cells.
Here, we have used immunoaffinity chromatograpy followed by tandem mass spectrometry to identify ASB11 interacting proteins.

Results

Identification of ASB11 complexes by immunoaffinity chromatography followed by tandem mass spectrometry

To identify proteins that bind to ASB11 in mammalian cells we employed immunoaffinity chromatography followed by tandem mass spectrometry.

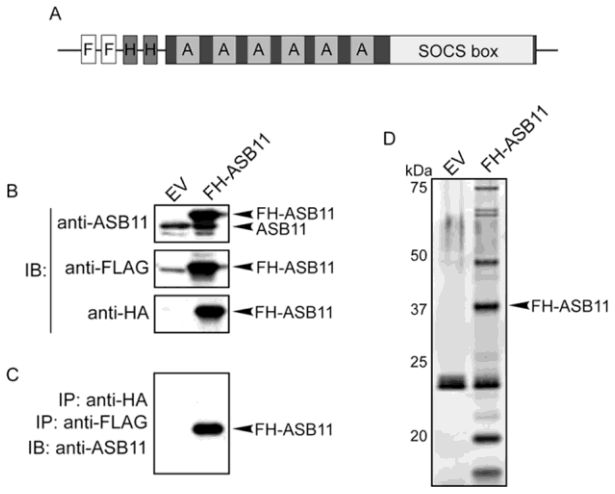

Figure 1: A. Schematic structure of the FLAG-HA tagged ASB11 (FH-ASB11) protein, showing the 6 ankyrin repeat in the N-terminal domain (A) and the C-terminal SOCS box domain. **B.** Expression of FH-ASB11 (right lane) detected by anti-ASB11 (upper panel), anti-FLAG (middle panel) and anti-HA (lower panel) antibodies. **C.** Expression of FH-ASB11 (right lane) was detected after double-immunoprecipitation (IP) with anti-FLAG and anti-HA antibodies followed by immunoblotting (IB) using an anti-ASB11 antibody. **D.** Co-immunoprecipitation of ASB11 complex components. Antibodies against FLAG and HA were used for double-immunoprecipitation from lysates of HEK293T cells expressing FH-ASB11 (right lane). EV: empty vector.

Human embryonic kidney 293T (HEK293T) cells were mock transfected or transfected with the N-terminally Flag-HA tagged ASB11 (FH-N-ASB11) construct (Fig.1A). To verify the expression of ASB11, cell lysates were analyzed by immunoblotting (IB) using anti-ASB11, anti-FLAG and anti-HA antibodies (Fig.1B). A specific band of approximately 40 kDa corresponding to FH-N-ASB11 was found in all cases.

Next, cell lysates were doubly immuno-precipitated with FLAG and HA resins, and approximately 10% of the final eluate was resolved by SDS-PAGE and either analyzed by immunoblotting (Fig.1C) or silver staining (Fig.1D). The remaining eluate was processed for mass spectrometry. We identify 194 putative interactors of ASB11 (Supplementary information Table S1). Approximately 15% of the identified

proteins were known integrants of the ubiquitin-proteasome pathway (Supplementary information Table S2) and, importantly, all components of the ECS complex were also found (Table 1). Together, these data confirmed a role of ASB11 as a substrate recognition subunit of the canonical ECS ubiquitin ligase complex, which targets proteins for ubiquitylation and subequent proteasomal degradation. In addition, another member of the ASB family, ASB13, coimmunoprecipitated with ASB11 suggesting a possible cross-regulation among ASB proteins.

ECS complex proteins	Accession Nr.	MW	EV	ASB11
Ankyrin repeat and SOCS box protein 11	IPI00103543	35 kDa	2	13
Transcription elongation factor B polypeptide 1	IPI00300341	12 kDa	3	9
Transcription elongation factor B polypeptide 2	IPI00026670	13 kDa	5	17
Cullin-5	IPI00216003	97 kDa	6	40
Cullin-2	IPI00014311	87 kDa	0	1
Isoform 1 of RING-box protein 2	IPI00033132	13 kDa	0	3
RING-box protein 1	IPI00003386	12 kDa	0	2

Table 1: Components of the ECS complex co-precipitated with ASB11. MW: molecular weight. EV:empty vector.

Biological validation of identified proteins of the ECS complex

To confirm that ASB11 indeed associate with components of the ECS complex, we first expressed FH-N-ASB11 in HEK293T cells and tested its capacity of binding to endogenous Cul5 and Rbx2 proteins. Immunoprecipitation with anti-FLAG and anti-HA antibodies followed by immunoblotting with specific antibodies, revealed that ASB11 is able to interact with Cul5 and Rbx2, allowing the formation of a canonical ECS complex (Fig.2B, lanes 1-3).

Recent studies have demonstrated that both SOCS box subdomains, BC box and Cul5 box, are essential for the interaction between ASB proteins and the Cul5-Rbx2 module (15). To investigate whether ASB11 also interacts with these molecules through its BC and Cul5 box, two distinct mutants of ASB11 were constructed. The mutant ASB11-BC had PF in place of LC in the consensus sequence [STP]L*XXX*[CSA]*XXX*Φ of the BC box, and the mutant ASB11-Cul had AAAA instead of LHLP in the consensus sequence Φ*XX*LPΦP*XX*Φ*XX*(Y/F)(L/I) of the Cul5 box (16) (Fig.2A). The ASB11 mutants

were expressed in HEK293T cells, and their abilities to interact with endogenous Cul5 and Rbx2 were examined. ASB15 was used as control (Fig.2B, lanes 4-6). The results revealed that endogenously expressed Cul5 and Rbx2 did not co-precipitated with neither the ASB11-BC nor the ASB11-Cul mutants.

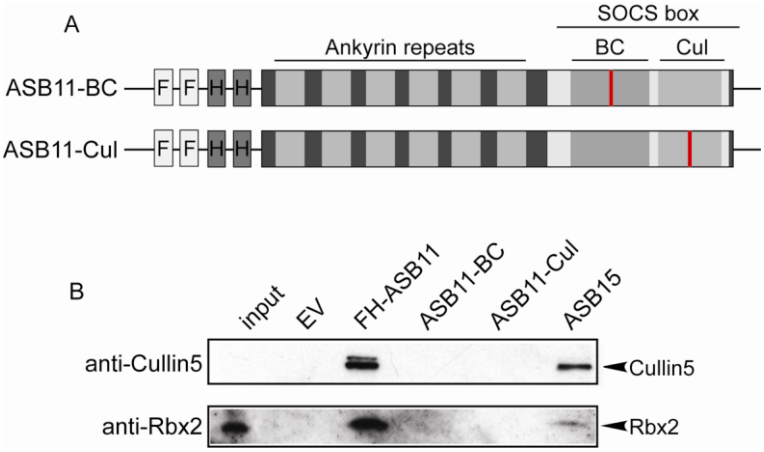

Figure 2: A. Schematic structure of mutant ASB11 proteins. The amino acids LC are replaced by PF in the consensus sequence of the SOCS box subdomain; BC box (ASB11-BC). The Cullin box subdomain presents an AAAA instead of a LHLP in its consensus sequence (ASB11-Cul). **B.** Endogenous Cullin5 (upper panel) and Rbx2 (lower panel) proteins were co-precipitated with full-length ASB11 (FH-ASB11) and ASB15 but not with ASB11 mutants lacking the consensus sequence of the BC (ASB11-BC) and Cul5 (ASB11-Cul) boxes. EV: empty vector.

These results showed that ASB11 interacted with Cul5 and Rbx2 through its intact SOCS box domain confirming that the BC box and Cul5 box conserved amino acid sequences shared by all members of the ASB family are essential for interaction with the Cul5-Rbx2 scaffold module.

Gene Ontology (GO) Analysis of ASB11-interacting Proteins

To understand the biological meaning behind the list of proteins identified in our experiment, we used the Database for Annotation, Visualization and Integrated Discovery (DAVID) to classify the data into specific categories based on cellular components, molecular functions and biological

processes, by highlighting the most relevant GO terms associated with our gene list.

The GO analysis revealed that 93 proteins, 52% of the total identified (p<0.01), were transmembrane (TM) proteins and 34 (19% of total, p<0.01) were proteins related to the endoplasmic reticulum (ER). Additionally, 49 proteins (27.5%, p<0.01) are known to participate in the transport machinery of the cells (Fig.3A). Interestingly, two web programs (SMART and HPRD) have predicted ASB11 itself carrying a TM domain (Fig.3B-C). However experiments showing the specific cell localization of ASB11 have not been provided yet.

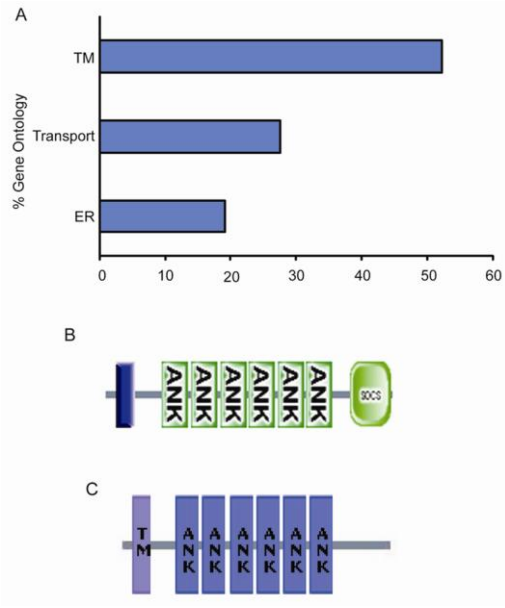

Figure 3: A. Putative ASB11 binding proteins identified by mass spectrometry and divided into groups based on gene ontology analysis. Transmembrane proteins (TM) represent 52% of the total of identified proteins; transport machinery-related proteins represent 27.5% and 19% were proteins of the endoplasmatic reticulum (ER). Transmembrane domain in ASB11 protein was predicted by (**B**) SMART and (**C**) HRPD web programs.

These data are consistent with our previous findings where Asb11 has been shown to bind, ubiquitylate and degrade the transmembrane Notch-ligand, DeltaA.

Discussion

Throughout the years, a large number of substrates have been identified for E3 ubiquitin ligases, progressively revealing the crucial importance of the ubiquitin-proteasome system in controlling the turnover of numerous

critical regulatory proteins involved in nearly all aspects of cellular processes. However, the task is still only in its infancy, and challenges ahead include unraveling the mechanisms by which E3 ligases confer specificity to ubiquitylation by recognizing target substrates. In this context, identification of substrates of E3 ligases is of utmost importance.

The SOCS box-containing proteins participate in the formation of E3 ligase complexes, forming a bridge between specific substrate-binding domains and the core complex of the E3 ubiquitin ligase. Many studies have reported ASB proteins, a subgroup of SOCS box proteins, to act as E3 ubiquitin ligases, targeting proteins for ubiquitylation and degradation. However, the processes of recognition, ubiquitylation and degradation of target substrates by ASB proteins remain to be elucidated.

In this study, we used affinity purification technique and mass spectrometry to identify putative interactors of the ankyrin repeat and SOCS box-containing protein 11, ASB11.

535 proteins were identified. After carefully analysis of the data, contaminants and unspecific proteins were removed, resulting in a list of 194 proteins. 15% of the total number of proteins was previously recognized as integrants of the ubiquitin-proteasome pathway (e.g. 26S proteasome regulatory subunits).

Studies have shown that elongin BC adapter proteins associate with SOCS box proteins and Cul-Rbx modules to form complexes of elongin BC-Cullin-Rbx-SOCS box, called ECS complexes. Specific components of the ECS complex were significantly present in our data, showing the highest numbers of unique peptides (e.g. Cullin5, ElonginB).

The interaction of ASB proteins with Cul5-Rbx2 modules requires conserved amino acid sequences of LC in its BC box and LPLP in its Cul5 box (15). Although these amino acid sequences are shared by numerous SOCS box proteins, including all ASB members, a few ASB proteins contain sequences different from the consensus motifs. In the case of ASB11 the conserved LPLP in the Cul5 box is replaced by LHLP. Thus, we next examined whether this slight divergence retain the ability to associate with Cul5-Rbx2 module. Indeed wild type ASB11 interacted with endogenously expressed Cul5 and

Rbx2, but not its mutant sequences. Therefore, the results suggest that ASB11 can interact with Cul5 and Rbx2, despite slight divergences in the consensus sequences seen in the Cul5 box and this interaction depends on intact conserved motif of both BC and Cullin boxes.

It has been proposed that the conserved cullin boxes, determine the association of SOCS box proteins with their specific Cul-Rbx module. The Elongin BC complex binds to the BC box region and links the substrate recognition subunit to heterodimers of either Cullin 2 (Cul2) and RING finger protein Rbx1 or Cullin 5 (Cul5) and Rbx2. Cullin boxes were then classified into two groups, Cul2 box and Cul5 box, on the basis of their sequence homology and binding specificity for either Cul2-Rbx1 or Cul5-Rbx2 modules (15,16). In this context, ASB proteins were shown to share the Cul5 box domain and interact with Cul5-Rbx2 to form E3 Ub ligases, instead of Cul2 or Rbx1. However, some studies reported ASB proteins to associate with Cul5-Rbx1 modules instead of Cul5-Rbx2 and in a lesser extent with Cul2 (17). Cullin2 and Rbx1 were also identified in our experiment, however, with a lower significance. These data provide evidences that ASB proteins may vary to form ubiquitylation complexes and it could be related with substrate specificity, proteins availability and biological functions.

Protein-protein interactions can now be examined by immunoprecipitation of the protein complex of interest allowing the identification of proteins that differentially and selectively interact to each other and are integral to their biological effects. In our study more than 50% of the proteins identified were transmembrane proteins, being almost 30% related to cell transport.

It is now established that Ub-mediated degradation of membrane proteins depends on a complex network of protein-protein interactions that control both the ubiquitylation reaction and the intracellular fate of the target substrate. A recently study has reported a novel E3 ubiquitin ligase family which constitutes membrane-bound molecules containing two transmembrane regions and a RING-CH domain. Forced expression of these novel E3s has been shown to reduce the surface expression of various

membrane proteins through ubiquitylation of target molecules (18). Accordingly, d-Asb11 in zebrafish was found to activate Notch signaling by ubiquitylating and degrading DeltaA, a transmembrane ligand for Notch receptors (11).

Despite the canonical role of ubiquitylation in mediating proteasome degradation, the protein modification by Ub has much broader and diverse functions. For example, monoubiquitylation of transmembrane proteins, influences their stability, protein-protein recognition, activity and intracellular localization (19).

Altogether, these results attempt us to speculate the function of ASB11 in ubiquitylating membrane proteins and, consequently, determining their cellular fate.

Material and Methods

Cell culture

HEK293T cells were maintained in Dulbecco's modified Eagle's medium (Invitrogen) containing 10% fetal calf serum. HEK293T cells were transfected using the calcium phosphate method as described by Dorrello et al., 2006.

Biochemical methods

Immunoprecipitation and immunoblotting were performed by standard methods and have been described previously (20). The primary antibodies used were: mouse monoclonal anti-FLAG (Sigma), anti-Actin (Santa Cruz Biotechnology), anti-HA (Covance), rabbit polyclonal anti-FLAG and anti-ASB11 (Sigma), anti-HA, anti-Rbx2 and anti-Cul5 (Santa Cruz Biotechnology).

Plasmids

For ASB11 transfections Hs ASB11 cDNA was cloned into BamHI and XhoI restriction sites of pcDNA3.

ASB11 mutants were generated using the QuickChange Site-directed Mutagenesis kit (Stratagene) according to manufacture's recommendations. All cDNAs were sequenced.

Purification of ASB11 interactors

HEK293T cells were transfected with pCDNA3-FLAG-HA-ASB11 and treated with 10 μM MG132 for 5 hours. Cells were harvested and subsequently lysed in lysis buffer (LB: 50 mM Tris-HCl pH 7.5, 150 mM NaCl, 1 mM EDTA, 0.5% NP40, plus protease and phosphatase inhibitors). ASB11 was immunopurified with anti-FLAG agarose resin (Sigma). After washing, proteins were eluted by competition with FLAG peptide (Sigma). The eluate was then subject to a second immunopurification with an anti-HA resin (12CA5 monoclonal antibody crosslinked to protein G Sepharose; Invitrogen) prior to elution in Laemmli sample buffer. The final eluate was separated by SDS-PAGE, and proteins were visualized by Coomassie colloidal blue (Invitrogen kit). Bands were sliced out from the gels and subjected to in-gel digestion. Gel pieces were then reduced, alkylated and digested according to a published protocol (Shevchenko et al., 1996). For mass spectrometric analysis, peptides recovered from in-gel digestion were separated with a C18 column and introduced by nano-electrospray into the LTQ Orbitrap XL (Thermo Fisher, Bremen). Peak lists were generated from the MS/MS spectra using MaxQuant (Cox and Mann, 2008), and then searched against the IPI Human database using Mascot search engine (Matrix Science). Carbaminomethylation (+57 Da) was set as fixed modification and protein N-terminal acetylation and methionine oxidation as variable modifications. Peptide tolerance was set to 7 ppm and fragment ion tolerance was set to 0.5 Da, allowing 2 missed cleavages with trypsin enzyme.

Silver staining

The final eluate of the purification described above was followed by silver staining (SilverQuest Silver staining kit, Invitrogen) according to manufacture's recommendations.

References

1. Finley D, Chau V. Annu Rev Cell Biol. 1991;7:25-69.
2. Weissman AM. Immunol Today. 1997 Apr;18(4):189-98.
3. Jackson PK, Eldridge AG, Freed E, Furstenthal L, Hsu JY, Kaiser BK, Reimann JD. Trends Cell Biol. 2000 Oct;10(10):429-39.
4. Pickart CM. Annu Rev Biochem. 2001;70:503-33.
5. Ardley HC, Robinson PA. Essays Biochem. 2005;41:15-30.
6. Kamura T, Sato S, Haque D, Liu L, Kaelin WG Jr, Conaway RC, Conaway JW. Genes Dev. 1998 Dec 15;12(24):3872-81.
7. Zhang JG, Farley A, Nicholson SE, Willson TA, Zugaro LM, Simpson RJ, Moritz RL, Cary D, Richardson R, Hausmann G, Kile BJ, Kent SB, Alexander WS, Metcalf D, Hilton DJ, Nicola NA, Baca M. Proc Natl Acad Sci U S A. 1999 Mar 2;96(5):2071-6.
8. Kile BT, Schulman BA, Alexander WS, Nicola NA, Martin HM, Hilton DJ. Trends Biochem Sci. 2002 May;27(5):235-41.
9. Piessevaux J, Lavens D, Peelman F, Tavernier J. Cytokine Growth Factor Rev. 2008 Oct-Dec;19(5-6):371-81. Epub 2008 Oct 22.
10. Hilton DJ, Richardson RT, Alexander WS, Viney EM, Willson TA, Sprigg NS, Starr R, Nicholson SE, Metcalf D, Nicola NA. Proc Natl Acad Sci U S A. 1998 Jan 6;95(1):114-9.
11. Diks SH, Sartori da Silva MA, Hillebrands JL, Bink RJ, Versteeg HH, van Rooijen C, Brouwers A, Chitnis AB, Peppelenbosch MP, Zivkovic D. Nat Cell Biol. 2008 Oct;10(10):1190-8. Epub 2008 Sep 7.
12. Diks SH, Bink RJ, van de Water S, Joore J, van Rooijen C, Verbeek FJ, den Hertog J, Peppelenbosch MP, Zivkovic D. J Cell Biol. 2006 Aug 14;174(4):581-92. Epub 2006 Aug 7.
13. Sartori da Silva MA, Tee JM, Paridaen J, Brouwers A, Runtuwene V, Zivkovic D, Diks SH, Guardavaccaro D, Peppelenbosch MP. PLoS One. 2010 Nov 19;5(11):e14023.
14. Donald S. Kirkpatrick, Carilee Denison & Steven P. Gygi. Nature Cell Biology 7, 750 - 757 (2005) doi:10.1038/ncb0805-750
15. Kohroki J, Nishiyama T, Nakamura T, Masuho Y. FEBS Lett. 2005 Dec 19;579(30):6796-802. Epub 2005 Nov 28.
16. Mahrour N, Redwine WB, Florens L, Swanson SK, Martin-Brown S, Bradford WD, Staehling-Hampton K, Washburn MP, Conaway RC, Conaway JW. J Biol Chem. 2008 Mar 21;283(12):8005-13. Epub 2008 Jan 10.
17. Heuzé ML, Guibal FC, Banks CA, Conaway JW, Conaway RC, Cayre YE, Benecke A, Lutz PG. J Biol Chem. 2005 Feb 18;280(7):5468-74. Epub 2004 Dec 8.
18. Ohmura-Hoshino M, Goto E, Matsuki Y, Aoki M, Mito M, Uematsu M, Hotta H, Ishido S. J Biochem. 2006 Aug;140(2):147-54. Review.
19. d'Azzo A, Bongiovanni A, Nastasi T. Traffic. 2005 Jun;6(6):429-41. Review.
20. Dorrello NV, Peschiaroli A, Guardavaccaro D, Colburn NH, Sherman NE, Pagano M. Science. 2006 Oct 20;314(5798):467-71.

Supplementary Information

#	Identified Proteins	Acces. Nr.	EV	ASB11
1	Cullin-5	IPI00216003	6	40
2	Transcription elongation factor B polypeptide 2	IPI00026670	5	17
3	Ankyrin repeat and SOCS box protein 11	IPI00103543	2	13
4	Isoform Long of Na/Ktransporting ATPase subunit alpha-1	IPI00006482	0	13
5	Isoform SERCA2A of Sarcoplasmic/endoplasmic reticulum Ca ATPase 2	IPI00177817	0	11
6	Isoform 1 of Protein transport protein Sec61 subunit alpha isoform 1	IPI00218466	0	10
7	Transcription elongation factor B polypeptide 1	IPI00300341	3	9
8	Receptor expression-enhancing protein 5	IPI00024670	0	9
9	Protein of unknown function DUF410 family protein	IPI00419575	0	7
10	Uncharacterized protein REEP6	IPI00646963	0	6
11	Ubiquitin-like protein 4A	IPI00005658	0	6
12	Uncharacterized protein MON2	IPI00465246	0	6
13	Large neutral amino acids transporter small subunit 1	IPI00008986	0	5
14	Ubiquilin-2	IPI00409659	0	5
15	253 kDa protein	IPI00152990	0	5
16	Isoform 3 of WD repeat domain phosphoinositide-interacting protein 4	IPI00642665	0	5
17	G protein pathway suppressor 1 isoform 2	IPI00156282	0	5
18	Autocrine motility factor receptor, isoform 2	IPI00423874	0	4
19	FUN14 domain containing 2	IPI00171769	0	4
20	Transmembrane protein 161A precursor	IPI00301841	0	4
21	Signal recognition particle receptor subunit beta	IPI00295098	0	4
22	Ankyrin repeat domain-containing protein 13A	IPI00217831	0	4
23	Mitotic spindle assembly checkpoint protein MAD2A	IPI00012369	0	4
24	Putative uncharacterized protein DKFZp686L20222	IPI00026689	0	4
25	Vitamin K-dependent gamma-carboxylase	IPI00305698	0	4
26	Serine/threonine-protein kinase 38	IPI00027251	0	4
27	Isoform 1 of Transmembrane and coiled-coil domain-containing protein 7	IPI00034201	0	4
28	Isoform 1 of RING-box protein 2	IPI00033132	0	3
29	Protein-tyrosine phosphatase-like A domain-containing protein 1	IPI00008998	0	3
30	UBX domain-containing protein 8	IPI00172656	0	3
31	ER degradation-enhancing alpha-mannosidase-like 3	IPI00009410	0	3
32	Isoform 2 of RING finger protein 126	IPI00155562	0	3
33	Isoform 1 of LAG1 longevity assurance homolog 1	IPI00019462	0	3
34	Isoform 3 of Fanconi anemia group I protein	IPI00306518	0	3
35	interleukin-1 receptor-associated kinase 1 isoform 3	IPI00060149	0	3
36	Ubiquilin-4	IPI00024502	0	3
37	Isoform 1 of Fanconi anemia group D2 protein	IPI00075081	0	3
38	Isoform 1 of Protein FAM62A	IPI00022143	0	3
39	Component of gems 4	IPI00027717	0	3
40	Isoform 1 of Carnitine O-palmitoyltransferase I, liver isoform	IPI00032038	0	3
41	LAG1 longevity assurance homolog 2	IPI00305304	0	3
42	Isoform 1 of Sn1-specific diacylglycerol lipase beta	IPI00385987	0	3
43	hypothetical protein LOC55793 isoform 1	IPI00413164	0	3
44	E3 ubiquitin-protein ligase RNF5	IPI00012608	0	2
45	hypothetical protein LOC84928	IPI00045764	0	2
46	Tumor necrosis factor superfamily, member 5-induced protein 1	IPI00644482	0	2
47	Solute carrier family 30 member 7	IPI00302605	0	2
48	RING-box protein 1	IPI00003386	0	2
49	Isoform 3 of Sigma 1-type opioid receptor	IPI00004267	0	2
50	Isoform 1 of Zinc transporter 9	IPI00552548	0	2

51	TDP43	IPI00025815	0	2
52	CLPTM1-like protein	IPI00151358	0	2
53	Isoform 2 of Import inner membrane translocase subunit TIM50	IPI00418497	0	2
54	Isoform 1 of Cytoplasmic FMR1-interacting protein 1	IPI00644231	0	2
55	Isoform 1 of Limb region 1 protein homolog	IPI00385238	0	2
56	Protein ADRM1	IPI00033030	0	2
57	Isoform 1 of Neutral alpha-glucosidase AB precursor	IPI00383581	0	2
58	CDNA FLJ12528 fis, clone NT2RM4000155	IPI00018632	0	2
59	Sortilin precursor	IPI00217882	0	2
60	Vesicle transport protein GOT1B	IPI00007061	0	2
61	Vacuolar ATP synthase subunit S1 precursor	IPI00784119	0	2
62	TGF-beta receptor type-1 precursor	IPI00005733	0	2
63	Isoform 1 of Fanconi anemia group A protein	IPI00006170	0	2
64	Uncharacterized protein KIAA0406	IPI00011702	0	2
65	Plasma alpha-L-fucosidase precursor	IPI00012440	0	2
67	Uncharacterized protein ASNA1	IPI00013466	0	2
68	Isoform 1 of Homocysteine-responsive endoplasmic reticulum	IPI00014171	0	2
69	ATP-binding cassette sub-family B member 10, mitochondrial precursor	IPI00015826	0	2
70	Isoform 3 of Protein YIF1B	IPI00063544	0	2
71	Isoform 1 of Signal peptide peptidase-like 3	IPI00152440	0	2
72	Isoform 2 of Ubiquitin carboxyl-terminal hydrolase isozyme L5	IPI00219512	0	2
73	Protein transport protein Sec61 subunit beta	IPI00220835	0	2
74	Isoform 1 of FAST kinase domain-containing protein 1	IPI00300186	0	2
75	40S ribosomal protein S4, Y isoform 1	IPI00302740	0	2
76	Isoform 1 of UPF0420 protein C16orf58	IPI00305627	0	2
77	UPF0467 protein C5orf32	IPI00382821	0	2
78	Isoform 2 of Condensin-II complex subunit G2	IPI00396058	0	2
79	Uncharacterized protein C8orf55 precursor	IPI00171421	0	1
80	FUN14 domain-containing protein 1	IPI00217081	0	1
81	Isoform 1 of Synaptic glycoprotein SC2	IPI00100656	0	1
82	Isoform 1 of Solute carrier family 35 member E1	IPI00101952	0	1
83	cDNA FLJ76313	IPI00006050	0	1
84	RING finger protein C13orf7	IPI00465370	0	1
85	BRI3-binding protein	IPI00103599	0	1
86	LGICZ1 protein	IPI00719125	0	1
87	4F2 cell-surface antigen heavy chain	IPI00027493	0	1
88	Conserved hypothetical protein	IPI00746458	0	1
89	Cullin-2	IPI00014311	0	1
90	Replication factor C subunit 5	IPI00031514	0	1
91	Translocation-associated membrane protein 1	IPI00219111	0	1
92	Phospholipase A-2-activating protein	IPI00218465	0	1
93	PRA1 family protein 3	IPI00007426	0	1
94	Etoposide-induced protein 2.4	IPI00023185	0	1
95	similar to C05G5.5	IPI00397764	0	1
96	Sodium-coupled neutral amino acid transporter 1	IPI00023030	0	1
97	Isoform 1 of Thyroid receptor-interacting protein 13	IPI00003505	0	1
98	Dymeclin	IPI00296211	0	1
99	Isoform 1 of Protein transport protein Sec61 subunit alpha isoform 2	IPI00414427	0	1
100	Corneodesmosin precursor	IPI00386809	0	1
101	KIAA0683	IPI00016868	0	1
102	Import inner membrane translocase subunit TIM44, mitochondrial	IPI00306516	0	1
103	Isoform 1 of Rhomboid domain-containing protein 1	IPI00152700	0	1
104	Electron transfer flavoprotein subunit alpha, mitochondrial precursor	IPI00010810	0	1
105	lysosomal-associated membrane protein 1	IPI00004503	0	1

106	Isoform Long of Ancient ubiquitous protein 1 precursor	IPI00001891	0	1
107	Protein PRO0628	IPI00006047	0	1
108	Rho-related BTB domain-containing protein 3	IPI00007132	0	1
109	Neutral amino acid transporter B	IPI00019472	0	1
110	GPI-anchor transamidase precursor	IPI00022543	0	1
111	Isoform 1 of C-X-C chemokine receptor type 4	IPI00028159	0	1
112	Isoform 1 of Zinc transporter ZIP3	IPI00029337	0	1
113	similar to Peripheral-type benzodiazepine receptor-associated protein 1	IPI00033009	0	1
114	Protein UNQ773/PRO1567 precursor	IPI00060800	0	1
115	Isoform 1 of Histone-lysine N-methyltransferase	IPI00102107	0	1
116	Signal peptidase complex catalytic subunit SEC11A	IPI00104128	0	1
117	Isoform 2 of Lysocardiolipin acyltransferase	IPI00166225	0	1
118	Uncharacterized protein ENSP00000312264	IPI00176824	0	1
119	Isoform 2 of AP-2 complex subunit sigma-1	IPI00183781	0	1
120	Neuronal acetylcholine receptor subunit alpha-5 precursor	IPI00295323	0	1
121	Uncharacterized protein C2orf18 precursor	IPI00550440	0	1
122	Isoform 1 of Protein cornichon homolog 4	IPI00000115	0	1
123	Isoform 2 of Probable hydrolase PNKD	IPI00001022	0	1
124	Importin subunit beta-1	IPI00001639	0	1
125	Isoform 4 of Nucleoporin NDC1	IPI00003455	0	1
126	Malignant fibrous histiocytoma-amplified sequence 1	IPI00003495	0	1
127	Isoform XB of Plasma membrane calcium-transporting ATPase 3	IPI00003831	0	1
128	Neutrophil defensin 1 precursor	IPI00005721	0	1
129	Isoform 1 of Surfeit locus protein 4	IPI00005737	0	1
130	Isoform 1 of TraB domain-containing protein	IPI00008732	0	1
131	TRAF-type zinc finger domain-containing protein 1	IPI00009146	0	1
132	ORM1-like protein 1	IPI00009364	0	1
134	Isoform 3 of LAS1-like protein	IPI00009917	0	1
135	Serine/threonine-protein phosphatase 6	IPI00012970	0	1
136	cDNA FLJ76992, highly similar to Homo sapiens synaptogyrin 1a	IPI00013940	0	1
137	ADP-ribosylation factor-like protein 6-interacting protein 1	IPI00014232	0	1
138	Isoform 1 of Zinc transporter ZIP14	IPI00014236	0	1
139	Isoform 1 of Protein SERAC1	IPI00014444	0	1
140	SCD5 protein	IPI00015151	0	1
141	Isoform 1 of CDK5 regulatory subunit-associated protein 1-like 1	IPI00015713	0	1
142	CDNA: FLJ22955 fis, clone KAT09907	IPI00015737	0	1
143	CKLF-like MARVEL transmembrane domain-containing protein 6	IPI00015801	0	1
144	Transmembrane emp24 domain-containing protein 2 precursor	IPI00016608	0	1
145	1-acyl-sn-glycerol-3-phosphate acyltransferase delta	IPI00016956	0	1
146	Protein transport protein Sec23B	IPI00017376	0	1
147	LMBR1 domain-containing protein 2	IPI00017940	0	1
148	Orphan sodium- and chloride-dependent neurotransmitter transporter	IPI00018071	0	1
149	ER lumen protein retaining receptor 2	IPI00018248	0	1
150	Immunoglobulin-binding protein 1	IPI00019148	0	1
151	C-4 methylsterol oxidase	IPI00019899	0	1
152	Isoform 1 of Solute carrier family 12 member 2	IPI00022649	0	1
153	Isoform 1 of Semenogelin-1 precursor	IPI00023020	0	1
154	Myeloid leukemia factor 2	IPI00023095	0	1
155	Uncharacterized protein ASPH	IPI00024572	0	1
156	Isoform 1 of SAPK substrate protein 1	IPI00027378	0	1
157	CAAX prenyl protease 2	IPI00031755	0	1
158	Uncharacterized protein C10orf35	IPI00060546	0	1
159	Isoform 2 of Phosphoglycerate mutase family member 5 precursor	IPI00063242	0	1
160	THO complex subunit 3	IPI00063729	0	1
161	Isoform 2 of Ubiquilin-1	IPI00071180	0	1

162	Isoform 2 of Plakophilin-1	IPI00071509	0	1
163	Isoform 1 of GPI transamidase component PIG-T precursor	IPI00100030	0	1
164	Isoform 2 of Cleft lip and palate transmembrane protein 1	IPI00107357	0	1
165	Solute carrier family 16 member 10	IPI00152879	0	1
166	Polymerase delta-interacting protein 2	IPI00165506	0	1
167	Isoform 1 of Integral membrane protein GPR177 precursor	IPI00171444	0	1
168	Isoform 1 of Protein-tyrosine phosphatase mitochondrial 1	IPI00174190	0	1
169	Uncharacterized protein SQSTM1	IPI00179473	0	1
170	Uncharacterized protein TTC27	IPI00183938	0	1
171	Isoform 1 of Centaurin-gamma-1	IPI00217393	0	1
172	Isoform 1 of Solute carrier family 35 member F2	IPI00293362	0	1
173	Eukaryotic translation initiation factor 2 subunit 3	IPI00297982	0	1
174	G protein-coupled receptor 50	IPI00299062	0	1
175	T-complex protein 1 subunit delta	IPI00302927	0	1
176	WD repeat-containing protein 34	IPI00306130	0	1
177	48 kDa protein	IPI00328383	0	1
178	Cullin-associated NEDD8-dissociated protein 2	IPI00374208	0	1
179	FOXP4 protein (Fragment)	IPI00386277	0	1
180	Nuclear pore complex protein Nup93	IPI00397904	0	1
181	Uncharacterized protein ENSP00000310225	IPI00398048	0	1
182	Isoform 2 of Protein FAM62B	IPI00409635	0	1
183	hypothetical protein LOC80097	IPI00410094	0	1
184	FAST kinase domain-containing protein 5	IPI00414973	0	1
185	Isoform 1 of Cytosol aminopeptidase	IPI00419237	0	1
186	Isoform 2 of Bromo adjacent homology domain-containing 1 protein	IPI00465088	0	1
187	RING finger and WD repeat domain-containing protein 3	IPI00478737	0	1
188	Putative uncharacterized protein DKFZp686H16220	IPI00552191	0	1
189	Ubiquitin-activating enzyme E1	IPI00645078	0	1
190	Uncharacterized protein ATP1B1	IPI00747849	0	1
191	Similar to Smad ubiquitination regulatory factor 2	IPI00868681	0	1
192	Isoform 2 of Limkain-b1	IPI00005146	0	1
193	similar to basic leucine zipper and W2 domains 1	IPI00005681	0	1
194	Isoform 2 of Otoferlin	IPI00216362	0	1

Table S1: ASB11 putative interactors identified by mass spectrometry

#	Identified Proteins	Acces. Nr.	Uni pep
1	26S protease regulatory subunit 4	IPI00011126	9
2	26S protease regulatory subunit 6A	IPI00018398	7
3	26S protease regulatory subunit 7	IPI00021435	13
4	26S protease regulatory subunit 8	IPI00023919	7
5	26S protease regulatory subunit S10B	IPI00021926	9
6	26S proteasome non-ATPase regulatory subunit 12	IPI00185374	8
7	26S proteasome non-ATPase regulatory subunit 14	IPI00024821	3
8	26S proteasome non-ATPase regulatory subunit 2	IPI00012268	6
9	26S proteasome non-ATPase regulatory subunit 3	IPI00011603	13
10	26S proteasome non-ATPase regulatory subunit 6	IPI00014151	12

11	26S proteasome non-ATPase regulatory subunit 7	IPI00019927	1
12	Isoform 1 of 26S protease regulatory subunit 6B	IPI00020042	6
13	Isoform 1 of 26S proteasome non-ATPase regulatory subunit 1	IPI00299608	5
14	Isoform 1 of Proteasome activator complex subunit 3	IPI00030243	6
15	Isoform 1 of Proteasome activator complex subunit 4	IPI00005260	2
16	Isoform 1 of Proteasome assembly chaperone 1	IPI00030770	1
17	Isoform 1 of Proteasome subunit alpha type-7	IPI00024175	11
18	Proteasome 26S non-ATPase subunit 11 variant (Fragment)	IPI00105598	8
19	proteasome 26S non-ATPase subunit 13 isoform 2	IPI00375380	8
20	proteasome 26S non-ATPase subunit 8	IPI00010201	3
21	Proteasome subunit alpha type-2	IPI00219622	5
22	Proteasome subunit alpha type-4	IPI00299155	9
23	Proteasome subunit alpha type-5	IPI00291922	8
24	Proteasome subunit alpha type-6	IPI00029623	12
25	Proteasome subunit beta type-1 precursor	IPI00025019	8
26	Proteasome subunit beta type-2	IPI00028006	8
27	Proteasome subunit beta type-3	IPI00028004	8
28	Proteasome subunit beta type-4 precursor	IPI00555956	6
29	Proteasome subunit beta type-6 precursor	IPI00000811	5
30	Proteasome subunit beta type-7 precursor	IPI00003217	6
31	Ubiquilin-2	IPI00409659	5
32	Ubiquilin-4	IPI00024502	3
33	ubiquitin specific protease 11	IPI00184533	1
34	Ubiquitin-activating enzyme E1	IPI00645078	1
35	Ubiquitin-like protein 4A	IPI00005658	6
36	Ubiquitin-like protein 7	IPI00305922	1

Table S2: Protein integrants of the Ubiquitin-Proteosome pathway.

CHAPTER 7

General Discussion

One of the most important and defining processes during development is the pattern formation of the various compartments in embryos. In an effort to discover the participants involved in regulating compartment size, we performed a differential display designed to isolate genes that are downregulated upon cell differentiation in *Danio rerio* (zebrafish) embryos. Zebrafish biological characteristics, as described in chapter 1, make it a valuable model organism for studies of vertebrate development and gene function allowing the identification of many genes involved in embryogenesis and human diseases. The full-length sequence of one down-regulated fragment under differentiation treatment during zebrafish embriogenesis revealed a gene homologous to the mammalian ankyrin repeat and suppressor of cytokine signaling (SOCS) box-containing protein 11 (*ASB11*), further referred to as *d-asb11*. Loss of function experiments resulted in premature neuronal differentiation and reduced cell proliferating compartment in embryos, whereas forced expression prevented neuronal differentiation and maintained precursor cell fate *in vivo* and *in vitro*. Thus, *d-asb11* first emerged as an essential gene responsible for maintaining proliferation of progenitors during zebrafish embryogenesis.

The d-Asb11 is a member of the ASB family which constitutes a conserved chordate-unique gene family characterized by variable numbers of N-terminal ankyrin repeats and a C-terminal SOCS box domain. Although still very little is known about ASB proteins, the information aggregated in chapter 2 provided a general view of the biological functions of the family as well as particular functions of its members. ASBs have been reported to regulate the turnover of protein substrates by interacting with and targeting them to degradation via the ubiquitin-proteasome pathway. ASB association with components of Cullin-based ubiquitylation complexes via the SOCS box domain is well established; however, ASB proteins seemed to vary to form ubiquitylation complexes and may act by additional regulation pathways. Furthermore, analysis of ASB transcripts levels revealed a tissue-specific expression pattern, indicating tissue-specific functions. ASB proteins were firmly implicated in the regulation of cell proliferation and

differentiation, important to maintain controlled cell growth and prevent tumor formation. Consistently, abnormal ASB expression was found in different cancer types. Therefore, more studies are necessary to investigate ASB proteins function and to define specific substrates by which ASBs interact with as well as to provide important information as the control of normal and pathological (i.e. cancer) compartment size in various systems during vertebrate development.

The evidences that ASB proteins are crucial regulators of compartment size and cell fate decisions, as well as the discovered of d-Asb11 maintaining cell undifferentiated state in the progenitor compartment of zebrafish embryos, prompted us to investigate more details of d-Asb11 molecular mode of function.

The study performed in the chapter 3 has successfully contributed to this question and showed that d-Asb11 is a key mediator of Delta-Notch signaling, acting at the level of DeltaA ubiquitylation, important in fine-tuning the lateral inhibition gradients between DeltaA and Notch and thereby regulating Notch signaling activity in a non cell-autonomous manner

The Notch signaling pathway represents a highly conserved mechanism to mediate signaling between adjacent cells, which ensures that an initially homogenous cell population differentiates to distinct fates, a process termed lateral inhibition. Thus, d-Asb11 acting on Notch pathway activation serves to maintain a cell in a proliferative state and to prevent its differentiation, sometimes promoting an alternative fate.

Although these findings presented a previously unrecognized function of the Asb11 protein in cell fate decisions, the importance of its specific domains in targeting substrates in a vertebrate organism was first demonstrated in the chapter 4, where we explored the biological functions of the cullin box domain of the d-Asb11. For that, we isolated a zebrafish mutant lacking the Cul5 box domain ($Asb11^{Cul}$) and found that homozygous zebrafish mutants for this allele were defective in Notch signaling as indicated by the impaired expression of Notch target genes. Importantly, $asb11^{Cul}$ fish were not capable to degrade the Notch ligand DeltaA during

embryogenesis, a process essential for the initiation of Notch signaling during neurogenesis. Accordingly, proper cell fate specification within the neurogenic regions of the zebrafish embryo was impaired. In addition, *asb11*^{Cul} mRNA was defective in the ability to transactivate a *her4::gfp* reporter DNA when injected in embryos. Thus, our study reporting the generation and the characterization of a metazoan organism mutant in the conserved cullin binding domain of the SOCS-box demonstrates a hitherto unrecognized importance of the SOCS-box domain for the function of this class of cullin-RING ubiquitin ligases and establishes that the d-Asb11 cullin box is required for both canonical Notch signaling and proper neurogenesis.

Subsequently experiments were initiated to identify further *in vivo* functions of d-Asb11, also using the hypomorphic mutant fish as a tool. d-Asb11 function in embryogenesis and adult organisms has not been fully explored, and thus, it was possible that d-Asb11 is relevant for compartment definition outside the neuronal system, prompting more comprehensive analysis of its *in vivo* expression. Indeed, d-Asb11 was well capable of activating Notch signal transduction outside the neuronal system as heterologous expression of this gene activates Notch reporters in a variety of cell types. Besides, analysis of *asb11* transcripts showed that the expression of this gene in muscle tissue is a pan-vertebrate characteristic; presenting a particular strong expression in mammalian muscle (mouse and human). Hence, in the chapter 5 we decided to characterize the function of d-Asb11 regarding to myogenesis.

Downregulation of d-Asb11 interfered with myotome formation during embryogenesis and adult muscle regeneration, whereas forced expression led to expansion of the muscle compartment both *in vitro* and *in vivo*. Importantly, we demonstrated that d-Asb11 is expressed beneath the basal lamina of adult zebrafish muscle fiber, and co-localized with a muscle satellite cell specific marker Pax7. This, together with the co-expression of d-Asb11 with label retaining BrdU slow-cycling cells, suggested that the d-Asb11 positive cells are the muscle satellite cells themselves. Interestingly, there are significantly less d-Asb11^{+} cells compared with Pax7^{+} cells in the adult muscle fibers. It is tempting to speculate that the d-Asb11 cells are

the primary stem cells, and thus, is activated and proliferates in response to muscle damage/injury. Thus, we concluded that d-Asb11 constitutes a novel regulator of primary and regenerative myogenesis.

The effects of *d-asb11* on embryonic myogenesis are remarkably similar to its effects on embryonic neural precursors, suggesting that *d-asb11* functions in a similar way in regulating both the neuroectodermal and mesodermal cell fates. Whether *d-asb11* is important for compartment size in the endodermal lineage, however, is questionable.

Furthermore, based on the evolutionary conservation of *d-asb11* with human *hASB9* and *hASB11*, it is tempting to hypothesize that the phenotypes we observed in the *d-asb11* mutants could be linked to human muscular diseases, prompting an investigation into the role of ASB11 in muscle pathology and the urgency to define its mode of action in molecular terms and especially to identify new binding partners.

Many studies have reported ASB proteins to act as E3 ubiquitin ligases, targeting proteins for ubiquitylation and degradation. However, the processes of recognition, ubiquitylation and degradation of target substrates by ASB proteins remain to be elucidated.

In chapter 6, we used affinity purification technique and mass spectrometry to identify putative interactors of the ASB11. 194 proteins were identified and 15% of the total number of proteins was previously recognized as integrants of the ubiquitin-proteasome pathway.

Studies have shown that elongin BC adapter proteins associate with SOCS box proteins and Cul-Rbx modules to form complexes of elongin BC-Cullin-Rbx-SOCS box, called ECS complexes. Specific components of the ECS complex were significantly present in our data, showing the highest numbers of unique peptides (e.g. Cullin5, ElonginB).

Indeed ASB11 can interact with Cul5 and Rbx2, despite slight divergences in the consensus sequences seen in the Cul5 box and this interaction depends on intact conserved motif of both BC and Cullin boxes.

In our study more than 50% of the proteins identified were transmembrane proteins, being almost 30% related to cell transport. A recent study has reported a novel E3 ubiquitin ligase family which constitutes membrane-

bound molecules containing two transmembrane regions and a RING-CH domain. Forced expression of these novel E3s has been shown to reduce the surface expression of various membrane proteins through ubiquitylation of target molecules. Accordingly, d-Asb11 in zebrafish was found to activate Notch signaling by ubiquitylating and degrading DeltaA, a transmembrane ligand for Notch receptors. These results attempt us to speculate the function of ASB11 in ubiquitylating membrane proteins and, consequently, determining their cellular fate.

Altogether my results provide important new insight on the action and function of ASB proteins, and especially ASB11, in regulating progenitor compartment expansion, possibly by controlling protein levels in the cells.

Summary

One of the most important and defining processes during development is the pattern formation of the various compartments in embryos. In an effort to discover the participants involved in regulating compartment size, we identified, in *Danio rerio* (zebrafish) embryos, a gene homologous to the mammalian ankyrin repeat and suppressor of cytokine signaling (SOCS) box-containing protein 11 (*ASB11*), further referred to as *d-asb11.* The d-Asb11 is a member of the ASB family which constitutes a conserved chordate-unique gene family characterized by variable numbers of N-terminal ankyrin repeats and a C-terminal SOCS box domain. ASBs have been reported to regulate the turnover of protein substrates by the ubiquitin-proteasome degradation pathway. Furthermore, ASB proteins were firmly implicated in the regulation of cell proliferation and differentiation; and abnormal ASB expression was found in different pathologies, including cancer. The evidences that ASB proteins are crucial regulators of compartment size and cell fate decisions, as well as the discovered of d-Asb11 maintaining cell undifferentiated state in the progenitor compartment of zebrafish embryos, prompted us to investigate more details of d-Asb11 molecular mode of function.

We first showed that d-Asb11 is a key mediator of Delta-Notch Signaling, acting at the level of DeltaA ubiquitylation, important in fine-tuning the lateral inhibition gradients between DeltaA and Notch and thereby regulating Notch signaling activity in a non cell-autonomous manner.

We next investigated the biological functions of the cullin box domain of the d-Asb11 SOCS box. For that, we isolated a zebrafish having a germline deletion of the cullin box subdomain ($Asb11^{Cul}$) and showed that this deletion resulted in loss of d-Asb11 activity. As a consequence, the animals were defective for Notch signaling and proper cell fate specification within the neurogenic regions of zebrafish embryos. These results established the first *in vivo* evidence that the cullin box is required for SOCS box functionality. Subsequently experiments were initiated to identify further *in vivo* functions of d-Asb11, also using the hypomorphic mutant fish as a tool.

Next we provided evidence that d-Asb11 is important in maintaining myogenic proliferation in the stem cell compartment of zebrafish embryos and muscle regenerative responses in adult animals. This finding is supported by the highly specific d-Asb11 expression found in proliferating satellite cells and revealed the new function of d-Asb11 as a regulator of zebrafish myogenesis. The apparent importance of d-Asb11 in multiple germ lines enforces the urgency to define its mode of action in molecular terms and especially to identify new binding partners.

For this purpose, we have applied immunoaffinity chromatograpy followed by tandem mass spectrometry to identify human ASB11 interacting proteins. The data confirmed the role of human ASB11 as a substrate-recognition that targets proteins for ubiquitylation and proteasomal degradation via the canonical ECS ubiquitin ligase complex. Furthermore, we speculated on a specific function of ASB11 in governing cellular fate of membrane proteins not only by mediating proteasome degradation but also by influencing protein stability, activity and intracellular localization.

Altogether our results provide important new insight on the action and function of ASB proteins, and especially ASB11, in regulating progenitor compartment expansion, possibly by controlling protein levels in the cells.

Samenvatting

Gedurende de embryogenese worden verschillende celsoorten (zenuwweefsel, spierweefsel) gevormd als voorlopercellen. Deze voorlopercellen vermenigvuldigen zich tot de uiteindelijke weefselgrootte en orgaangrootte is bereikt. Grootte van weefsels en organen definieert soorten, stuurt evolutie en is verstoord bij kanker, het is dus van belang de regulatoren van orgaangrootte te kennen. Eerder onderzoek in onze onderzoeksgroep, voorafgaand aan het door mij in dit proefschrift beschreven onderzoek omvatte een genetische screen in zebravissen, en daarbij werd ontdekt dat het gen ***asb11*** bepaald hoe groot de hersenen van de zebravis worden. De moleculaire mechanismen die ten grondslag liggen aan dit effect alsook het belang van *asb* genen in de controle van compartimentgrootte in het algemeen bleef ononderzocht. Het doel van het dit proefschrift was daarom verdere duidelijkheid te verschaffen m.b.t. de werking en functie van ASB eiwitten in het regelen van compartimentgrootte. De "**outline of this thesis**" beschrijft de verschillende onderdelen van deze dissertatie en hun onderlinge samenhang.

Voor dit onderzoek besloot ik gebruik te maken van zebravis, een organisme dat belangrijke voordelen biedt, zoals de mogelijkheid om snel met quasigenetische methodologie (morpholino's, mRNA injectie etc.) de actie van eiwitten te onderzoeken, maar ook een organisme dat gedurende de embryonale fase doorzichtig is en dat zich buiten het moederlichaam ontwikkelt en ook nog eens een snelle generatietijd bezit. Een meer uitvoerige inleiding in de zebravis biologie geef ik in **hoofdstuk 2**. Een meer specifieke discussie over de biologie van ASB eiwitten in hun algemeenheid en in het speciaal een analyse van hun mogelijke rol in sturen van compartimentgrootte, gebaseerd op het corpus van de aanwezige biomedische literatuur en electronische databestanden, is te vinden in **hoofdstuk 3**. Van deze discussie wordt duidelijk dat *asb11* waarschijnlijk compartiment expansie drijft door het aanjagen van de zogenaamde Delta-Notch signalering en dit concept wordt in de volgende twee hoofdstukken experimenteel uitgewerkt.

In **hoofdstuk 4** wordt aangetoond, gebruik makend van gidsgenen die louter tot expressie komen na de activatie van specifieke ontwikkelingsbiologische paden, dat specifiek Notch-Delta signaal transductie wordt aangedaan door veranderingen in de dosering van ASB11. Dit effect kon worden teruggebracht tot een essentiele rol van het *asb11* gen in het tot stand brengen van de zogenaamde “laterale inhibitie”. Notch-Delta signalering ontstaat in cel-paartjes waar één cel veel Notch bevat en de andere veel Delta. Omdat het ASB11 eiwit Delta afbreekt verandert de verhouding tussen de relatieve Delta hoeveelheden in een celpaar en kan de laterale inhibitie haar werk doen. Interessant is dat de primaire structuur van *asb11* inderdaad elementen bevat die er op wijzen dat *asb11* via een proces dat we ubiquitinatie noemen eiwitten kan afbreken. Een voorspelling van de bevindingen gedaan in hoofdstuk 4 zou dan ook zijn dat de genetische ablatie van deze elementen de werking van *asb11* zou ondergraven.

Deze hypothese werd direct getest in **hoofdstuk5**. Ofschoon nog nooit eerder in een organisme een zogenaamde cullinbox genetisch uit het genoom werd verwijderd, is dit element evolutionair zeer geconserveerd in ubiquitine ligases. Ik heb daarom een zebravis mutant geïsoleerd die dit element van *asb11* mistte. Het bleek dat deze deletie inderdaad een gemankeerde ASB11 functie tewerkstelde met onder andere een geringe expansie van het centraal zenuwstelsel die gepaard ging met de afwezigheid van Delta-Notch signalering tijdens de ontwikkeling van dit orgaan. Deze studies bevestigden niet alleen het belang van het *asb11* gen in het bepalen van compartimentgrootte, maar bevestigden ook voor het eerst met genetische methoden in metazooën dat de evolutionaire conservering van de cullin-box in ubiquitine ligases een reflectie is van een essentiële functie van deze sequentie voor de ubiquitinering.

Het belang van *asb* genen voor het aansturen van compartimentgrootte werd verder duidelijk door studies beschreven in **hoofdstuk 6**. Het bestuderen van expressie van de verschillende *asb* genen in muis en vis leidde tot de hypothese dat ook tijdens de ontwikkeling van de spier *asb*

genen belangrijk zouden zijn. En inderdaad was een cullinbox mutant geremd in spieruitgroei, terwijl overactivatie van *asb* genen tot expansie van het spierstelsel leidde. Blijkbaar spelen *asb* genen in meerdere kiembanen van de vertebraat een belangrijke rol in het sturen van expansie van compartimenten.

Een dergelijke belangrijke rol van *asb* genen in de fysiologie van de vertebraat maakt het nog belangrijker dat we exact begrijpen hoe *asb11* moleculair precies werkt. Daarom ben ik in een studie, beschreven in **hoofdstuk 7**, op zoek gegaan middels geavanceerde massa spectrometrie technieken naar inter-acterende eiwitten van het ASB11. De resultaten laten zien dat ASB11 alle componenten van het traditionele ECS ubiquitine ligase systeem bindt en brengt dus verdere klaarheid in hoe *asb11* haar fundamentele functie in de patroonvorming kan uitvoeren.

Een synthese van de onderzoeksresultaten verkregen alsmede een plaatsbepaling van deze synthese in het totaal van de aanwezige biomedische kennis wordt gegeven een discussie verwerkt in **hoofdstuk 8**. Er wordt geconcludeerd dat met name zolang het *asb11* gen tot expressie komt het progenitor compartiment kan expanderen door een ubiquitine-machinerie afhankelijke activering van Delta-Notch signalering. Differentiërende signalen zoals vitamine A zuur remmen de expressie van asb11 en markeren het eind van progenitor en compartimentexpansie en het begin van functionele differentiatie.

About the author

Maria Augusta Sartori da Silva was born on the 24th of September 1983 in Piracicaba, Brazil. In 2001 she finished her pre-graduate education in Biochemistry at Technical School "Conselheiro Antonio Prado", Campinas (Brazil).

In 2003 she enrolled Biological Sciences higher studies at Pontifical Catholic University of Campinas (PUCCAMP), Campinas, Brazil, where she graduated in January 2007. During the course of her studies; she performed undergraduate research for 2 years in the Signal Transduction Laboratory, in the Institute of Biology at University of Campinas, Brazil. She worked on the project entitled "Induction of myeloid leukaemia cells death by natural products", under the supervision of Prof.dr. Carmen Verissima Ferreira and specialized in Molecular Biology.

In July 2007 she started her PhD studies at University Medical Center Groningen, in Groningen, The Netherlands, as an ALW PhD fellow, under the supervision of Prof.dr. Maikel Peppelenbosch, afterwards moving to Erasmus-MC in Rotterdam. In January 2008 she started collaboration with Dr. Dana Zivkovic at Hubrecht Institute, in Utrecht, where she performed experiments using zebrafish. In the end of 2009 she started collaborating with Dr. Daniele Guardavaccaro (Hubrecht) and Albert Heck's group (University of Utrecht) where she performed biochemistry and mass spectrometry experiments. In 2010 she carried out experiments in mice in collaboration with Dr. Vanesa Muncan at Leiden University Medical Center.

The result of her research is presented in this thesis.

List of Publications

Diks SH, **Sartori da Silva MA**, Hillebrands JL, Bink RJ, Versteeg HH, van Rooijen C, Brouwers A, Chitnis A, Peppelenbosch MP and Zivkovic D. *d-Asb11 is an essential mediator of canonical Delta-Notch signaling*. **Nature Cell Biology.** 2008.

Sartori da Silva MA, Tee JM, Paridaen J, Brouwers A, Runtuwene V, Zivkovic D, Diks SH, Guardavaccaro D, Peppelenbosch MP. Essential role for the d-Asb11 cul5 Box domain for proper notch signaling and neural cell fate decisions in vivo. **PLoS One**. 2010.

Ferreira CV, **Sartori da Silva MA**, Justo GZ. Nanocosmetics and nanomedicines: New approaches for skin care. *Chapter 12: Zebrafish as a suitable model for evaluating nanocosmetics and nanomedicines.* **Springer Publishing Company**. 2011.

Tee JM, **Sartori da Silva MA**, Rygiel AM, Muncan V, Brouwers A, Bink R, van den Brink GR, van Tijn P, Zivkovic D, Kodach LL, Diks SH, Guardavaccaro D, Peppelenbosch MP. ***d-****Asb11 is a novel regulator of embryonic and adult regenerative myogenesis.* Submitted.

Sartori da Silva MA and Peppelenbosch MP. *Size matters: the emerging role of ASB proteins in controlling cell fate decisions and cancer development* (Review). Submitted.

Acknowledgements/Agradecimentos

Foremost, my utmost gratitude to my first supervisor and dear friend Prof. Carmen Verissima Ferreira who made possible the achievement of this PhD and whose support and encouragement I will never forget.
I especially want to thank my supervisor, Prof. Maikel Peppelenbosch, for his patience, motivation, enthusiasm, immense knowledge and guidance during my research.
I owe my most sincere gratitude to Dana Zivkovic and Daniele Guardavaccaro who gave me the opportunity to work with their groups at the Hubrecht Institute and gave me valuable help during my research.
I warmly thank to all those who have helped me with my lab work; my labmates, specially Anke and Roberto and staff coleagues for the use of the facilities.
I would like to thank my colleagues and friends for providing a stimulating and fun environment at work.
I offer my sincere regards to all of those who supported me in any respect during the completion of this PhD.

Amigos e família:
Agradeço aos amigos que ficaram no Brasil por estarem presente todas as vezes que retornei. E por me fazerem sentir que a amizade verdadeira sobrevive ao tempo e a distância!
Aos amigos que encontrei aqui, obrigada por trazerem um pouquinho do Brasil com vocês, seja no sotaque gostoso, nos abraços fortes, nas saudades divididas ou no sorriso que escapa fácil do rosto do brasileiro. Alguns de vocês serão amigos para toda a vida. Obrigada por terem feito parte da minha vida!
Família, devo tudo a vocês, minha vida, minha força, minhas conquistas. Obrigada pelo apoio, pelo amor e pelos puxões de orelha quando mereci. Pai, mãe, vó e Chico, vocês são tudo na minha vida! Amo vocês!

PhD Portfolio Summary

Summary of PhD training and teaching activities

Name PhD student: Maria Augusta Sartori da Silva **Erasmus MC Department:** Gastroenterology and Hepatology	**PhD period:** July 2007 to July 2011 **Promotor:** Prof. dr. M. Peppelenbosch **Copromotor:** Dr. D. Guardavaccaro

1. PhD training

	Year	Workload (hours/ECTS)
General Courses		
- Kinome Profiling Course	2008	1 ECTS
- Laboratory Animal Science	2009	4 ECTS
- PhD Masterclass – Cancer Genomics & Developmental Biology	2009	1 ECTS
- Proteomics and mass spectrometry	2010	1.5 ECTS
- Digital pictures: data integrity & display	2010	1 ECTS
- PhD Masteclass - Cancer Genomics & Developmental Biology	2010	1 ECTS
Presentations		
- 2nd Symposium on Stem Cell, Development and Regulation, Amsterdam	2008	2 ECTS
- 3rd Symposium on Stem Cell, Development and Regulation, Amsterdam	2009	2 ECTS
- 4th Symposium on Stem Cell, Development and Regulation, Amsterdam	2010	2 ECTS
International Conferences		
- 5th European Zebrafish Genetics & Development Meeting, Amsterdam (Netherlands)	2007	3 ECTS
- 8th International Conference on Zebrafish Development & Genetics, Winsconsin (USA)	2008	3 ECTS
- 6th European Zebrafish Genetics & Development Meeting, Rome (Italy)	2009	3 ECTS

2. Teaching activities

	Year	Workload (hours/ECTS)
Supervising Master's theses		
- Anirudh Prahallad	2010	3 ECTS